ALMA MATER STUDIORUM - UNIVERSITÀ DI BOLOGNA

FACOLTA' DI INGEGNERIA

CORSO DI LAUREA IN INGEGNERIA CIVILE

Ingegneria Civile,Chimica, Ambientale e dei Materiali

TESI DI LAUREA

in
Advanced Structural Mechanics

"In-Plane Cyclic Behavior of Substandard Confined Masonry: Full-Scale Experiments, Finite-Elements Modeling and Incremental Dynamic Analysis."

CANDIDATO
Marco Cavigli

RELATORE:

Dott. Ing. Alessandro Marzani

CORELATORI:

Dott. Ing. Nicola Buratti
Dott. Ing. Fabio Matta

"In-Plane Cyclic Behavior of Substandard Confined Masonry: Full-Scale Experiments, Finite-Element Modeling and Incremental Dynamic Analysis"

Contents

Contents

Contents

"In-Plane Cyclic Behavior of Substandard Confined Masonry: Full-Scale Experiments, Finite-Element Modeling and Incremental Dynamic Analysis"

Contents

Acknowledgement

"In-Plane Cyclic Behavior of Substandard Confined Masonry: Full-Scale Experiments, Finite-Element Modeling and Incremental Dynamic Analysis"

Contents

"In-Plane Cyclic Behavior of Substandard Confined Masonry: Full-Scale Experiments, Finite-Element Modeling and Incremental Dynamic Analysis"

Contents

iv

"In-Plane Cyclic Behavior of Substandard Confined Masonry: Full-Scale Experiments, Finite-Element Modeling and Incremental Dynamic Analysis"

Chapter 1

1. Introduction

1.1 Objectives

The issue of the seismic performance and safety of existing masonry structures is characterized by numerous uncertainties and as in our case by a real lack of sufficient knowledge.

The aim of this work is to understand the seismic behavior of "Sub standard Confined Masonry Structures", characterized by substandard materials and poor design knowledge, with the scope to reduce the design's uncertainty and the number of victims involved in the seismic event.

In fact this technique is used in zones of high seismic hazard and the scope of this work it is to define, through a rational basis, the "Seismic Performance Factors" that, when properly implemented in the seismic design process, will result in equivalent safety against collapse in an earthquake, comparable to the inherent safety against collapse intended by current seismic codes, for building with different seismic-force-resisting systems [1].

This aim was been achieved through the following steps:

- investigation of materials, design and construction practices that result in substandard confined masonry structures;

- experimentation of three full scale walls with the aim to characterize the in plane behavior;

- development of an efficient FE model capable of predicting the behavior of the CM walls;

- validation of the FE model (elementary archetype);

- development of three houses' models based on the elementary archetype;

- testing the houses' models with 10 different type of unscaled accelerograms through the Incremental Dynamic Analysis;

- implementation of Push Over Test;

- validation of the Capacity Curve using the dynamics tests results;

- definition of the Global Ductility Factor and the Behavior Factor.

"In-Plane Cyclic Behavior of Substandard Confined Masonry: Full-Scale Experiments, Finite-Element Modeling and Incremental Dynamic Analysis"

Chapter 1

1.2 Back ground and literature review

1.2.1 Confined Masonry

The construction of confined masonries starts in 1908, after the Messina earthquake, becoming one of the most popular and inexpensive structural construction system used for housing.

This construction is common for low-rise residential buildings and individual houses in many areas of Latin America, Indian subcontinent and Asia as well as some parts of Europe.

In these buildings masonry shear walls are often the only structural element assumed to provide resistance to gravitational and seismic lateral loads. It consists basically of masonry panels confined by vertical and horizontal elements usually of reinforced concrete. The horizontal members are called bond-beams and vertical members are called tie-columns.
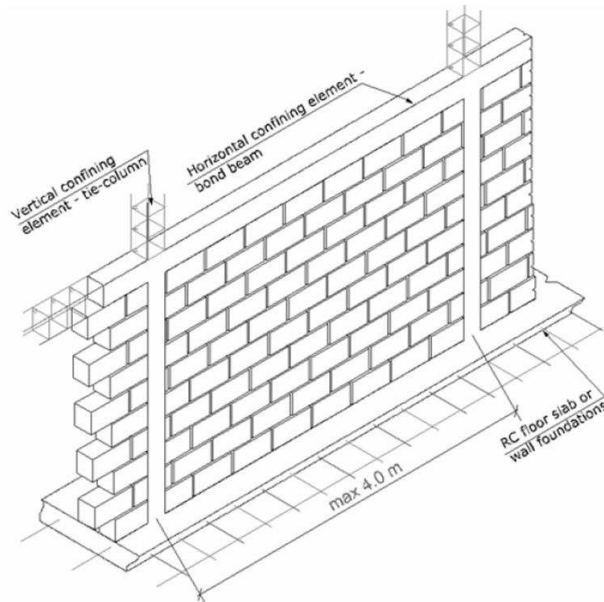
Figure 1 Example of Confined Masonry [2]

Tie-columns have a square section whose dimensions are usually equal to the wall thickness. In respect to the bond beams, their width is the wall thickness and the depth is usually equal to 20-25 cm (8-10 in).

The crucial point is that this technique has evolved essentially through an informal process based on experience, and that it has been incorporated in formal construction through code requirements and design procedures that are mostly rationalizations of the established practice, even after having been validated by structural mechanics principles and experimental evidence.

In spite of masonry experimental research programs conducted in many countries, the behavior of confined masonry shear walls is still not very well know.

"In-Plane Cyclic Behavior of Substandard Confined Masonry: Full-Scale Experiments, Finite-Element Modeling and Incremental Dynamic Analysis"

Chapter 1

1.2.2 Failure Modes

In order to investigate the Seismic behavior of Masonry Structures, a comprehensive literature review was conducted [3-4-5-6-10]. The first things we have to define is "Failure Mode", that is the core of the structural design of buildings. A failure mode is a mechanism by which a component in a building stop to be able to resist the loads applied on it.

The goal of structural design is identifying the possible mechanism that could bring about failure, predicting the force or deformation that failure by this mechanism will occur, and determining if this force or deformation capacity is larger than expected demands on the structure. There are two general types of failure modes: non-structural failure modes and structural failure modes. For the first modes, they result only in collapse of the failed component itself. This happens because non structural elements do not support other members. For a structural point of view, such elements are only required to resists the forces applied to them directly, such as self-weight or inertial force. Structural failure modes involve the failure of structural members, or members that are relied upon to support other components of the building. If a structural failure mode occurs, the result is collapse of part or all the building.

As shown in picture 2, we have tree typical distributions of forces:

vertical, in plane lateral forces and out of plane lateral forces.
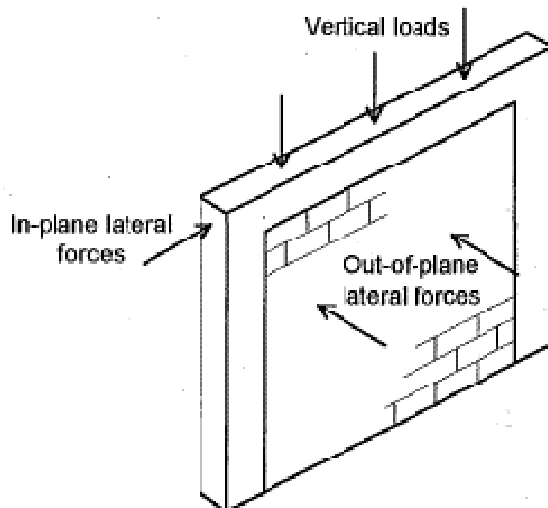
Figure 2 Confined Masonry wall with loads [7]

From the damaging observation, after a seismic event, it is possible to define two different categories in which divide the seismic behavior of Masonry structure: the first mode we consider the collapse's kinematics connected with the out of plane behavior of masonry walls (rocking) and the second mode's mechanisms that involve the in-plane behavior of masonry walls, damaged typically for shear or flexure.

"In-Plane Cyclic Behavior of Substandard Confined Masonry: Full-Scale Experiments, Finite-Element Modeling and Incremental Dynamic Analysis"

Chapter 1

And it is just the second mode that have a relevant role under seismic action as will be explained in 1.2.4. In fact also in code [8-9] the seismic-force-resisting element considered in the analysis are those work in their plane. The typical mechanisms for the second mode are shown in picture 3.
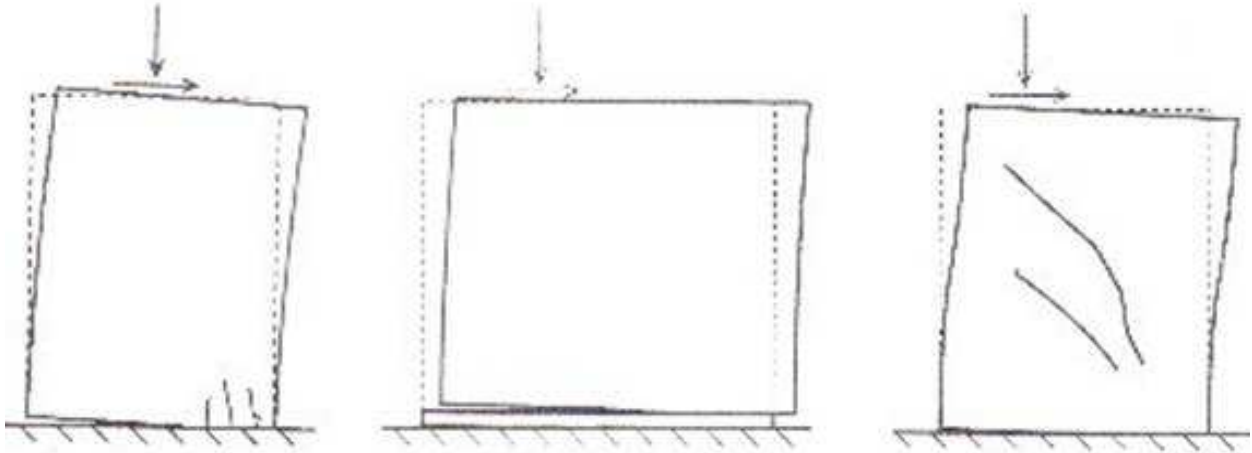
Figure 3 Failure Mechanisms [7]

In plane failures occur in walls parallel to the direction of earthquake shaking. Generally resisting forces in the in-plane direction is an efficient way for a structure to transfer lateral forces to the foundation and that it is the way in which the masonry structures works.

Three failure modes can result from confined masonry walls carrying lateral loads in-plane: diagonal shear failure, sliding shear failure and in-plane bending failure.

1.2.2.1 Diagonal Shear Failure

It is a typical in plane mechanism observed in well-proportioned confined masonry structures. Several approaches can be used to idealize the force transfer that brings about diagonal shear failure. One of them it is illustrated in figure 4, in which the force transfer is achieved through a compression strut and a tension tie.
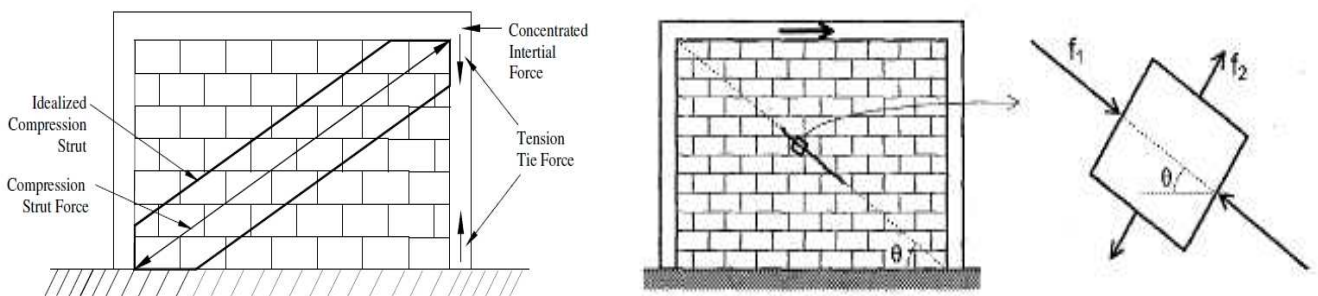
Figure 4 Shear Failure [10-11]

"In-Plane Cyclic Behavior of Substandard Confined Masonry: Full-Scale Experiments, Finite-Element Modeling and Incremental Dynamic Analysis"

Chapter 1

Referred to the literature it is possible to assume that the width of the diagonal strut it is equal to one third of its length and its thickness it is the same of the panel.

As diagonal cracking increases, the compression strut becomes less effective in transferring compressive force. To compensate, the tie columns work to distribute the horizontal inertial force off the main diagonal, in effect widening the compression strut.

Increasing the load increase also the number of struts inside masonry and for a certain point of view we can image it like in figure 5:
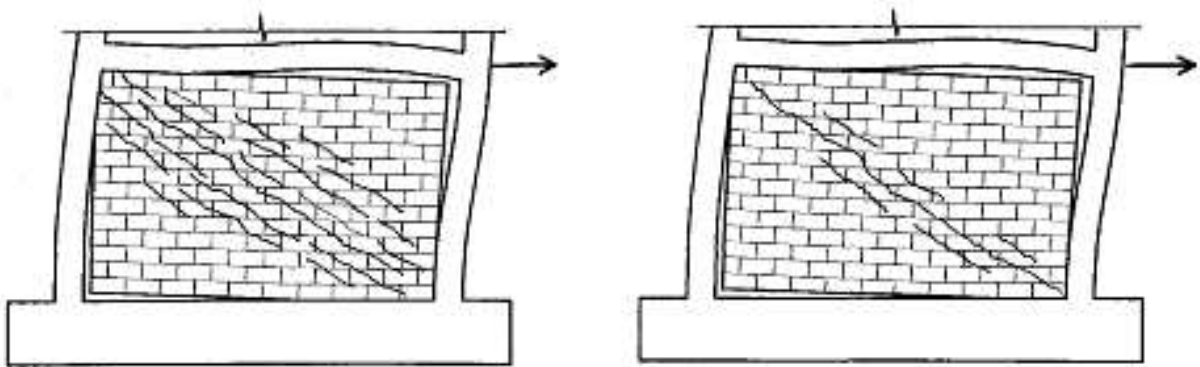
Figure 5 Increasing of Struts [11]

1.2.2.2 Sliding Shear Failure

In this type of failure, a horizontal crack forms in the mortar joint across a portion or the entire length of the panel and then it extends into the tie columns. Once the tie columns have failed in shear, failure occurs by the wall sliding along the horizontal joint. It happens only if the resistance of the mortar joint is very weak.
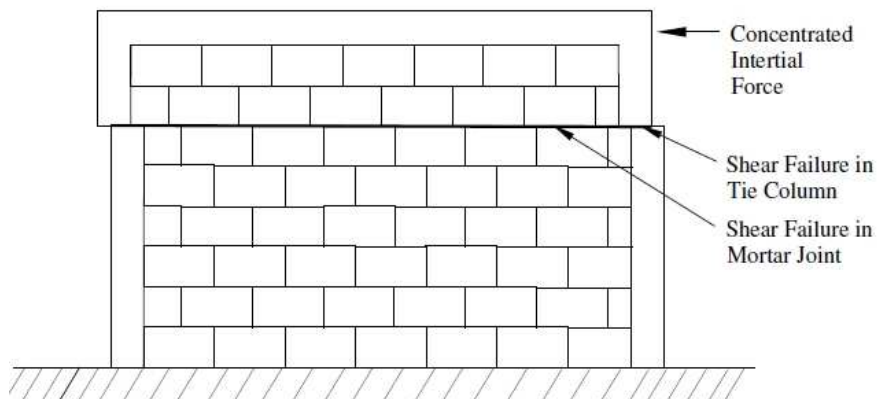
Figure 6 Sliding Shear Failure [10]

"In-Plane Cyclic Behavior of Substandard Confined Masonry: Full-Scale Experiments, Finite-Element Modeling and Incremental Dynamic Analysis"

Chapter 1

1.2.2.3 In-Plane Bending Failure

Horizontal and vertical loads cause compression stresses at one end of the wall and tensile stresses at the other. Assuming the tie column does not participate, the wall fails when the tension strength of the mortar at the tension end is exceeded, causing the wall to tip over.
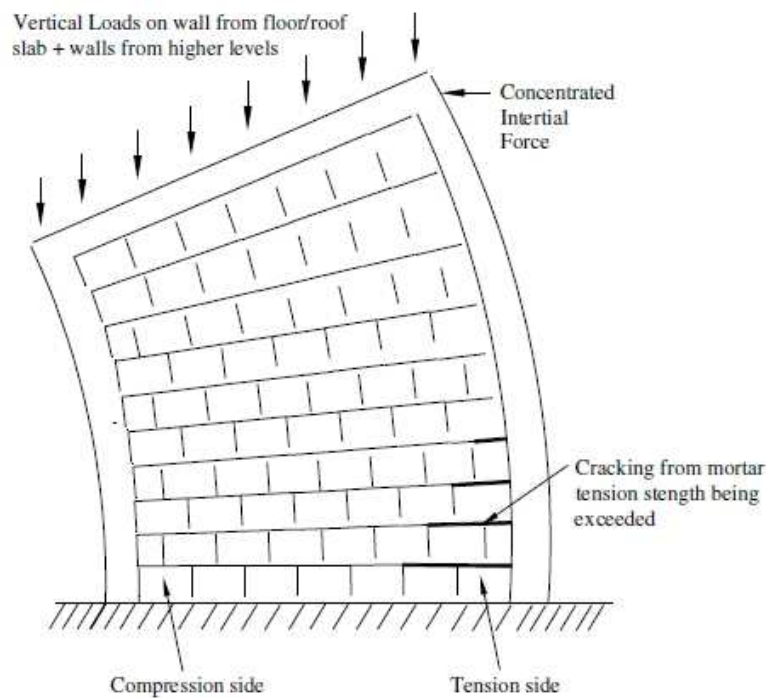
Figure 7 Bending Failure [10]

1.2.3 Confined Masonry Buildings, Seismic Behavior

It is really important to understand how this structures work to resist earthquake forces.

Earthquake introduces stress into buildings by accelerating and displacing the base of the building. Since no lateral forces are applied to the building above the ground, the walls, floors and roof stay in their original positions. The foundation, however, wants to drag the rest of the building along with it since everything is connected together. To do so, the structural elements must apply forces on the superstructure to get it move with the foundation.

The forces applied by the structural elements works to overcome the inertia, or resistance to change the initial conditions of the superstructure, and hence are referred to as inertial forces. The inertia of a component of a building is directly proportional to its mass. Thus, much heavier will be a wall,

"In-Plane Cyclic Behavior of Substandard Confined Masonry: Full-Scale Experiments, Finite-Element Modeling and Incremental Dynamic Analysis"

Chapter 1

a floor etc., and larger will be the force that must be developed in the structural elements to make it move with the foundation.

To make easier to understand the seismic response of a structure, instead of consider earthquake loads as ground displacements and acceleration, sometimes we can consider the base of the structure to remain still, and apply equivalent lateral loads on the building equal to the inertial forces caused by ground motion. The two systems are structurally equivalent, but the latter is usually easier to understand and interpret. Figure 4 illustrates the two ways of conceptualizing earthquake loads.
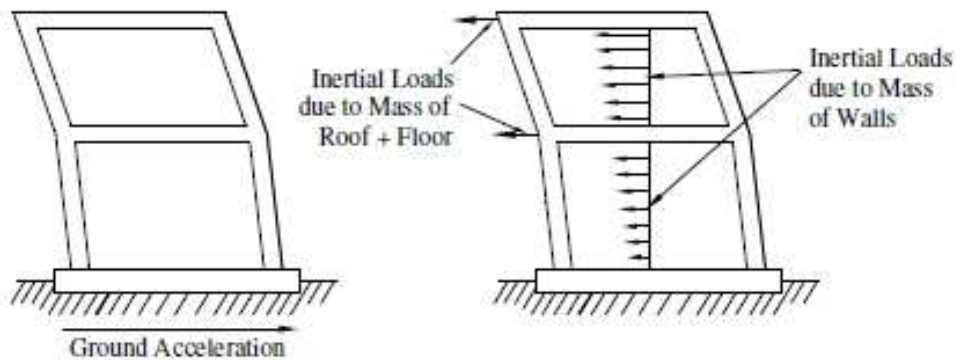
Figure 8 Idealization of earthquake demands [10]

We have to underline that the magnitude and direction of seismic loads continually change during the seismic event. In seismic design have to be determine the maximum demands in each direction and designing the structure to resists them.

The equivalent lateral force visualization of earthquake loads will be used to explain how a confined masonry structure transmits earthquake forces to the foundation. Referring to Figure 5 below, the inertial forces on a CM building are concentrated where most of the mass is: at the floor and roof levels, and in the masonry walls themselves. The red arrows show the inertial forces on each component applied to the component's center of mass, the blue arrows illustrate how the inertial forces transfer to supporting elements, and the green arrows represent forces on components transferred from other components [10].

"In-Plane Cyclic Behavior of Substandard Confined Masonry: Full-Scale Experiments, Finite-Element Modeling and Incremental Dynamic Analysis"

Chapter 1
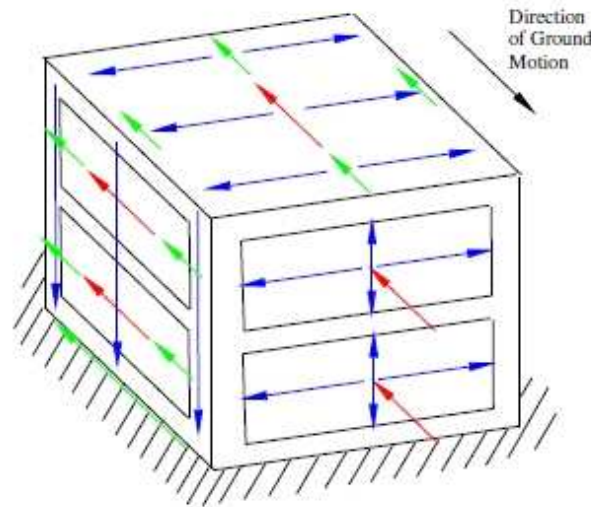
Figure 9 Inertial Loads in CM [10]

Analyzing the members of the simple structures in figure 5, it is possible to understand that the masonry walls perpendicular to the direction of shaking are much weaker and more flexible than the wall parallel to the direction of shaking. So these elements transfer their inertial forces to the much stiffer elements bordering the walls. The roof and the floor transmit the inertial forces from their own mass, along with the forces transferred to them from the walls perpendicular to the direction of shaking, to the walls parallel to the direction of shaking. To do so, roofs and floors deform in plane (since all deformations are parallel to the plane of the roof or floor) as a diaphragm, and as a result, are referred to as diaphragm elements. The walls parallel to the direction of shaking have the responsibility of transferring inertial forces from their own mass, the diaphragms and the walls perpendicular to shaking down to the foundation, where it is transmitted to the surrounding soil. These walls perform this function by deforming in-plane in shear and bending (second mode).

1.2.4 Seismic Design

In reference to the Italian Code NTC2008 and American Code ASCE 7, the seismic design it is related to the seismic behavior of the structure we want to design.

In other words the point it is if the structure can dissipate energy or not.

If the structure can't dissipate energy we have to design in an linear-elastic way, in which the design load it is the linear-elastic load that come from the analysis. In the other case, it is possible to reduce

"In-Plane Cyclic Behavior of Substandard Confined Masonry: Full-Scale Experiments, Finite-Element Modeling and Incremental Dynamic Analysis"

Chapter 1

the response spectrum of the structure and design it with a less load instead of the elastic load, reducing the cost of the structure.

As an example it is shown in figure 10 a diagram in which it is clear the difference between design in linear-elastic hypothesis or design with an elastic-plastic behavior:
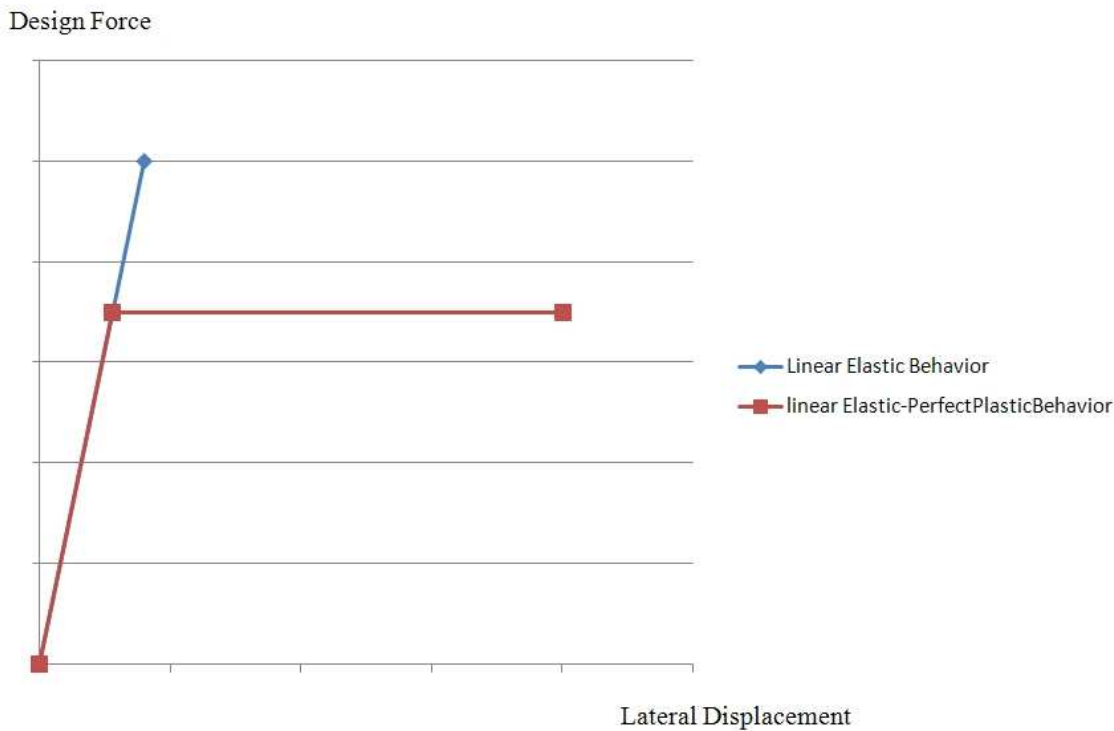
Figure 10 Elastic Behavior vs Elastic-Plastic Behavior

Seismic codes are developed with the intent of ensuring serviceability requirements during frequent moderate earthquakes and life safety during a major earthquake. Therefore, in the latter case extensive damage to the structure may be acceptable so long as collapse is prevented.

Design seismic forces are obtained by reducing a linear elastic response spectra by a response modification factor R (Ve/V)[9] or using q (structure factor) [8] and member forces are determined through linear elastic analysis[12].

In addition, a displacement amplification factor C_d is used to compute the expected maximum inelastic displacement from the elastic displacement induced by the seismic design forces.

"In-Plane Cyclic Behavior of Substandard Confined Masonry: Full-Scale Experiments, Finite-Element Modeling and Incremental Dynamic Analysis"

Chapter 1

Figure 11 Seismic Performance Factor described by NEHRP

Usually R and C_d recommended by the codes depend on the period of the structure, the structural system type and the structural ductility.

1.2.5 Numerical Modeling

The different techniques proposed in the literature for idealizing this structural type can be divided into two groups, namely, local or micro-models and simplified or macro-models. The first group involves the models in which the structure is divided into numerous elements to take account of the local effects in detail, whereas the second group includes simplified models based on a physical understanding of the behavior of the CM wall. In the later case, a few elements are used to represent the effect of the element as a whole. It is evident from experimental observations that these structures exhibit a highly nonlinear elastic behavior, and the most important factors contributing to the non linear behavior arise from material non linearity. These factors can be summarized as follows:

- Infill Panel: cracking and crushing of the masonry, stiffness and strength degradation.
- Surrounding Frame: cracking of the concrete, yielding of he reinforcing bars, local bond slip.
- Panel-Frame Interfaces: degradation of the bond –friction mechanism, variation of the contact length.

"In-Plane Cyclic Behavior of Substandard Confined Masonry: Full-Scale Experiments, Finite-Element Modeling and Incremental Dynamic Analysis"

Chapter 1

After the considerations done before, and a comprehensive literature review, the seismic behavior of Confined Masonry structures it is modeled through macro modeling in which it was supposed that the wall under seismic action will act with a strut and tie mechanism whit considering also the friction between the masonry units. Figure 10 illustrate it.
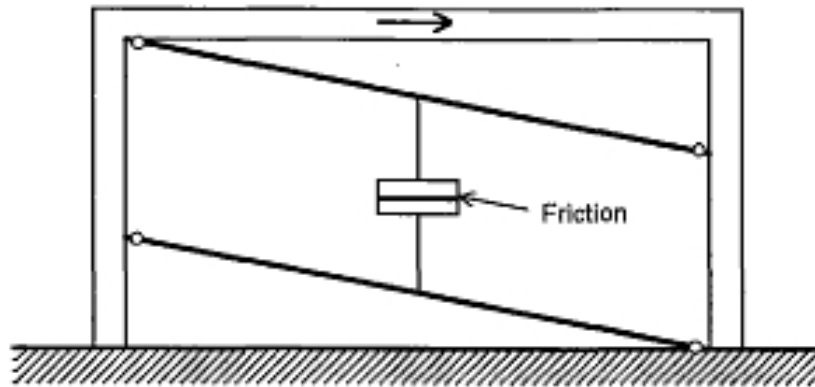
Figure 8 CM Modeling

The diagonal strut model is widely accepted as a simple and rational way to describe the influence of the masonry inside the frame.

"In-Plane Cyclic Behavior of Substandard Confined Masonry: Full-Scale Experiments, Finite-Element Modeling and Incremental Dynamic Analysis"

Chapter 2

2. Mechanical Characterization of the Materials

2.1 Introduction

In order to investigate the materials, design and construction practice that result in substandard confined masonry structures, a comprehensive literature review was done.

In Confined Masonry, as we explained before, we have an unreinforced masonry wall panel surrounded by horizontal and vertical "confining" members called bond beams and tie columns. The masonry wall panel consists of units bonded with mortar and confining elements constructed of reinforced concrete (RC). In some cases the units in a masonry walls are toothed at tie column locations to create better interlock between the wall and tie column. In a CM system, the masonry wall panel assume the role to transmit all lateral and gravity loads to the buildings foundation. The bond beams and tie columns work to hold the wall together under earthquake. The RC confining elements improve the connections between wall-roof-floor enabling the structure to better act together as a unit during a seismic event, that it is what we call box behaviour, that it is really important to make the structure able to resist a lateral action.

The important features in CM structures are the materials quality and the detailing used in the design as shown in Figure 11.
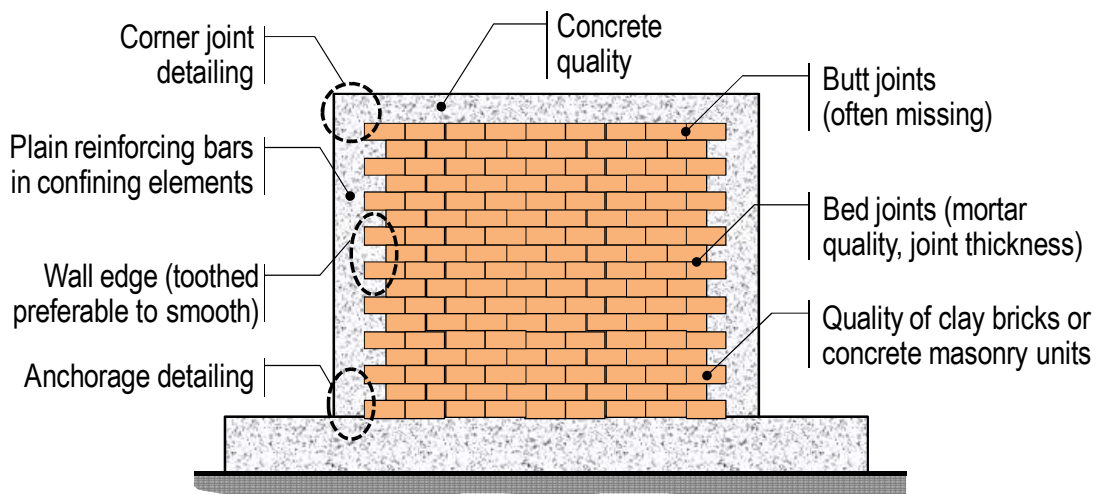
Figure 11 Typical Design and construction practice

"In-Plane Cyclic Behavior of Substandard Confined Masonry: Full-Scale Experiments, Finite-Element Modeling and Incremental Dynamic Analysis"

Chapter 2

2.2 Specimens Dimensions and material (Walls, Units, Mortar, Frame)

Confined masonry walls are made of units, "confining" elements and bonding materials like mortar. What we want to do now it is to define what are the standard dimensions and typologies of material used in substandard CM walls to define a full scale specimen that can represent the real physical behavior of that element. The point was to design a test that was able objectively to represent this type of construction, characterized from a really substandard materials and also design approach, using a restrict number of specimens.

2.2.1 Wall Dimensions

The height of the walls is inside a range between 2.20-2.50 m (7.2-8.2 ft). The length between 2-4 m (6.2-13 ft). The column depth is usually equal to the wall thickness, between 15-20 cm (6-8 in). The depth of the confining beam varies between a range of 20-25 cm (8-10 in), and its width between 15-20 cm (6-8 in) in function of the wall thickness.

2.2.2 Blocks (Units)

There are a lot of masonry units that are used in CM. We can divide them in respect to the materials, geometry and distribution of cores. We can have concrete blocks, solid concrete bricks, clay blocks and clay bricks (each one solid or hollow). The most common are hollow concrete blocks with a net area about 55%-60% of the gross cross section. They are also typically made near the construction site, and that means that the choose of the materials it is correlated to the materials they have.
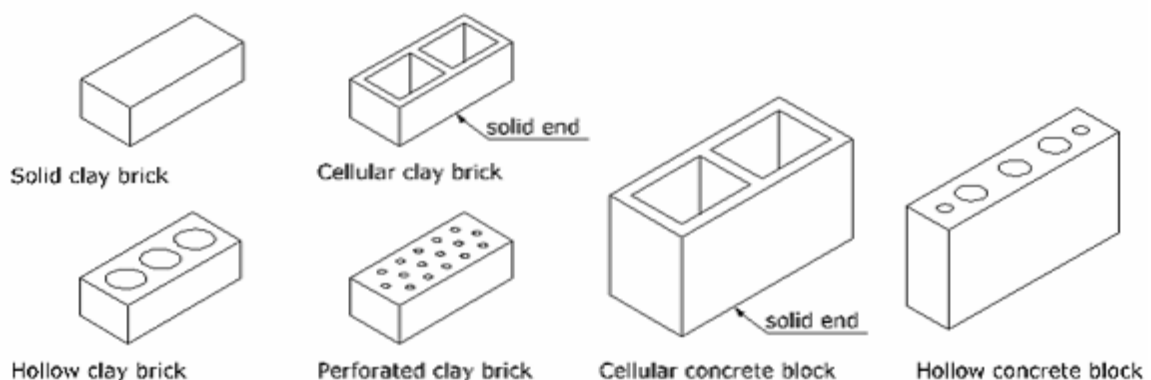
Figure 12 Types of masonry units [2]

"In-Plane Cyclic Behavior of Substandard Confined Masonry: Full-Scale Experiments, Finite-Element Modeling and Incremental Dynamic Analysis"

Chapter 2

Below there is a table in which we can see the strength of the different types of units.

Table 1 Strentgh in masonry units [14]

Type of masonry unit	class	σ'_{PKm} Kg/cm²	σ'_{PK} Kg/cm²	Net section
Solid clay brick	A	120	80	>80% gross section
Solid clay brick	B	75	45	>80% gross section
Hollow clay block	A	120	85	>60% gross section
Hollow clay block	B	75	50	>40% gross section
Hollow concrete block	I	65	45	>40% gross section
Hollow concrete block	II	65	45	>40% gross section
Hollow concrete block	III	50	30	>40% gross section

2.2.3 Mortar

Portland cement and lime mortar are the most used. Their compressive strength ranging between 5-10 MPa (730-1450 psi). The bed joints thickness varies between 1-2.5 cm (0.375-1.0 in). For the builders the head joints are not considered important so their thickness change between 0-1 cm (0-0.375 in).

Figure 1 Thick of mortar bed joints

"In-Plane Cyclic Behavior of Substandard Confined Masonry: Full-Scale Experiments, Finite-Element Modeling and Incremental Dynamic Analysis"

Chapter 2

2.2.4 Concrete

The concrete it is casted in place, so it isn't typically compacted. The use of round and smooth aggregates in conjunction with smooth bars and ties determine the presence of large voids and poor bond with the steel. The compressive strength of typical substandard concrete varies between 8-12 Mpa (1150-1750psi).

The poor compression strength in units, mortar and concrete is due to lower quantity of filler. As we can see to the below figures, poor materials used in confined masonries are combined with no accuracy to the design details.

Figure 12 Unconsolidated concrete at the interface with masonry

Figure 13 Lack of bond

"In-Plane Cyclic Behavior of Substandard Confined Masonry: Full-Scale Experiments, Finite-Element Modeling and Incremental Dynamic Analysis"

Chapter 2
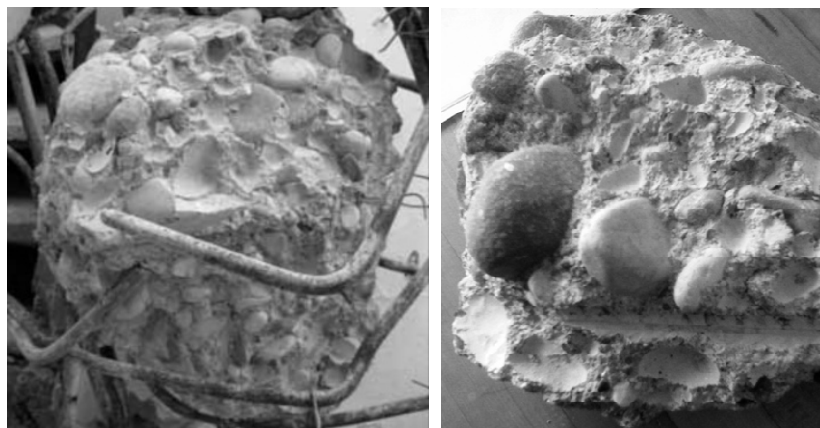
2.2.5 Steel Reinforcement

The longitudinal reinforcement of beams and pillars typically consist in four bars with a tensile strength of about 280-420 Mpa (40610-61000 psi). The ties are smooth bar equally spaced with no decrease in spacing at the column or beam and no bends.

(a)   (b)

(c)   (d)   (e)

In fact, as we can see from picture (a) and (b) they made open stirrups with large spacing between steel tie, and not deformed steel bars (picture d-e) it inducing buckling of the longitudinal bars and failure mechanisms of the walls.

"In-Plane Cyclic Behavior of Substandard Confined Masonry: Full-Scale Experiments, Finite-Element Modeling and Incremental Dynamic Analysis"

Chapter 2

2.3 Mechanical Characterization of the Materials

As we explain before, the goal of the first part of the work was to be able to design and construct a limited number of full scale specimens that were able to represent what is done in common practice of building CM structures. Once defined from the literature review what were the range of dimension and strength of the constituents, we started to produce them. In order to characterize the mechanical properties and define the constitutive models of the materials used, following the American Codes [9], the following experiments were performed.

2.3.1 Compression Test on single blocks (ASTM C140)

To define the compressive strength of the concrete units six tests were carried out.

A single block was instrumented with four 0.5 cm (0.2 in) displacement transducers, one strain gage and one 445 kN (100 Kip) load cell. In figure 14 it is illustrated the test.

Figure 14 Test Set Up

"In-Plane Cyclic Behavior of Substandard Confined Masonry: Full-Scale Experiments, Finite-Element Modeling and Incremental Dynamic Analysis"

Chapter 2
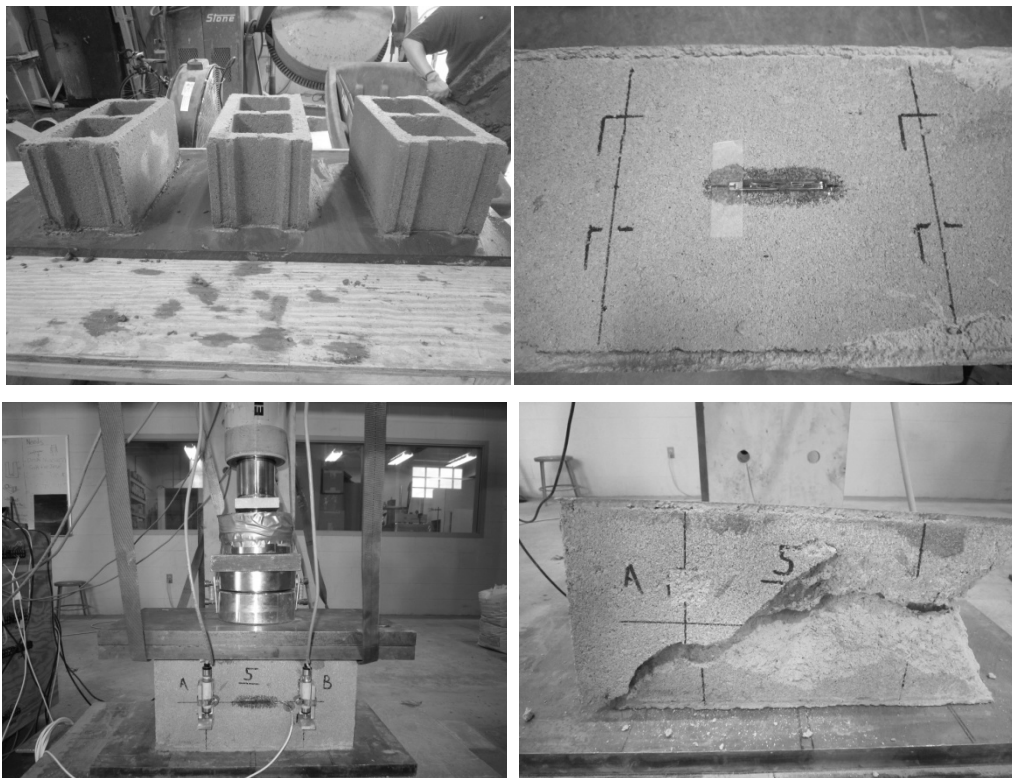
Below the average results are reported. The net cross section area is 39141.21204 mm^2.

Table 2 ASTM C140 Results

Specimen	Comp. Strength (MPa) on net area	Modulus of Elasticity (MPa)	Poisson's ratio
Block #1	7.37	4670.70	-
Block #2	6.97	4390.40	-
Block #3	6.82	6874.80	-
Block #4	7.38	5493.30	0.87
Block #5	7.59	6128.00	0.62
Block #6	7.01	7077.50	0.77
Average	**7.19**	**5772.45**	**0.75**
stdev	0.30	1117.73	
COV %	**4.164**	**19.363**	

2.3.2 Compression Test on two-block prisms (ASTM C1314)

Three tests were carried out on two-blocks prisms instrumented with four vertical 0.5 cm (2in) displacement transducers, two horizontal 0.5 cm (0.2 in) displacement transducers and one 445 kN (100 kip) load cell.

Figure 15 Test Instrumentation

"In-Plane Cyclic Behavior of Substandard Confined Masonry: Full-Scale Experiments, Finite-Element Modeling and Incremental Dynamic Analysis"

Chapter 2

Average results are reported in table 3.

Table 3 ASTM C1314

Specimen	Comp. Strength (MPa) on net area	Modulus of Elasticity (MPa)	Poisson's ratio
Prism #1	7.37	10985	0.779
Prism #2	6.97	13241	1.104
Prism #3	6.82	9670.5	1.058
Average	**7.05**	**11298.83**	**0.980**

2.3.3 Compression Test on concrete cylinders (ASTM C39)

This test was very important to know if the cement used to cast bond beams and tie column was representative of what often used in developing areas. Six concrete cylinders 10x20 cm (4x8 in) with a cross section of 8107.08056 mm^2 were taken from each wall.

Table 4 Wall 1 ASTM C39

Specimen	Comp. Strength (MPa)	Modulus of Elasticity (GPa)
Wall 1-1	9.13	12.53
Wall 1-2	11.78	11.14
Wall 1-3	9.38	11.18
Wall 1-4	11.85	11.67
Wall 1-5	12.34	9.43
Wall 1-6	9.10	12.49
Average	**10.60**	**11.41**
stdev	1.54	1.15
COV %	**14.564**	**10.039**

"In-Plane Cyclic Behavior of Substandard Confined Masonry: Full-Scale Experiments, Finite-Element Modeling and Incremental Dynamic Analysis"

Chapter 2

Table 5 Wall 2 ASTM C39

Specimen	Comp. Strength (MPa)	Modulus of Elasticity (GPa)
Wall 2-1	13.25	14.51
Wall 2-2	14.33	15.17
Wall 2-3	12.03	12.68
Wall 2-4	12.98	14.69
Wall 2-5	12.78	14.83
Wall 2-6	13.95	11.49
Average	**13.00**	**13.64**
stdev	0.70	1.49
COV %	**5.368**	**10.906**

Table 6 Wall 3 ASTM C39

Specimen	Comp. Strength (MPa)	Modulus of Elasticity (GPa)
Wall 3-1	12.43	14.57
Wall 3-2	12.50	12.66
Wall 3-3	13.40	14.38
Average	**12.78**	**13.87**

2.3.4 Compression test on mortar cylinders (ASTM C109)

Six tests were carried out on mortar cylinders sampled during the construction of walls and instrumented with three vertical 0.5 cm (0.2in) displacement transducers and tested in a 0.14 MPa (20 psi) load cell. The specimens dimensions were 7.5x15 cm (3x6 in).

"In-Plane Cyclic Behavior of Substandard Confined Masonry: Full-Scale Experiments, Finite-Element Modeling and Incremental Dynamic Analysis"

Chapter 2

Table 7 ASTM C 109

Specimen	Comp. Strength (MPa)	Modulus of Elasticity (GPa)
Type N #1	8.513	11.050
Type N #2	9.575	12.076
Type N #3	8.075	12.251
Type N #4	7.459	-
Type N #5	7.599	-
Type N #6	7.537	10.692
Type N #7	9.690	12.751
Type N #8	8.293	10.444
Average	**8.34**	**11.54**
stdev	0.88	0.94
COV %	**10.547**	**8.144**

2.3.5 Flexural test on blocks and mortar prisms (ASTM C348)

Three point bending test was used to define the flexural strength of mortar and blocks.

Table 8 ASTM C348 Blocks Prisms

Specimen	Flexural Strength (MPa)	Flexural Strength (psi)
#1	1.63	236.85
#2	1.83	265.52
#3	1.61	233.15
#4	1.53	221.72
#5	1.81	262.37
#6	1.82	263.33
Average	**1.70**	**247.16**
stdev	0.13	18.87
COV %	**7.634**	**7.634**

"In-Plane Cyclic Behavior of Substandard Confined Masonry: Full-Scale Experiments, Finite-Element Modeling and Incremental Dynamic Analysis"

Chapter 2

Table 9 ASTM C348 Mortar Prisms

Specimen	Flexural Strength (MPa)	Flexural Strength (psi)
CM #1	6.23	903.81
CM #2	6.15	892.37
CM #3	6.97	1011.12
CM #4	6.62	960.14
CM #5	6.61	959.01
CM #6	5.80	840.78
Average	**6.40**	**927.87**
stdev	0.42	60.61
COV %	**6.532**	**6.532**

2.3.6 Shear tests on mortar joints (BS EN 1052-3:2003)

This test was performed with three units of CM under three different precompression levels to define the cohesion and friction coefficient of the mortar joints.


Figure 16 Test Set Up

"In-Plane Cyclic Behavior of Substandard Confined Masonry: Full-Scale Experiments, Finite-Element Modeling and Incremental Dynamic Analysis"

Chapter 2
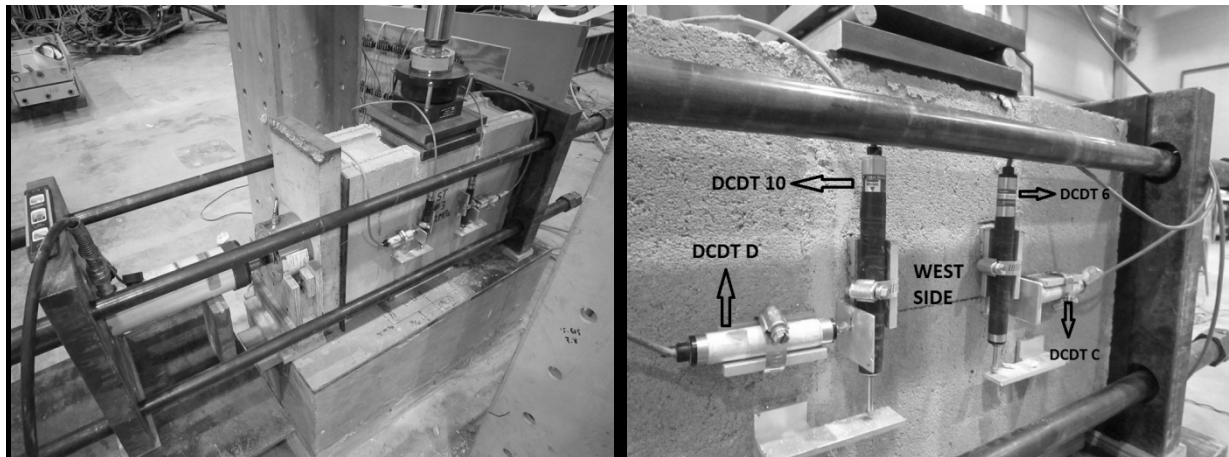
Table 10 BS EN 1052-3:2003

	Compressive Stress (MPa)			
Precompression (MPa)	**0.1**	**0.2**	**0.3**	**0.5**
Shear Stress (MPa)	0.153	0.276	0.370	0.430
	0.167	0.307	0.378	-
	0.186	0.298	0.387	-
Average	**0.169**	**0.294**	**0.378**	**0.430**

2.3.7 Flexural test on mortar joints (ASTM E754)

Four point bending tests in five seven-blocks specimens were carried out to obtain the modulus of rupture of masonry.

Table 11 ASTM E754

Specimen	Modulus of rupture (MPa)	Modulus of rupture (psi)
Prism #1	0.16	23.24
Prism #2	0.16	22.98
Prism #3	0.21	30.60
Prism #4	0.19	27.52
Prism #5	0.10	14.25
Average	**0.18**	**26.08**
stdev	0.03	3.66
COV %	**14.029**	**14.029**

"In-Plane Cyclic Behavior of Substandard Confined Masonry: Full-Scale Experiments, Finite-Element Modeling and Incremental Dynamic Analysis"

Chapter 2

2.3.8 Compression test on small masonry walls (BS EN 1052-1:1999)

To have a better idea about the compression behavior of masonry, compression tests on small walls were conducted. The smalls walls were built with ten masonries units and instrumented with two vertical 10 cm (4in) potentiometers, one 5 cm (2in) horizontal displacement transducers one 445 kN (100 kip) load cell and one pressure transducer to measure the maximum vertical load and pressure. The results are on line with the average of substandard confined masonry units.

Table 12 BS EN 1052-1:1999

Specimen	Comp. Strength (MPa) on net area	Modulus of Elasticity (GPa)
Wall #1	4.52	7.359
Wall #2	3.69	8.179
Wall #3	4.71	7.621
Average	**4.31**	**7.72**

"In-Plane Cyclic Behavior of Substandard Confined Masonry: Full-Scale Experiments, Finite-Element Modeling and Incremental Dynamic Analysis"

Chapter 3

3. Experimental Program

The experimental program was intended to define the in-plane behaviour of Confined Masonry walls subject to a cyclic displacement. The goal was to make a test that was able to represent objectively this type of technique, characterized from highly substandard materials and design approach, using a restrict number of specimens. Once defined the constituents properties and sure that were inside substandard range, three types of confined masonry walls were designed, built and tested.
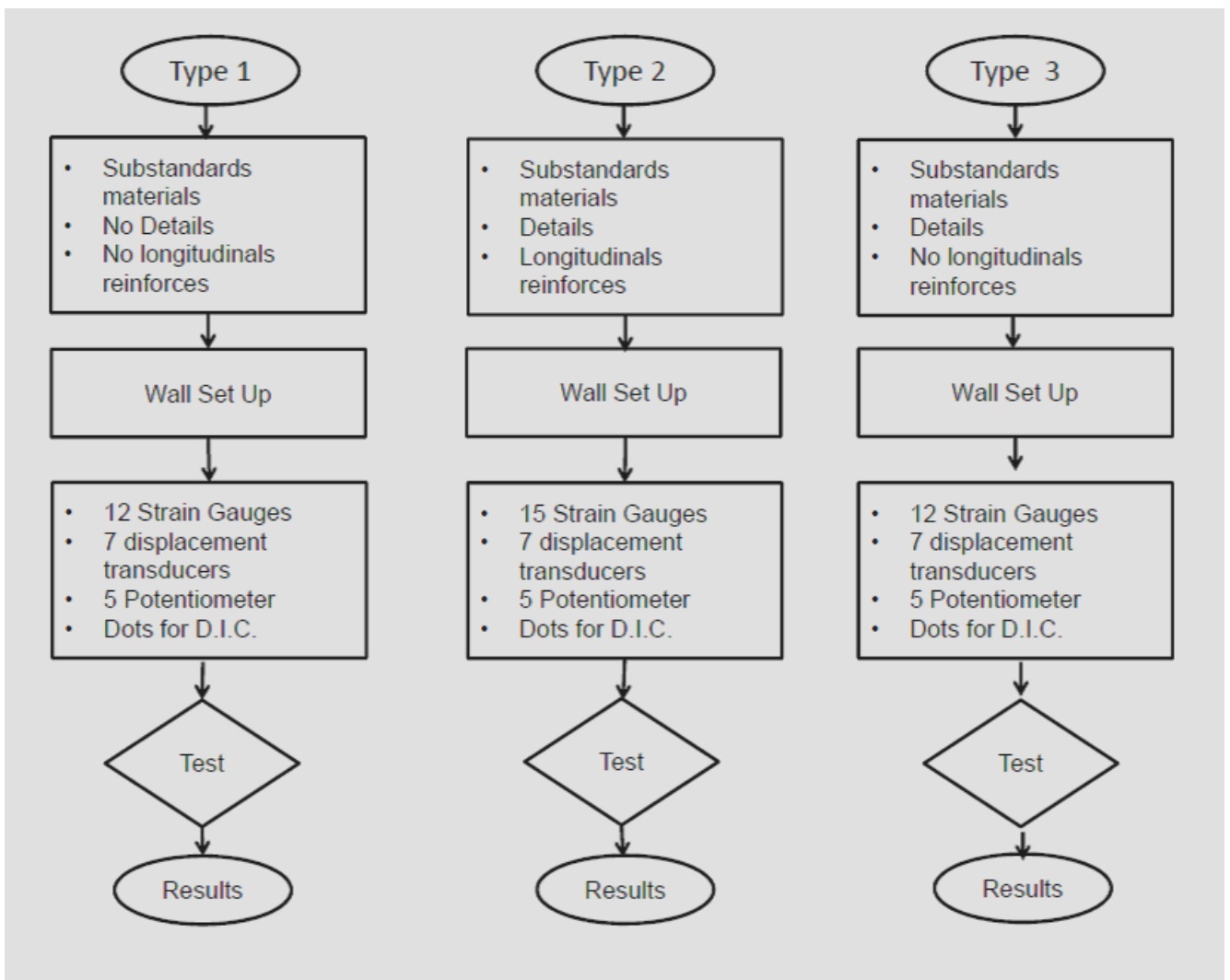
Figure 17 Experimental Program

"In-Plane Cyclic Behavior of Substandard Confined Masonry: Full-Scale Experiments, Finite-Element Modeling and Incremental Dynamic Analysis"

Chapter 3

Below in figure 18 it is illustrated the scheme for shear compression test of cantilever wall. The benchmark from where it is started the test design:
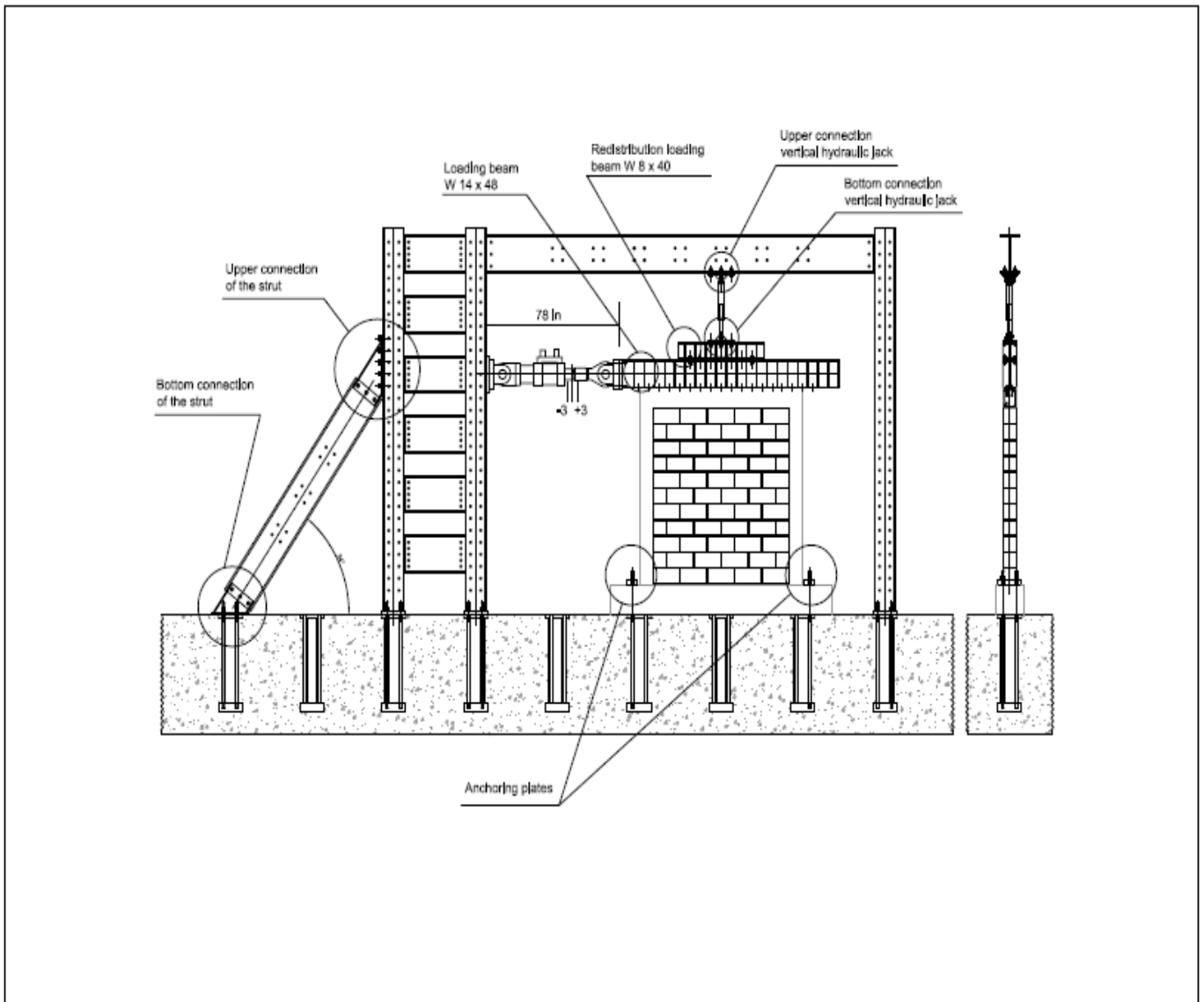
Figure 18 Example of the Test Scheme

3.1 Test set up, instrumentations and procedure

Three Confined Masonry walls made of 40x20 cm (15.625x7.625 in) concrete blocks, cement mortar and reinforced concrete frame were built. They were designed to contain inside strain gauges, potentiometers, displace transducers and a side was treated with white cement paint to contain dots for digital image correlation.

The dimensions of the three specimens were 250x243x20 cm (98x95.625x7.625 in).

"In-Plane Cyclic Behavior of Substandard Confined Masonry: Full-Scale Experiments, Finite-Element Modeling and Incremental Dynamic Analysis"

Chapter 3
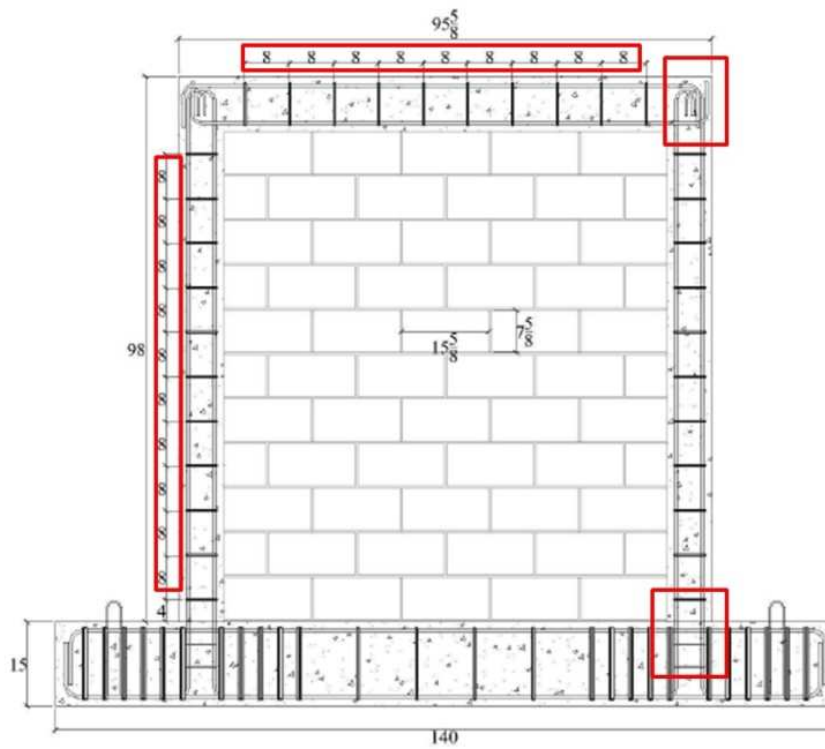
Figure 19 Type 1 No Detail
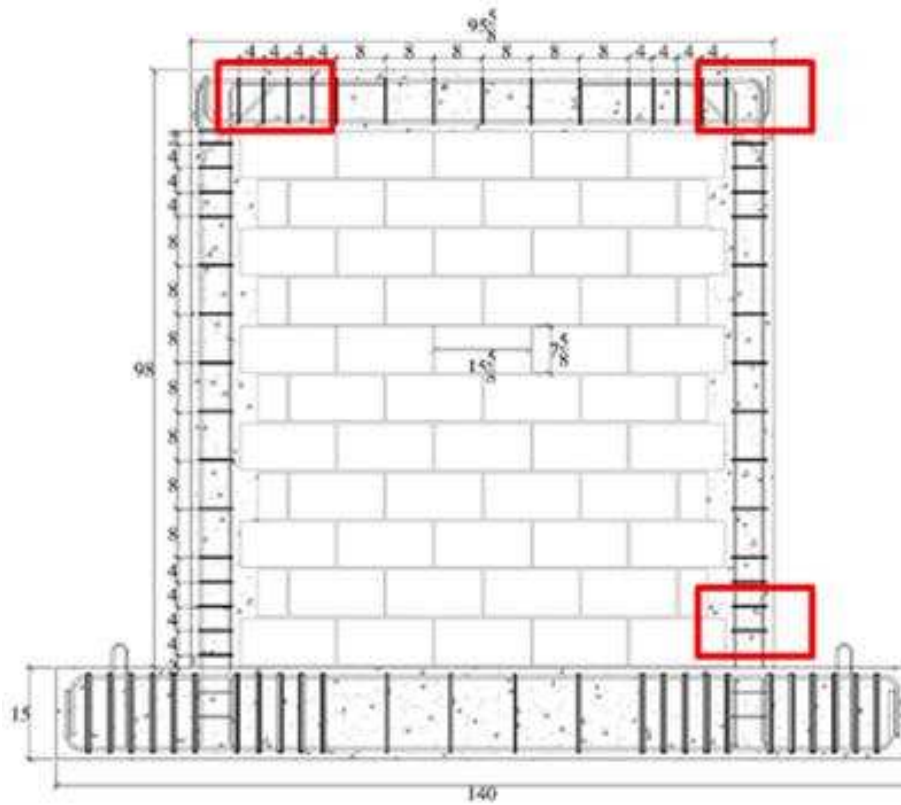
Figure 20 Type 2-3 in evidence the engineering details

"In-Plane Cyclic Behavior of Substandard Confined Masonry: Full-Scale Experiments, Finite-Element Modeling and Incremental Dynamic Analysis"

Chapter 3

As it is underlined in figure 19, type one specimen represent a lack of engineering knowledge like anchorage length and distance between tie bars .

That specimen was instrumented with twelve strain gauges, seven displacement transducers and five potentiometers.

Figure 21 shows the instruments positions:
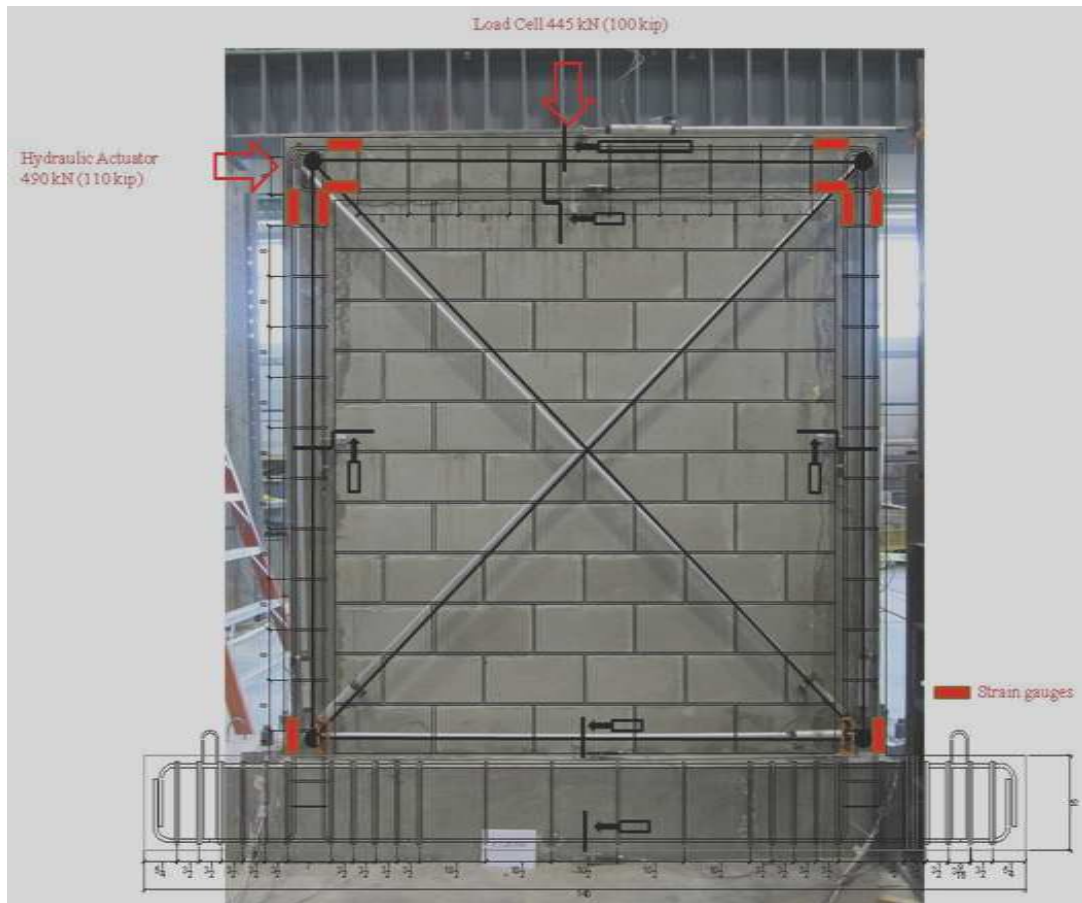
Figure 21 Set Up Type 1 Specimen

Type one specimen was used as benchmark specimen.

Below in figures 22 (a) and (b) represent respectively the set up for type two and type three specimens.

Type two specimen was retrofitted using longitudinal aluminum bars with the scope to increase the wall confinement and consequentially the system strength. It was instrumented with seven displacement transducers, five potentiometers and additional strain gauges to measure the aluminum strain.

"In-Plane Cyclic Behavior of Substandard Confined Masonry: Full-Scale Experiments, Finite-Element Modeling and Incremental Dynamic Analysis"

Chapter 3

Type three wall represented the same physical conditions of the type one but with engineering details. It is a good way to start building in growing countries subject of seismic hazard. Figures 24 shows the other side of specimens that was prepared for the digital image correlation.
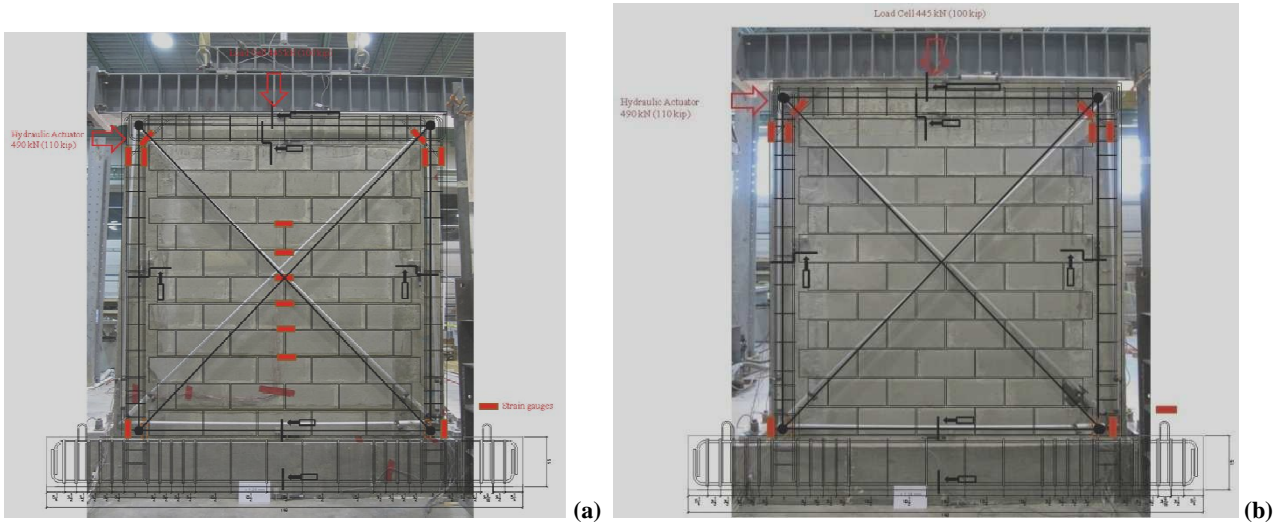

Figure 22 (a) Type two (b) Type three
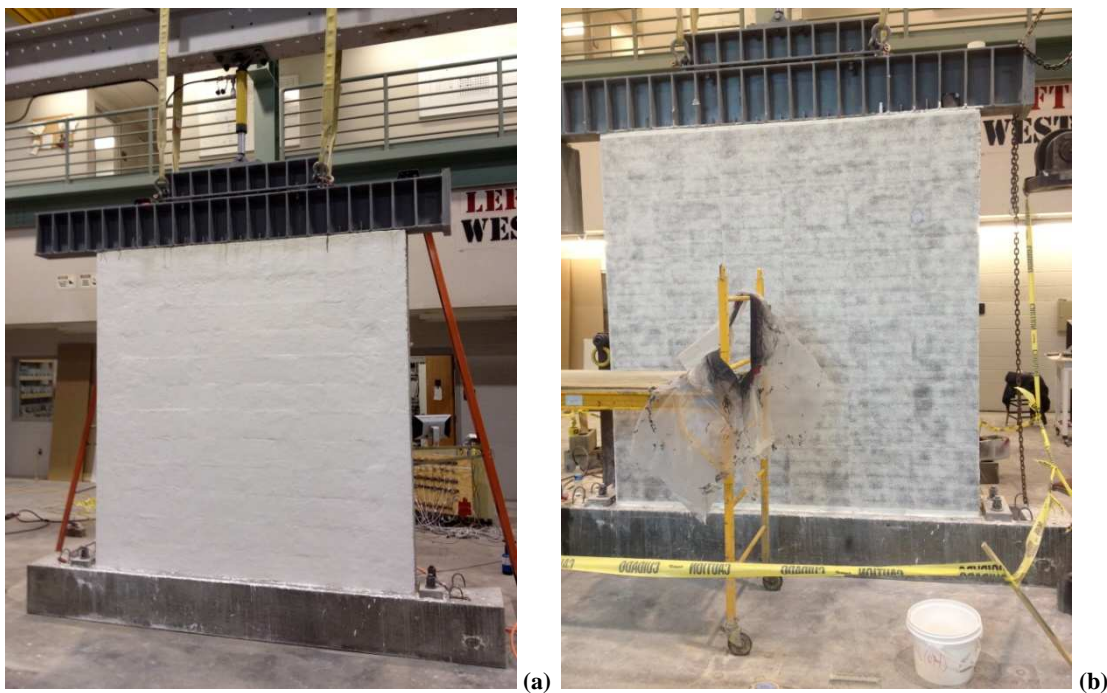
Figure 23 (a) Painted (b) Ready for DIC

3.2 In-Plane Cyclic Shear-Compression Tests

Three specimens for evaluating the seismic behavior of Confined Masonry walls were sized 250x243x20 cm (98x95.625x7.625 in) and tested under cyclic load.

"In-Plane Cyclic Behavior of Substandard Confined Masonry: Full-Scale Experiments, Finite-Element Modeling and Incremental Dynamic Analysis"

Chapter 3

Confined masonry walls were tested with a cantilever-type boundary condition, with fixed base and top end free to rotate, by applying centered and constant vertical load of 90 kN given from 445kN (100 kip) load cell to obtain the shear type failure mode. Horizontal cyclic displacements, with increasing amplitude and the presence of four plateau used to take pictures for the digital image correlation were applied. Figure 24 a and b represent the applied load, choosen from [3].
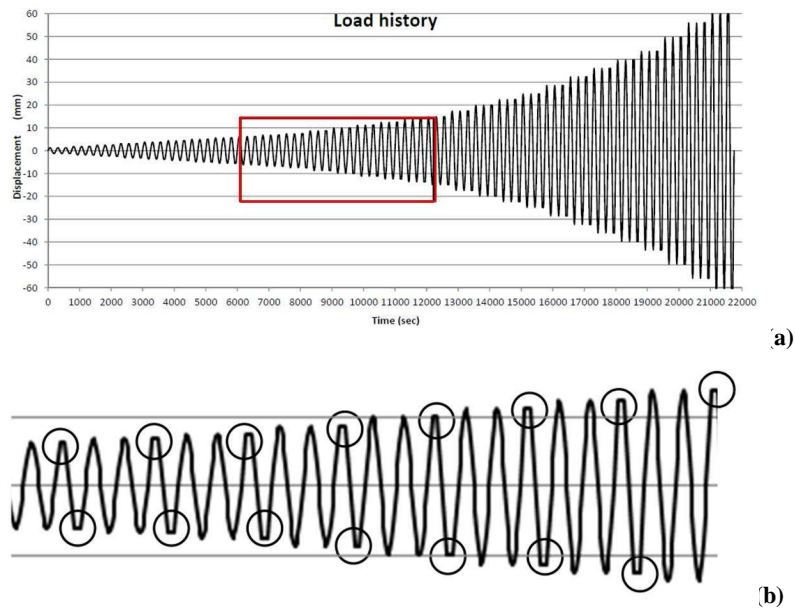
Figure 24 (a) Load History (b) Plateau for DIC

During in-plane cyclic tests, the confined masonry walls attained three main limit states, which were used to idealize observed behavior. At first, specimens responses were linear elastic, with similar stiffness values. When sliding mechanism occurs, it causes the development of horizontal cracks and the masonry's behavior changes and it starts working as strut and tie. At this point, the base shear continues to increase until the yielding point. From this point, with the increasing of cracks' dimensions, the strut area starts decreasing with the base shear until the ultimate displacement.

3.3 Experimental results

Plotting the lateral force versus the lateral displacement relative to the mid-span of the tie beam (control point), are obtained the hysteretic force-displacement diagrams for each tested specimens.

"In-Plane Cyclic Behavior of Substandard Confined Masonry: Full-Scale Experiments, Finite-Element Modeling and Incremental Dynamic Analysis"

Chapter 3

In figure 25 are plotted the three diagrams, from which it is possible to analyze the structural behavior of the walls including initial stiffness, change of CM walls behavior with relative decreasing of stiffness due to the damage, shear forces and associated deformations and overall deformability. Form figure 25 it is evident that improving the detailing the average lateral force and the average displacement capacity increase considerably.
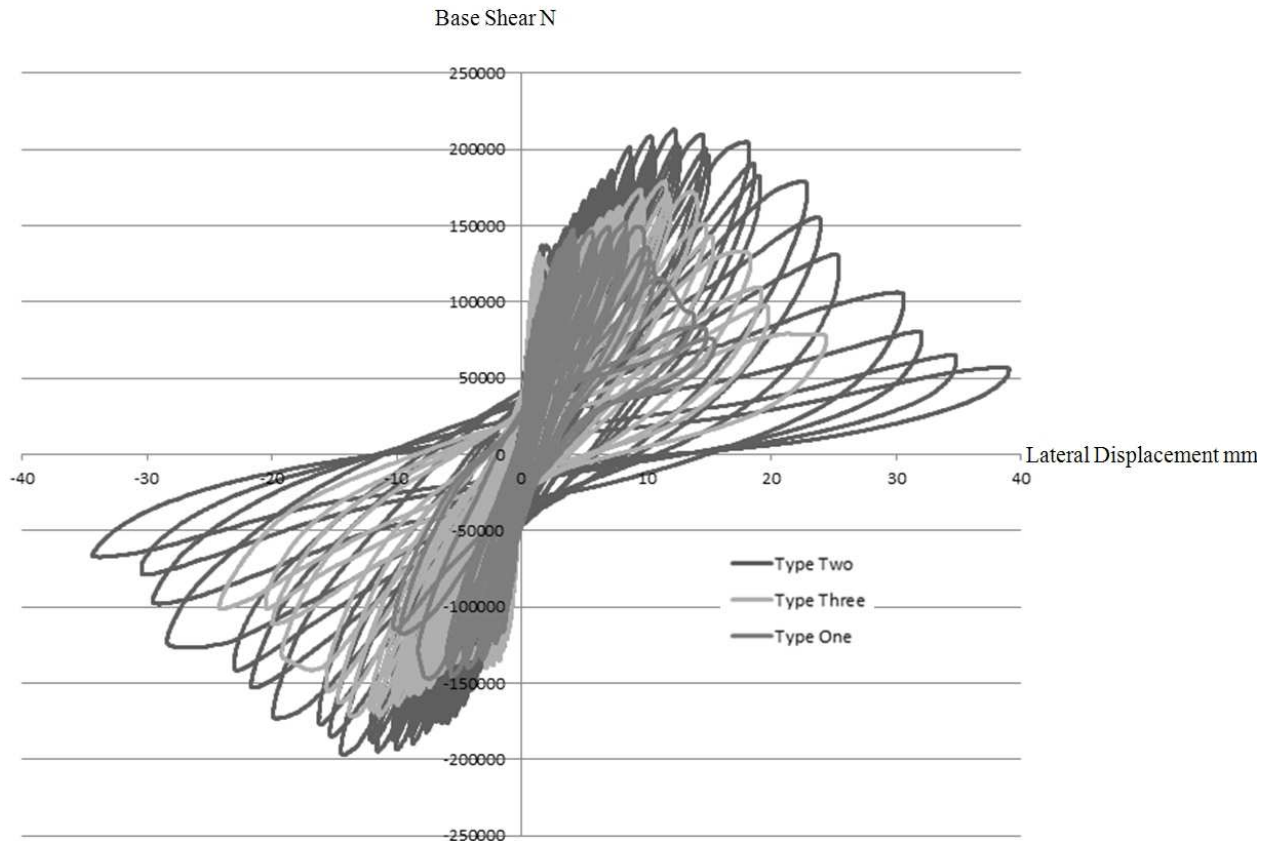
Figure 25 Hysteretic Force-Displacement Diagram

In respect to the effect of longitudinal aluminum strips the average lateral force capacity increases by 40% and the average lateral displacement by 180%.

Have to been underline that the seismic response of buildings is related not only to strength and displacement capacity (members ductility), but also to typical parameters of cyclic behavior such as energy dissipation capacity, stiffness degradation and viscous damping coefficient, according to damage propagation.

To completely understand the tests results, with the help of a simple Matlab script, are also illustrate in figure 26 the positive and negative peaks of each load cycle for the three specimens tested.

"In-Plane Cyclic Behavior of Substandard Confined Masonry: Full-Scale Experiments, Finite-Element Modeling and Incremental Dynamic Analysis"

Chapter 3
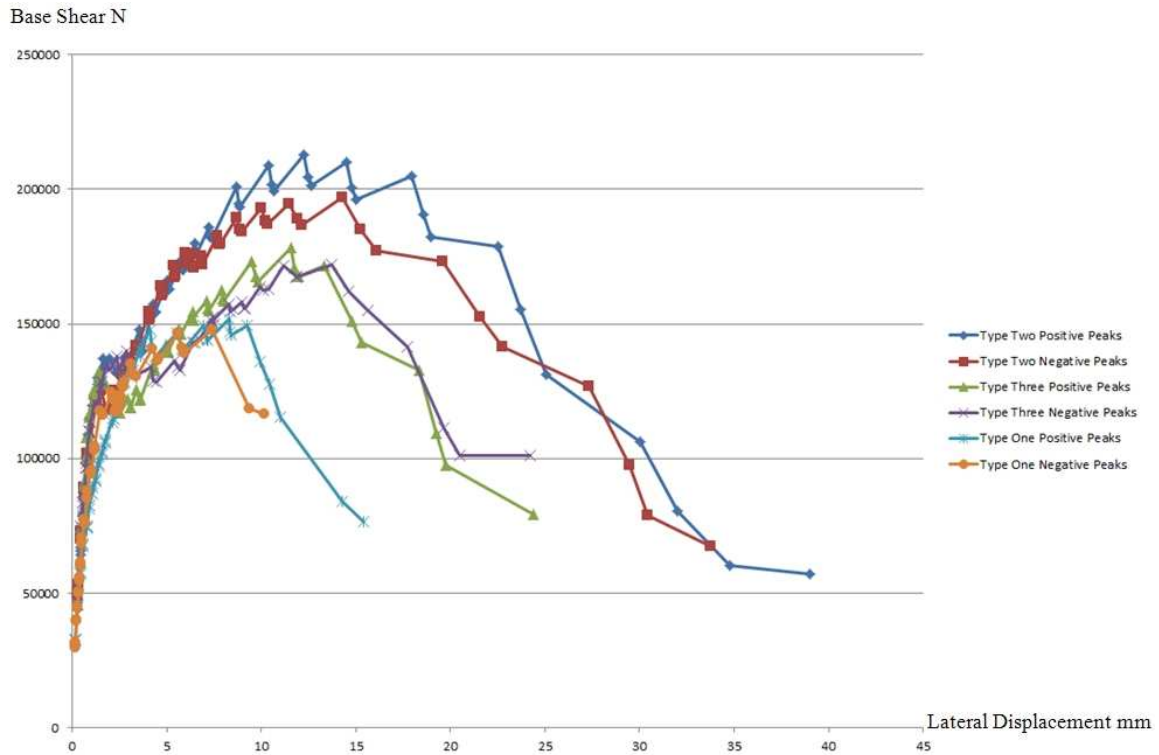
Figure 26 Peacks Diagram

Negative and positive peaks are plotted in the same quadrant, because in that way it is possible to evaluate for first how the test was done, in fact the two curve have to be almost the same. In that particular case, the discrepancies between the type One curves are due to a local failure mechanism that happened at the top right corner as shown in figure 27, where it was formed an hinge.
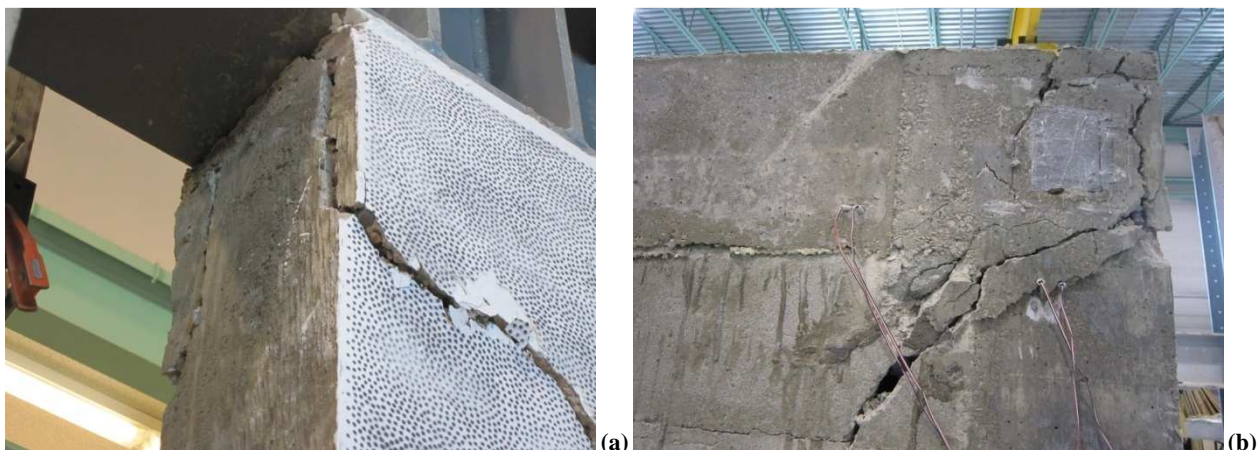
Figure 27 Corner hinge (a) DIC side (b) Instrumented side

Below will be illustrate the Digital Image Correlation Results and the cracks pattern for each specimens with the scope to lay the bases for the numerical modeling Hypothesis.

"In-Plane Cyclic Behavior of Substandard Confined Masonry: Full-Scale Experiments, Finite-Element Modeling and Incremental Dynamic Analysis"

Chapter 3

3.4 Digital Image Correlation results and Crack Pattern

Three Digital image correlation test were carried out. Two 5 Megapixel camera and one computer were used to do it. This analysis technique permits to define the strain field and so to solve the mechanicals laws directly.

Below it is reported the algorithm used in DIC analysis.
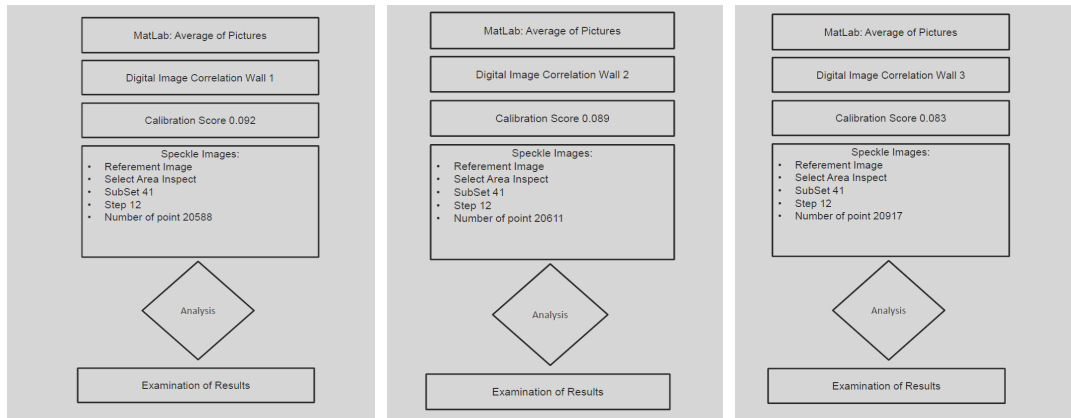
Figure 28 DIC Algorithm

Once defined what is the way to obtain the results, the really important aspect of this type of analysis it is that is possible to see how and where the strain is localized. In that side, it took a really important weight to define the behavior under cyclic load of each specimen.

As is shown in figure 29, it is clear that CM walls, with the rising of the first cracks, starts having a strut and tie behavior. The wall's diagrams are referred to exx1 that represent the strain in the x-direction. Hot range color indicate tension, cold range color compression.

"In-Plane Cyclic Behavior of Substandard Confined Masonry: Full-Scale Experiments, Finite-Element Modeling and Incremental Dynamic Analysis"

Chapter 3
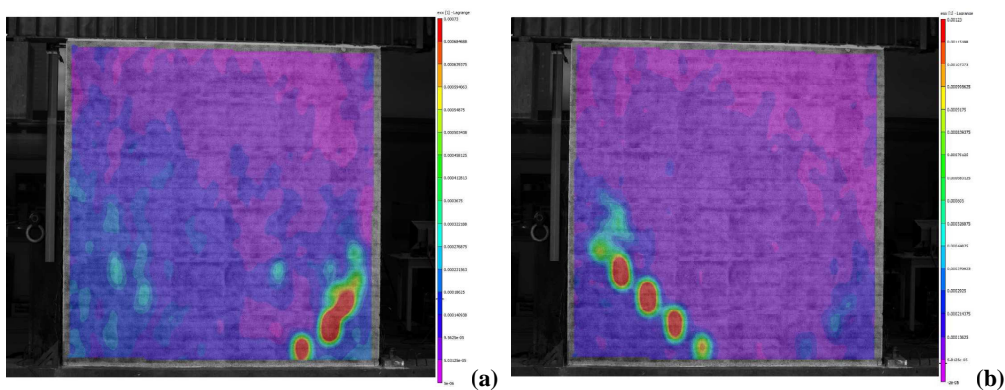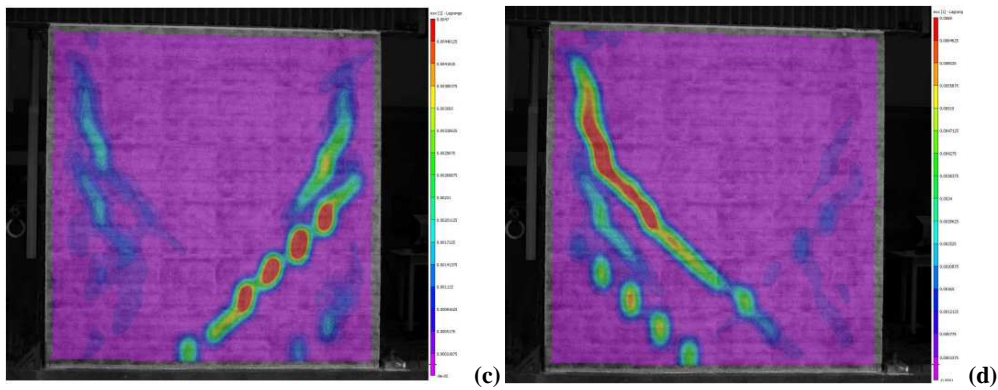
Figure 29 (a-b) First cracks (c-d) Typical Shear failure cracks

In order to give a full view of damage degree below is shown the cracks pattern of type one specimen.
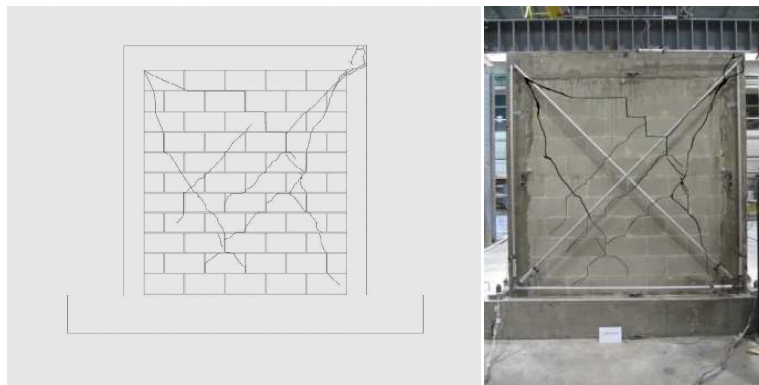

Figure 30 Crack Pattern

Type two specimen digital image analysis are reported in figure 31, it is clear also in that case the strut behavior of retrofitted CM wall, with another important aspect, that the tooth presence doesn't change the system answer.

"In-Plane Cyclic Behavior of Substandard Confined Masonry: Full-Scale Experiments, Finite-Element Modeling and Incremental Dynamic Analysis"

Chapter 3
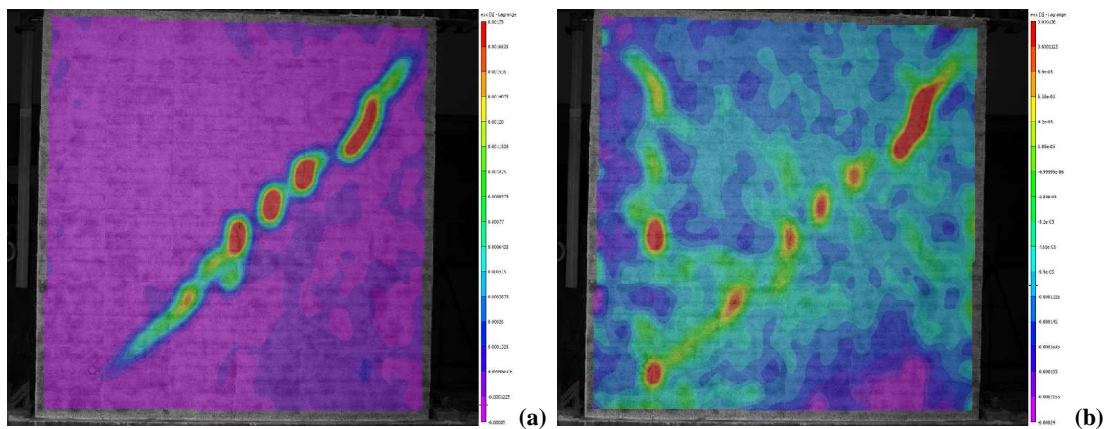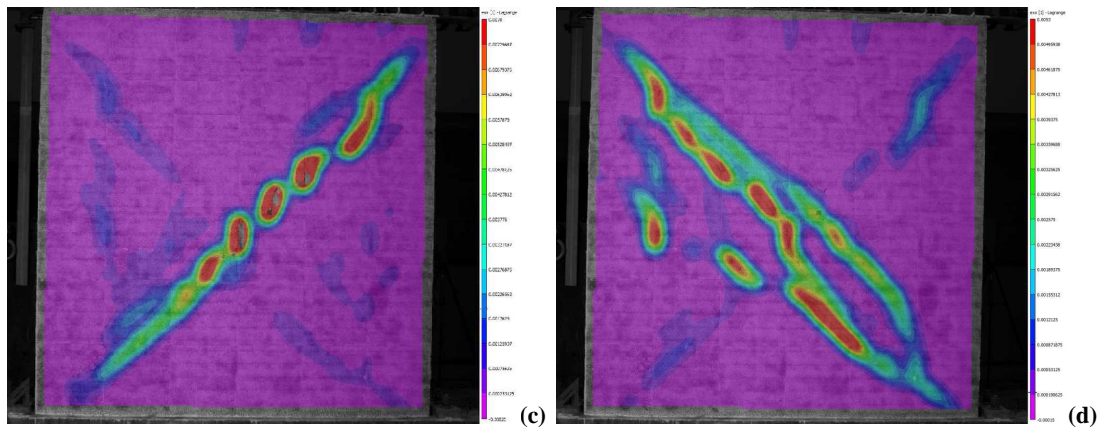
Figure 31 DIC Type Two wall (a-b) Cracks Begin (b-c) Shear Failure

In that case, the presence of the aluminum strips increase a lot the compression of the wall, but not the stiffness carrying the damage degree more high as we can see from the figure 32.
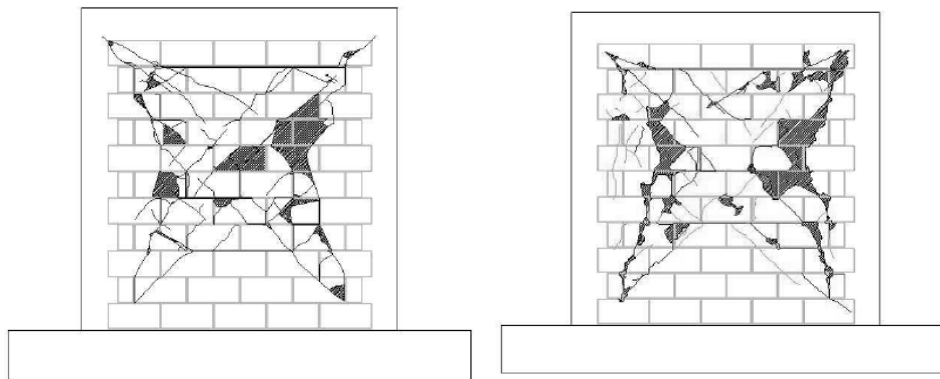

Figure 32 Crack Pattern

The third in-plane shear test was performed on type three wall. This is the specimen used to validate the numerical model. The choice to create an archetype that was able to represent this specimen belong to two reason, the first as shown in figure 26, its load capacity and ultimate displacement are in the middle between a really not engineering technique and a retrofitted wall and the second because the presence of normal but functional engineering detail has give good results. Below are illustrated DIC results and the crack pattern of type two wall.

"In-Plane Cyclic Behavior of Substandard Confined Masonry: Full-Scale Experiments, Finite-Element Modeling and Incremental Dynamic Analysis"
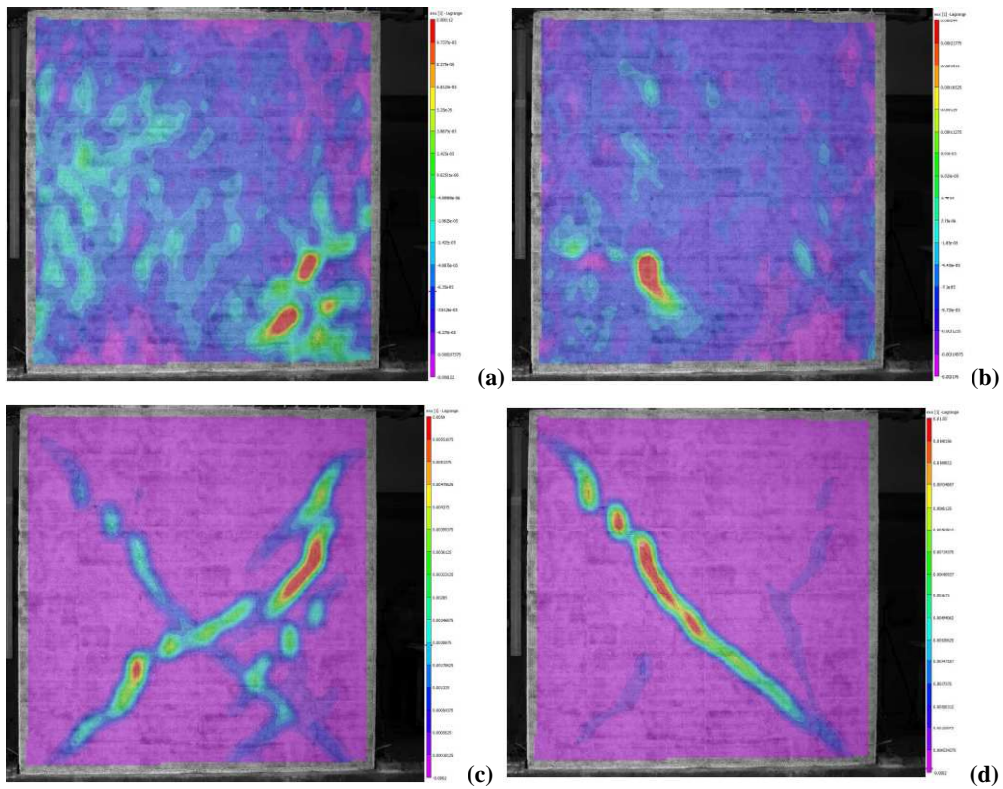
Chapter 3

**Figure 32 DIC Type Two wall (a-b) Cracks Begin (b-c) Shear Failure**
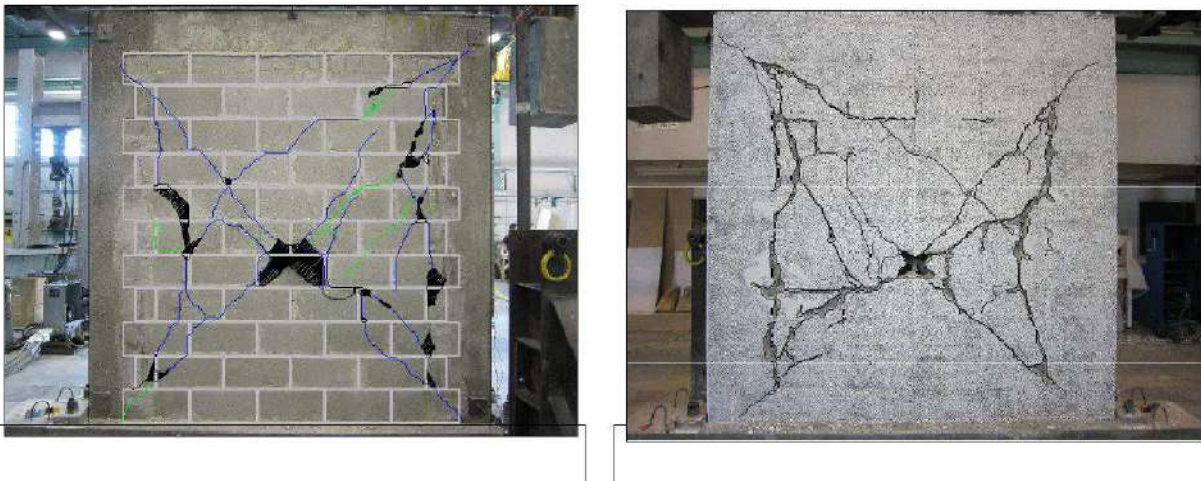
Figure 33 Type Three Wall Crack Pattern

Another test was carried out, the in plane behavior of confining frame. This test was really important, as will explained in chapter 4, for calibrate the archetype. Below is reported the Force-lateral displacement Hysteretic diagram.

"In-Plane Cyclic Behavior of Substandard Confined Masonry: Full-Scale Experiments, Finite-Element Modeling and Incremental Dynamic Analysis"

Chapter 3
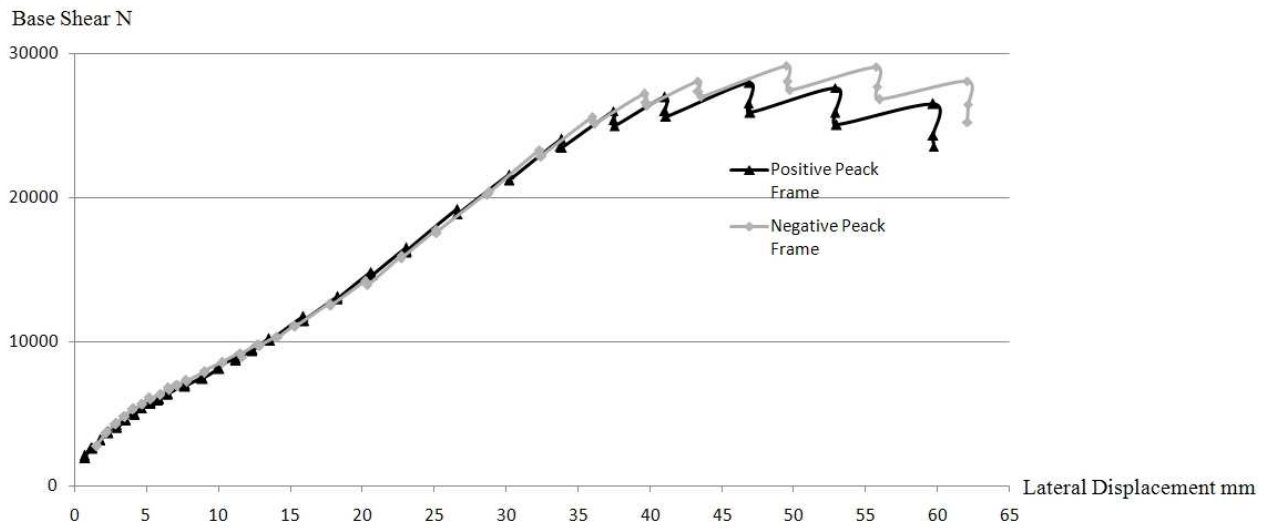
Figure 34 Force-Lateral Displacement Hysteretic Diagram

Have to be point out that the frame was damaged, because it was the confining frame for Type Two wall.

Figure 35 Frame Set up

"In-Plane Cyclic Behavior of Substandard Confined Masonry: Full-Scale Experiments, Finite-Element Modeling and Incremental Dynamic Analysis"

Chapter 4
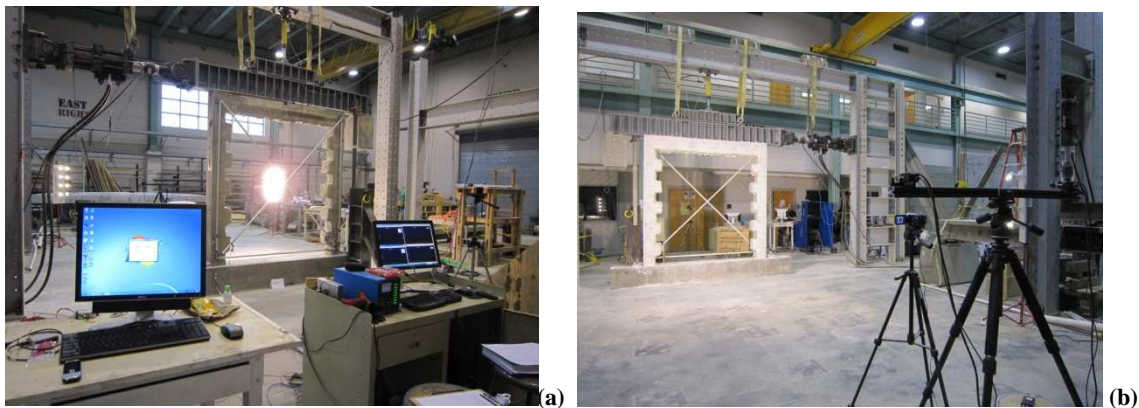
4. Numerical Modeling

After a comprehensive literature review [15-16-17-18-19-20-21] act to know how other authors treat the problem, to identify the practices and the parameters that govern the problem and to define what was the best modeling approach, a macro modeling approach, based on the assumption done in previous chapters was choosen. Also the choice of the program had a relevant weight, and at the end the numerical analysis was done using Seismostruct, a free license program. For first have to be defined the meaning of archetype. An archetype is a prototypical representation of a seismic-force-resisting element. Archetypes are intended to reflect the range of design parameters and element attributes that are judged to be reasonable representations of the feasible design space and have a measurable impact on system response. Once validated it, how will be show in next chapter, it is possible to define the space of the construction made of archetype and using non linear analysis it is possible to define the seismic response of the proposed seismic-force-resisting system.

Below is reassumed the numerical modeling process:
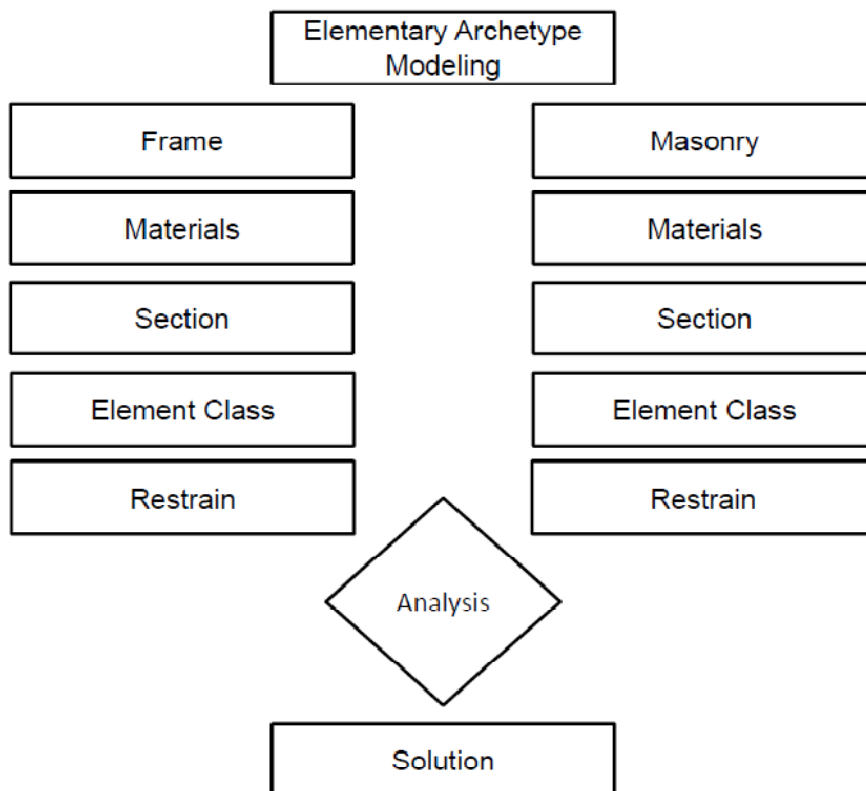
Figure 36 Process to define the Archetype

"In-Plane Cyclic Behavior of Substandard Confined Masonry: Full-Scale Experiments, Finite-Element Modeling and Incremental Dynamic Analysis"

Chapter 4

4.1 Hypothesis

Based on the meaning of Confining Masonry walls, namely unreinforced masonry walls built first and then confined with cast in-place reinforced concrete, the first assumption was that wall and frame work like a parallel system. In figure 37 is shown the meaning:
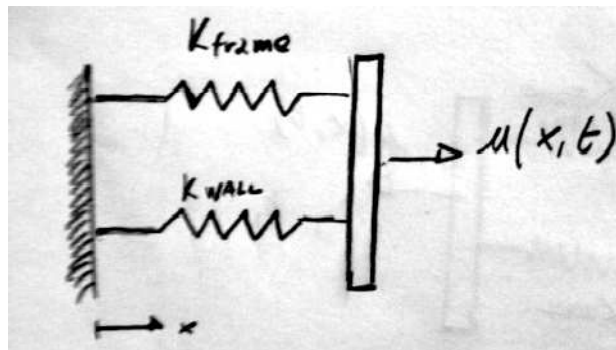

Figure 37 Process to define the Archetype

With this assumption, it was possible to split the modeling problem into two element, the frame and the masonry wall. It is also assumed that the frame works for flexural deformation and the walls for shear.

4.2 Frame Modeling

To modeling the frame the following data were used:

- Column section 193.675x193.675 mm^2 ;
- Beam section 193.657x254 mm^2;
- Longitudinal reinforce 4Ø12 S400;
- Rectangular Hoops 1 Ø12/100 mm S200;
- Rebar cover thickness 34.95 mm.

The constitutive law used for concrete is Mander et Al.[1988] Model. To describe completely the mechanical characteristics of the material, five parameter had to be defined.

"In-Plane Cyclic Behavior of Substandard Confined Masonry: Full-Scale Experiments, Finite-Element Modeling and Incremental Dynamic Analysis"

Chapter 4

In table 13 are defined the parameters:

Table 13

Parameter	Explanation
f_c	Cylindrc Compression Strength
f_t	Traction Strength
ε_c	Strain at the maximum strength
k_c	Confining Factor
γ	Weight of concrete

The element class used was inelastic plastic hinge frame element. This type of element permit to concentrate such inelasticity within a fixed length of the element, as proposed by Scott and Fenves [2006]. The advantages of such formulation is a full control/calibration of the plastic hinge length. In fact, the tests was done for a damaged frame, and the model, at the beginning had to follow the same curves, so, in base of the assumption found in [22-23-24], the first step was to model a damaged frame, or better to define the plastic hinge length to model the real cyclic response of the frame. Two limit curves will shown in figure 38, the first that represent the frame without damage and a plastic hinge length equal to a 16.67% of the length of the column and the second one, that represent a complete damage of the frame with a plastic hinge length equal to the 33% of the length of the column. Once made the elementary archetype, using a non linear static analysis in displacement control, we obtain the numerical results shown in figure 38 and 39 that are plotted with the test results.
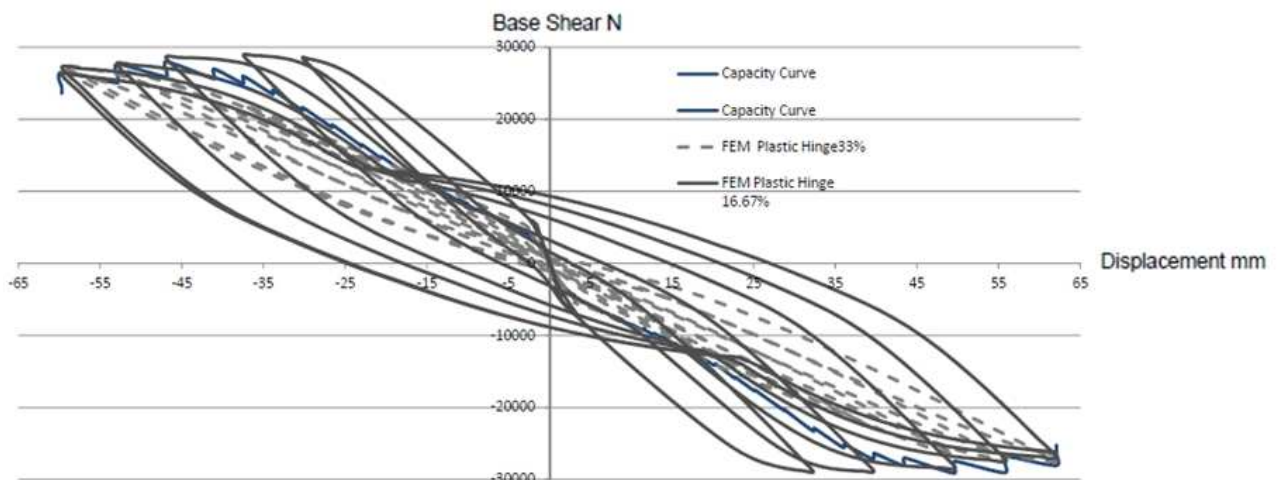

Figure 38 Frame Modeling

"In-Plane Cyclic Behavior of Substandard Confined Masonry: Full-Scale Experiments, Finite-Element Modeling and Incremental Dynamic Analysis"

Chapter 4

Defined what were the upper and lower limit curve, after a lot of numerical test, the real frame behavior was obtained. In fact, as is shown in figure 39, the plastic hinge after type two wall test was equal to the 28% of the length of the column, and that means, how we can see from the force-lateral displacement diagram, the dissipative properties of the frame weren't been exhausted. That's have to be point out, because for a seismic point of view, what we will find it is the wall behavior, that have less ductility properties than the frame. It is also true that one of the first hypothesis we find from literature review was that the frame role was only to confine the wall, and not bearing loads.
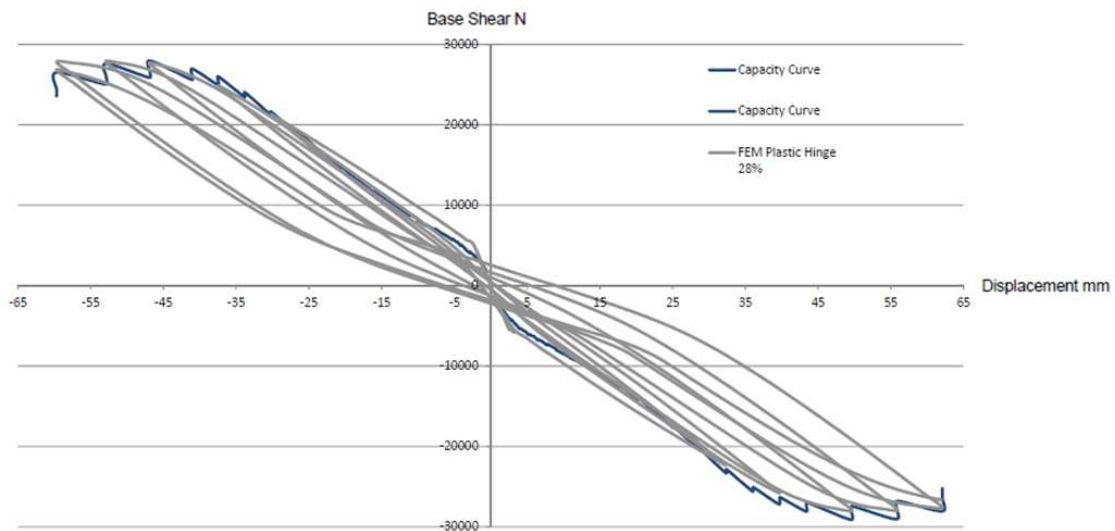

Figure 39 Analitycal Modeling of the Frame

Once defined the frame element properties and checked that it was working well (validation using test results), we started the confined wall modeling.

4.3 Confined Masonry wall Modeling

To modeling the non-linear behavior of infill panels in frame structures it is used a four nodes masonry panel element, developed and initially programmed by Crisafulli [11] and implemented in Seismostruct by Blandon [2005].

As it is shown in figure 40, each panel is represented in Seismostruct by six strut members.

"In-Plane Cyclic Behavior of Substandard Confined Masonry: Full-Scale Experiments, Finite-Element Modeling and Incremental Dynamic Analysis"

Chapter 4
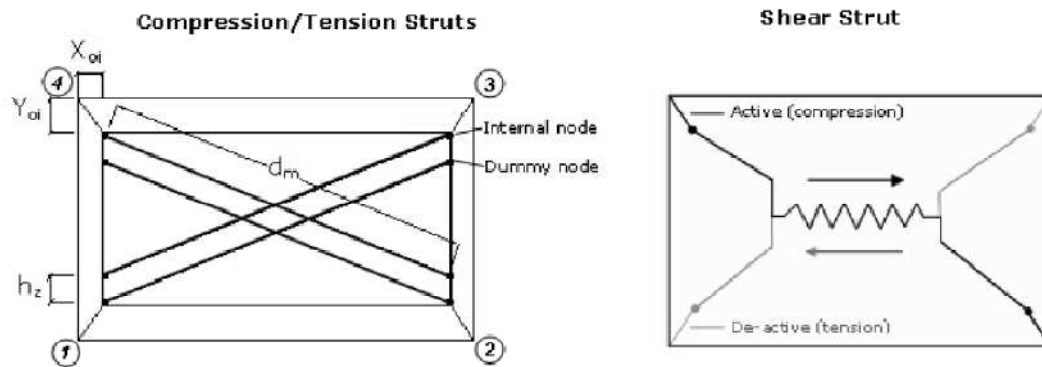
Figure 40 Infill Element

Each diagonal direction features two parallel struts to carry axial loads across two opposite diagonal corners and a third one to carry the shear from the top to the bottom of the panel. This latter strut only acts across the diagonal corners and a third one to carry the shear from the top to the bottom of the panel. This latter strut only acts across the diagonal that is on compression, hence its activation depends on the deformation of the panel. The axial load struts use the masonry strut hysteresis model, while the shear strut uses a dedicated bilinear hysteresis rule.

To fully characterize this type of element, these are the parameters that have been defined:

- strut curve parameters:
- shear curve parameters;
- infill panel thickness;
- out of plane failure drift;
- strut area 1;
- strut area 2;
- equivalent contact length;
- horizontal and vertical length;
- proportion of stiffness assigned to shear;
- specific weight.

4.3.1 Strut curve parameters

This is the masonry infill strut model, developed and initially programmed by Crisafulli and implemented in Seismostruct by Blandon to be used in association with the infill panel element.

"In-Plane Cyclic Behavior of Substandard Confined Masonry: Full-Scale Experiments, Finite-Element Modeling and Incremental Dynamic Analysis"

Chapter 4

The first things have to be underlined it is that this curve was studied assuming small hysteretic cycles. 17 parameters need to be defined in order to fully characterize this response curve, and must be underline that a lot of them are experimental parameters.

Table 14

Parameter	Explanation
E_m	Inizial Young Modulus
$f_{m\theta}$	Diagonal Compression Capacity of the panel
f_t	Bond-strnght of the interface frame-wall
ε_m	Strain at Maximum Stress
ε_{uk}	Ultimate Strain
ε_{cl}	Strain after which cracks partially close
ε_1	Strut Area reduction strain
ε_2	Residual Strut Area strain
gu	Starting unloading stiffness factor
ar	Strain reloading factor
ach	Strain inflection factor
ba	Complete unloading strain factor
bch	Strain inflection factor
gpu	Zero stress Stiffness factor
gpr	Reloading Stiffness factor
ex1	Plastic unloading Stiffness factor
ex2	Repeated cycle Strain factor

Have to be underlined that the last nine parameters are all empirical parameters and related to cyclic loading. In addition, sensitivity studies have also shown that only three of them play a significant role:

- reloading stiffness factor;
- strain inflection factor;
- plastic unloading stiffness factor.

4.3.2 Shear curve parameters

The shear strength results as the combination of two mechanisms, namely, bond strength and friction resistance between the mortar joints and the bricks. The shear strength can thus be expressed as the sum of the initial shear bond strength τ_0 and the product of coefficient of friction μ and the normal compressive force in perpendicular direction to the bed joints. This approach to

"In-Plane Cyclic Behavior of Substandard Confined Masonry: Full-Scale Experiments, Finite-Element Modeling and Incremental Dynamic Analysis"

Chapter 4

estimate shear resistance is pragmatically adopted by design codes, independently of the failure mechanism being developed in the infill panel. To fully characterize this response curve 4 parameters have to be defined:

Table 15

Parameter	Explanation
τ_0	Shear bond strength
μ	Friction coefficient
τ_{max}	Maximum shear strength
α_s	Empirical factor. It represents the ratio between the maximum shear stress and the average stress in the panel

Below it is shown the way in which were defined these parameters.
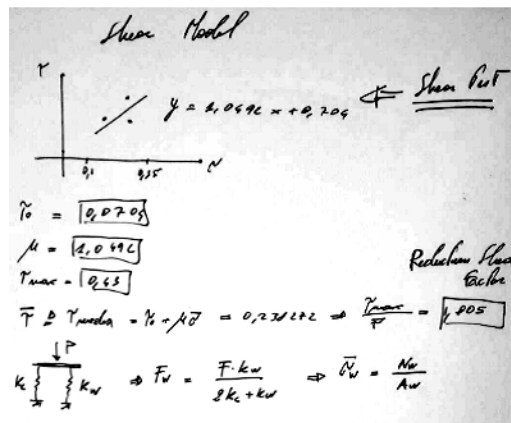
Figure 41

4.3.3 Panel thickness

This value could be considered as equal to the width of the panel bricks alone or include also the contribute of the plaster.

4.3.4 Out of plane failure drift

Introduced in percentage of storey height, it take in account the possibility that if out of plain behavior occur, the panel do not give contribution in react to seismic response.

4.3.5 Strut Area 1

Strut area 1 it is the initial strut area value. In according with different authors, in the figure below it is represented how it is defined.

"In-Plane Cyclic Behavior of Substandard Confined Masonry: Full-Scale Experiments, Finite-Element Modeling and Incremental Dynamic Analysis"

Chapter 4
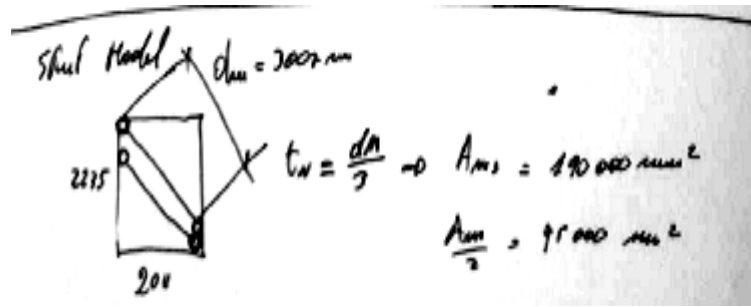
Figure 42 Strut Area 1

4.3.6 Strut Area 2

Defined a percentage of strut Area1, it represent the residual strut area, after that damaging has taken the wall.

4.3.7 Equivalent contact length

Introduced as percentage of the vertical height of the panel, effectively yielding the distance between the internal and dummy nodes (node 1-2-3-4 figure 40) and used as to somehow take due account of the contact length between the frame and the infill panel.

4.3.8 Horizontal and vertical offsets

X_{oi} and Y_{oi} introduced as percentage of the horizontal and vertical dimensions of the panel, are parameters that provide the distance between the external corner nodes and the internal ones.

4.3.9 Proportion of stiffness assigned to shear

It represent the proportion of the panel stiffness that should be assigned to the shear spring:

$$K_a = (1 - \gamma_s)\frac{A_{ms} Em}{2\, dm}$$

$$K_s = (\gamma_s)\frac{A_{ms} Em}{2\, dm} \cos^2\theta$$

With the following means:

K_a = Strut stiffness;

K_b = Shear stiffness;

γ_s = proportion of stiffness assigned to shear.

"In-Plane Cyclic Behavior of Substandard Confined Masonry: Full-Scale Experiments, Finite-Element Modeling and Incremental Dynamic Analysis"

Chapter 4

4.3.10 Specific weight γ

It is the specific weight of the masonry wall.

4.4 Numerical results

Once defined the parameters necessary to the element characterization, in-plane cyclic numerical test were carried out. The walls element was tested with cantilever-type boundary conditions, with fixed nodes at the base and the same displacement-rotation of nodes at the top.

Two vertical static load, representing the compression load that loads cell give to specimen, were applied and an horizontal time history displacement load was applied at top level.

Figure 43 (a) shows the element, (b) illustrates the Base Shear-Lateral Displacement diagram.

(a)   **(b)**

Figure 43

"In-Plane Cyclic Behavior of Substandard Confined Masonry: Full-Scale Experiments, Finite-Element Modeling and Incremental Dynamic Analysis"

Chapter 5
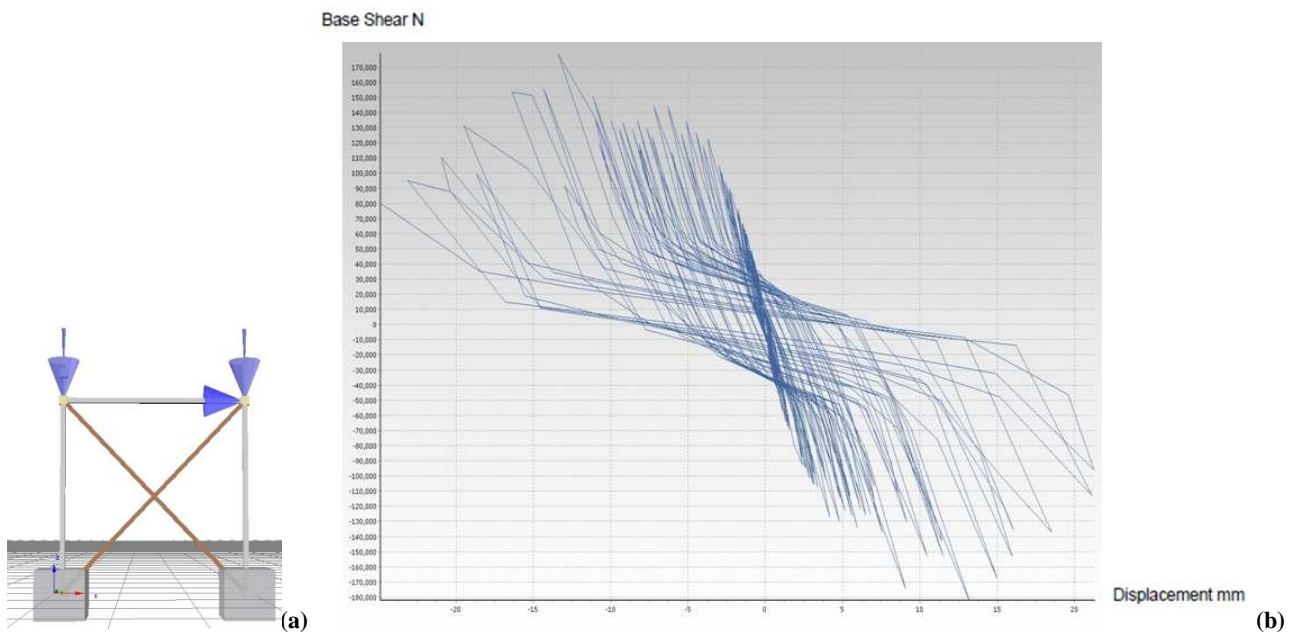
5. Validation of the Model and Results of Analyses

5.1 Comparison between analytical and experimental results

As is shown in below diagram, the numerical model reproduce the behavior of confined masonry wall after that the first cracks start happening. The Force-Lateral displacement hysteretic diagram of laboratory test presents two typical behaviors, the first, in which the stiffness is leaded by sliding mechanism, and the second, after that cracking begins, in which the stiffness decreases and the wall starts a strut and tie behavior. It is this the behavior that we wanted reproduce with numerical modeling, because from the first crack to the end the element starts dissipate energy. For a seismic analysis, be able to reproduce this mechanism makes possible to define the ultimate displacement of the element and quantify the value of the q factor with whom the linear elastic response spectrum can be scaled.
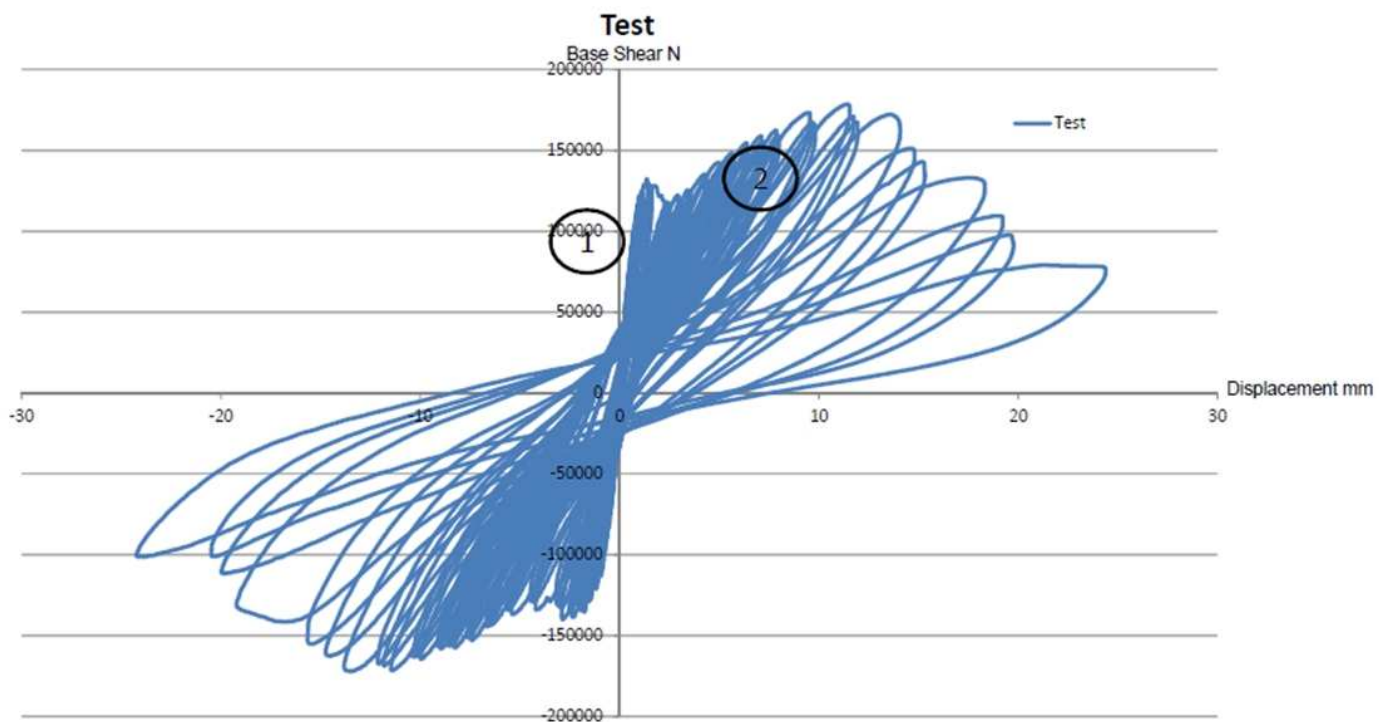
Figure 44 Force-Lateral Displacement Hysteretic curve diagram

Below are represented two limit curves, the first with the 50% of shear stiffness and the second one with the 10%. The point is that for this type of element, it is not take into account that the shear stiffness (sliding mechanism) decreasing as it is shown in figure 45.

"In-Plane Cyclic Behavior of Substandard Confined Masonry: Full-Scale Experiments, Finite-Element Modeling and Incremental Dynamic Analysis"

Chapter 5
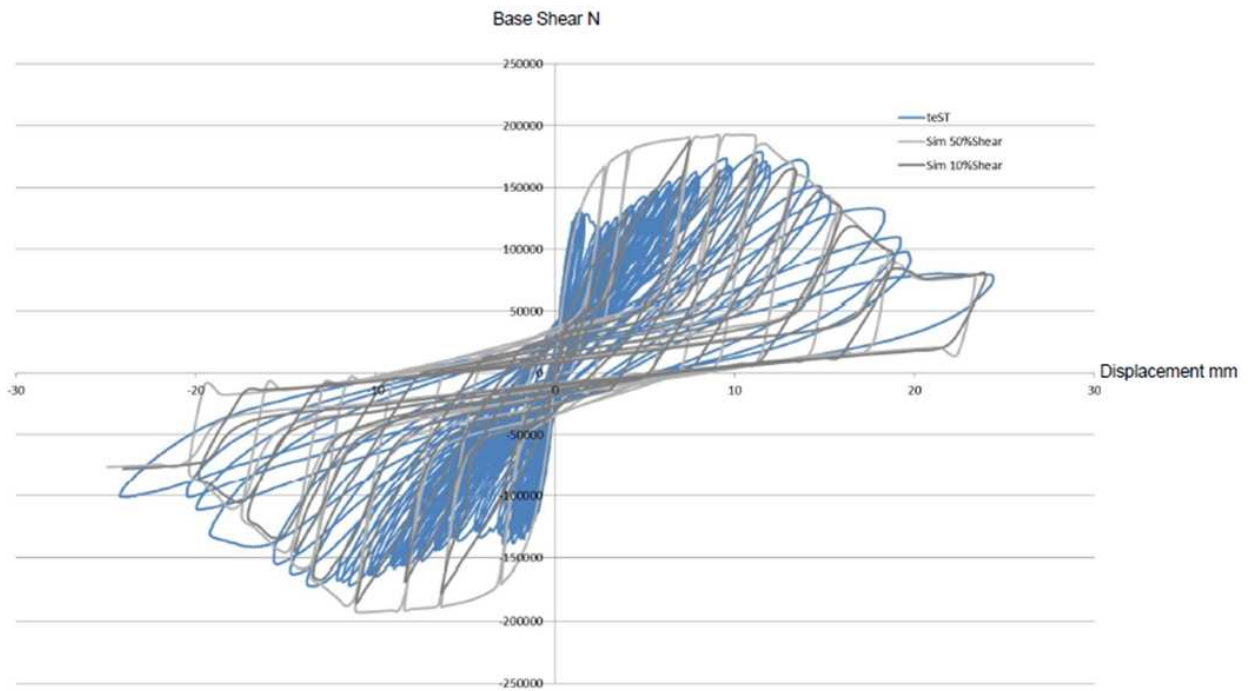
Figure 45 Numerical limit curves

Using the same time history analysis load, the numerical model's result are shown in figure 46. It is possible to recognize that the model represent the strut and tie behavior of tested CM wall, not reaching the first stiffness.
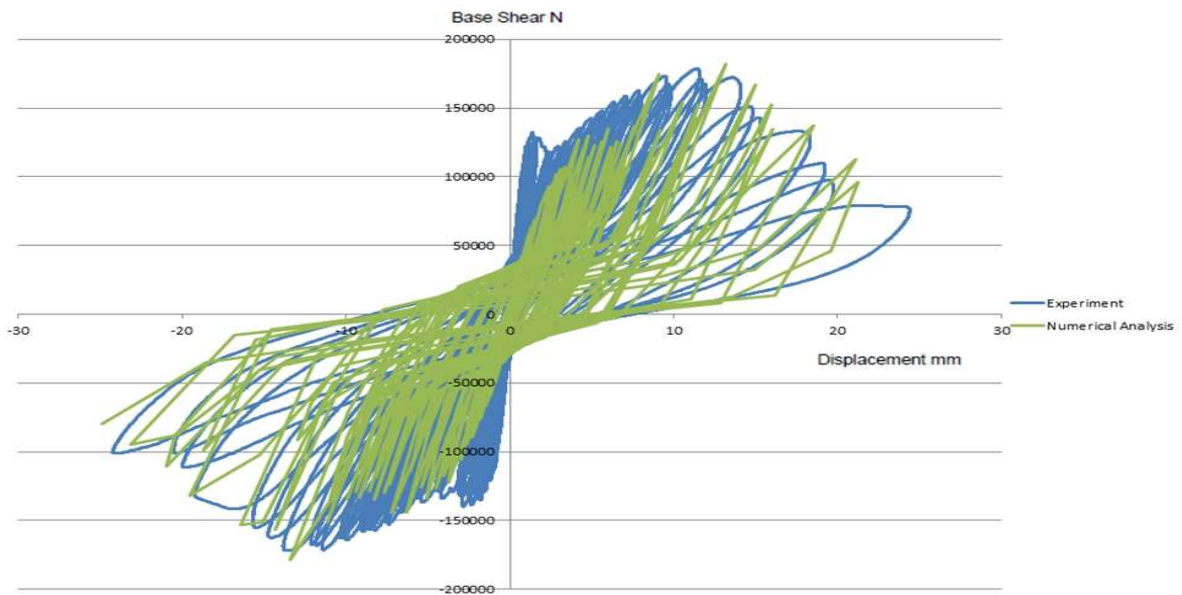

Figure 46 Comparison Experimental and Analytical results

"In-Plane Cyclic Behavior of Substandard Confined Masonry: Full-Scale Experiments, Finite-Element Modeling and Incremental Dynamic Analysis"

Chapter 5

5.2 Definition of "q" factor for elementary Archetype

A push over test in displacement control for the elementary archetype was carried out and following the theory found in [3] an idealization of the numerical envelope through a bi-linear schematization was done. Once done it, it is possible to define, from the bi-linear curve, what is the element ductility factor μ. Defined μ we can quantify the q value, under this hypothesis:

- $q = \mu$ ➔ if we consider the same displacement assumption;
- $q = \sqrt{2\mu - 1}$ ➔ if we consider same area assumption.
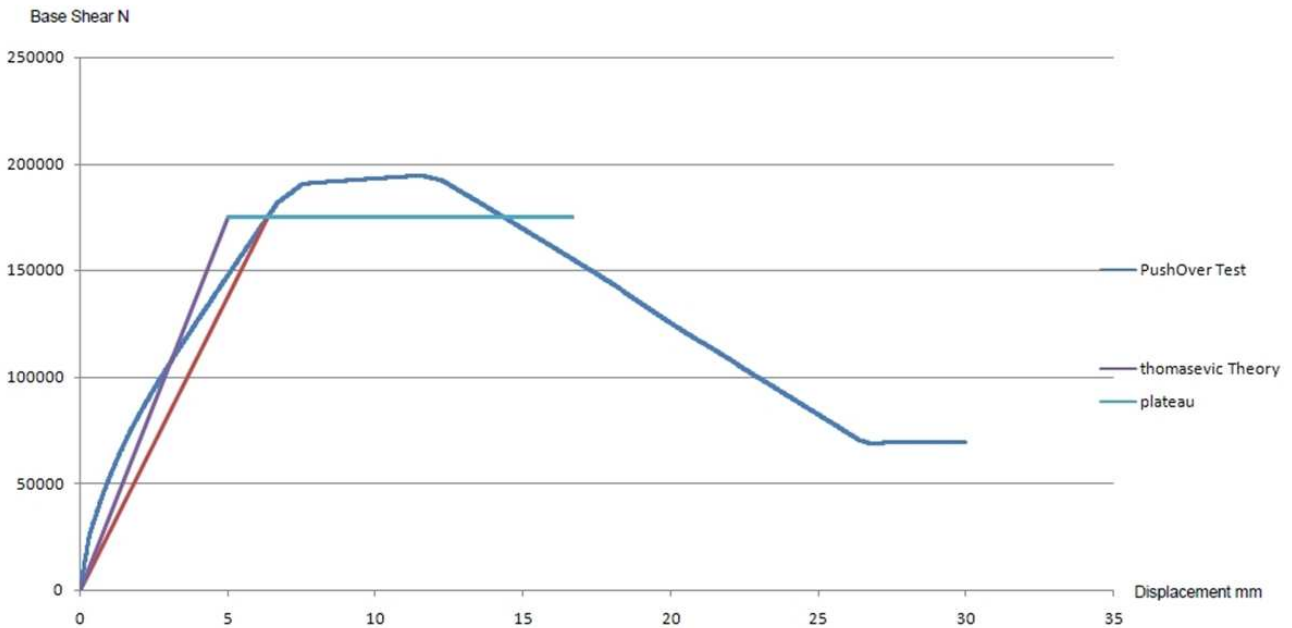
Figure 46 Capacity curve (blue) of elementary archetype ,red violet and light blue represent two types of bi-linearization

To do the bi-linearization, three limit state have to be defined:

- crack limit H_{cr}, d_{cr};
- maximum resistance H_{max}, d_{max};
- ultimate state H_u, d_u.

In that way it is possible to quantify:

- global ductility factor = $\mu_u = d_u / d_e$;
- over strength = $\gamma_u = Hmax / H_u$.

To better define the meaning of this quantity, below is reported figure 47.

"In-Plane Cyclic Behavior of Substandard Confined Masonry: Full-Scale Experiments, Finite-Element Modeling and Incremental Dynamic Analysis"

Chapter 5
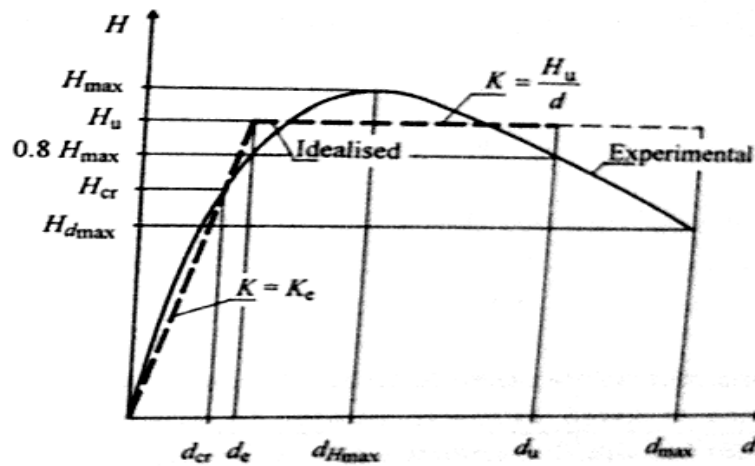
Figure 47 Idealization of archetype capacity curve [3]

Referring to the figure 46, two types of bi-linearization were done. Both have got the same plateau, the violet was built using the [3] theory, and the red with the assumption that the linear trait finish with the percentage of 90% of maximum base shear. The reason of this assumptions derive for the point that the numerical model shows only the strut and tie behavior, losing the first stiffness with the crack limit state. Here are shown the global ductility factors obtained using [3] of ours assumption:

Table 16 q factor for elementary archetype

q using [3]	3.326
q same displacement	2.62
q same areas	2.01

5.3 Conclusions

Two bi-linearizations were carried out and three different values of q were found. After a comprehensive literature review, it is possible to affirm that normal confined masonry wall elements have a q factor in a range between 3-4, and that in this case, in which the sub-standards materials are proved, 2 it seems the most reasonable choice.

"In-Plane Cyclic Behavior of Substandard Confined Masonry: Full-Scale Experiments, Finite-Element Modeling and Incremental Dynamic Analysis"

Chapter 6

6. Evaluation of q factor for Confined Masonry Building

Once defined the elementary archetype and its validation through laboratory tests results, three confined masonry house were modeled, ten non scaled accelerograms were chosen and 60 incremental dynamics analysis were carried out to define the non linear dynamic behavior of the three structures. Also 6 push over tests in displacement control were done and validated using the incremental dynamic analysis and a reasonable q factor values to design was defined.

6.1 Houses Archetypes

After a comprehensive literature review act to define the dimensions of typical confined masonries houses, and using some plans found in [27], three houses were defined and modeled. One of the most important point was to decide how idealize the slab mass, and after some consideration it be decided to concentrate it in the geometrical centroid. As it can be seen from figures 48-49-50 b the first type represent the case in which in one direction there are two coupled confined masonry walls, the second is made by single confined masonry units and the third whit a torsion resistant element. This choice belong to the aim to verify if there was substantial change of behavior between the three constructive typologies.

Below, in figures, are shown the three models and the relative plans.


(a)   (b)
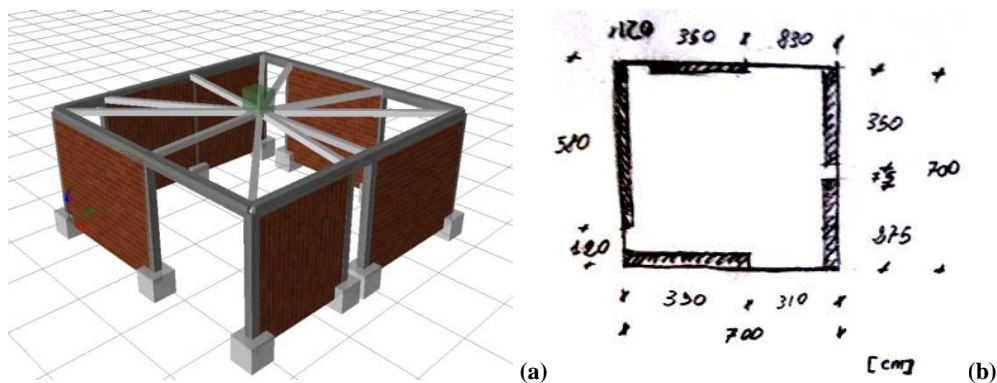
Figure 48 (a) Numerical model House type 0ne, (b) Plan

"In-Plane Cyclic Behavior of Substandard Confined Masonry: Full-Scale Experiments, Finite-Element Modeling and Incremental Dynamic Analysis"

Chapter 6
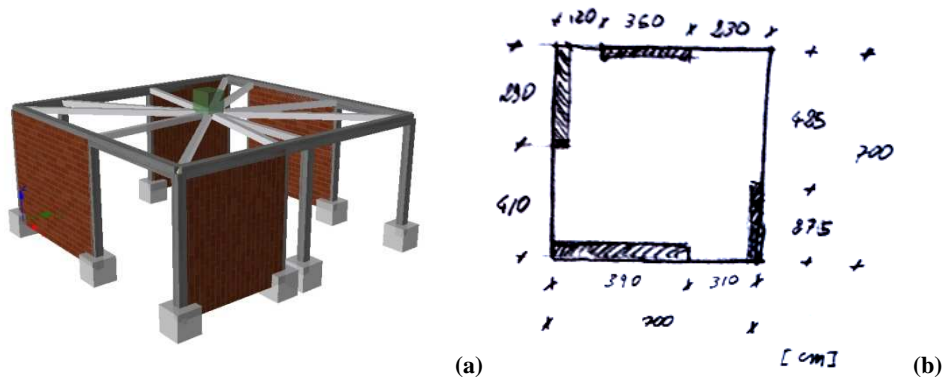
Figure 49 (a) Numerical model House type two, (b) Plan
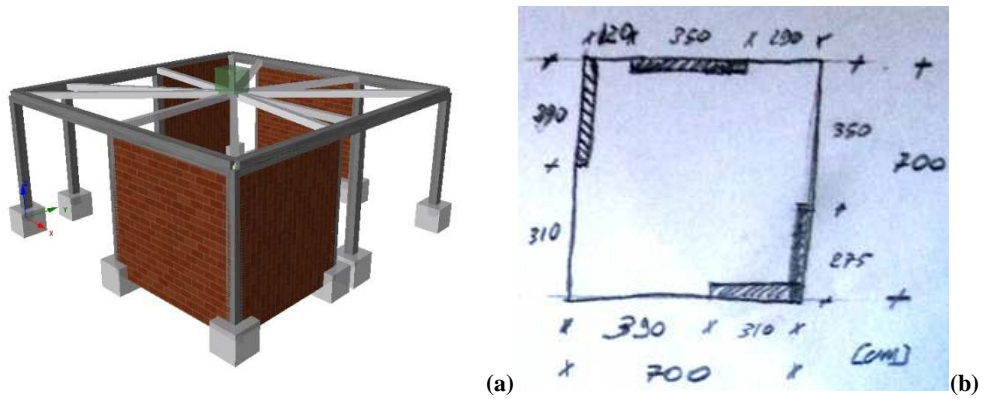

Figure 50 (a) Numerical model House type three, (b) Plan

The eight of each wall it is 3 m and the confining members section is 20x20 cm for the tie columns and 25x20 cm for the tie beams. The top slab was modeled as a rigid diaphragm.

Using the eigenvalues analysis, the intrinsic properties of each house were calculated and shown in table 17.

Table 17

Intrinsic Properties	Natural Pulse [rad/sec]	Natural Frequency [Hz]	Fundamental Period [sec]
house type one x direction	92.86	14.78	0.068
house type one y direction	128	0.05	20.37
house type two x direction	91.02	0.07	14.5
house type two y direction	93.5	0.068	14.88
house type three x direction	94.5	15.04	0.066
house type three y direction	98.4	15.66	0.064

Using this values it is possible to know the PSA [g] relative to each one house in x and y direction.

"In-Plane Cyclic Behavior of Substandard Confined Masonry: Full-Scale Experiments, Finite-Element Modeling and Incremental Dynamic Analysis"

Chapter 6

6.2 Accelerograms

The form of seismic action to be used in seismic resistance verification depends on the importance and complexity of the structure under consideration. In the case of structures with regular structural configuration, such as masonry structures, the calculation are simplified by taking into account only one horizontal component of the seismic ground motion and analyzing the structure in each orthogonal direction separately [25]. Since the natural accelerograms rpresent an interesting option to use in the non linear dynamic analysis of the structures[26], ten of them from PEER were chosen and implemented in the incremental dynamic analysis tests.

Basically the incremental dynamic analysis is a parametric analysis method that has recently emerged in several different forms to estimate more thoroughly structural performance under seismic loads. The concept it is scaling an acceleration time history and taking the drift-base shear curve and the scaled acceleration-drift curve.

After that, doing a push over test it is possible to define q factor dividing the Dynamic force (PSA*mass) for the 90% of the maximum base shear found with a push over test.

The accelerograms were chosen in respect to this assumptions:

- Magnitude range between 6.2-7.3;
- Soil type(referred to NTC 2008 type B-C);
- Maximum epicenter distance (0-15 Km).

Table 18

Non scaled accelerogam	Magnitude	Fault tipe	V_{30} [m/s]	f [Hz]
Parkfield 1966	6.19	Strike Slip	236.8	0.25
El Centro 1979	6.53	Strike Slip	208.9	0.12
Victoria Mexico 1980	6.33	Strike Slip	274.5	0.25
Morgan Hill 1984	6.19	Strike Slip	270.8	0.25
Superstition Hill1987	6.54	Strike Slip	208.7	0.16
Duzce Turkey 1999	7.14	Strike Slip	276	0.10
Erzican Turkey 1992	6.69	Strike Slip	274.5	0.12
Kocaeli Turkey 1999	7.51	Strike Slip	297	0.06
Kobee Japan	6.9	Strike Slip	609	0.12
Landers 1992	7.28	Strike Slip	379.3	0.07

"In-Plane Cyclic Behavior of Substandard Confined Masonry: Full-Scale Experiments, Finite-Element Modeling and Incremental Dynamic Analysis"

Chapter 6

For each one non scaled accelerogram it was carried out an IDA in x and y direction, using a scaling factor that goes from 0.25 to 8.

6.3 Incremental Dynamic Analysis

Once choose the ten accelegrom, based on the assumption done before, 60 incremental dynamics analysis were carried out. In fact, each unscaled ground motion record, applied to the base, was applied to each structures type in x and y direction. As an example, in figure below it is rapresented this schematization:

(a)   (b)
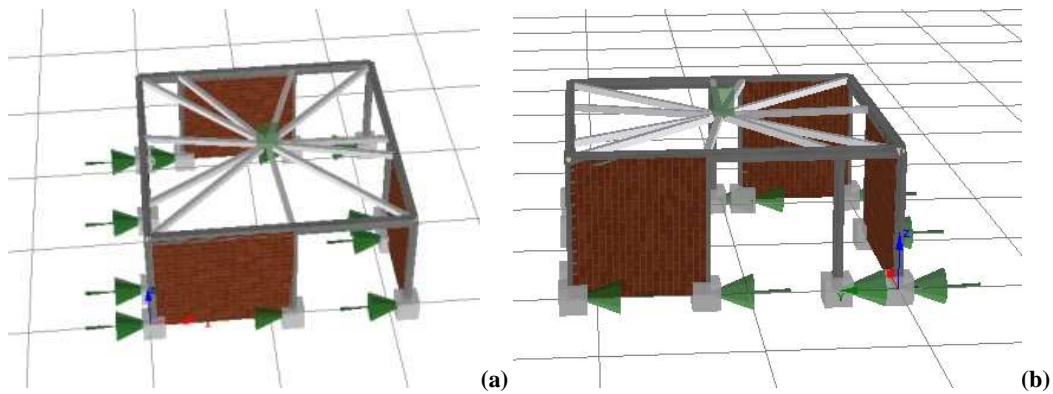
Figure 51 (a) Base load applied in x direction, (b) Base load applied in y direction

The ground motion forms of each record are shown below:


(a)   (b)

"In-Plane Cyclic Behavior of Substandard Confined Masonry: Full-Scale Experiments, Finite-Element Modeling and Incremental Dynamic Analysis"

Chapter 6

(c)

(d)

(e)

(f)

(g)

(h)

"In-Plane Cyclic Behavior of Substandard Confined Masonry: Full-Scale Experiments, Finite-Element Modeling and Incremental Dynamic Analysis"

Chapter 6

(i) **(e)**
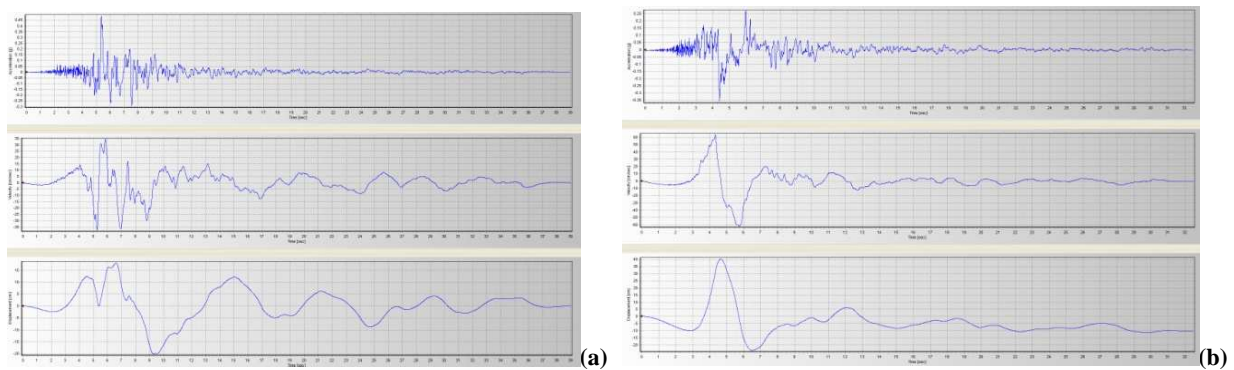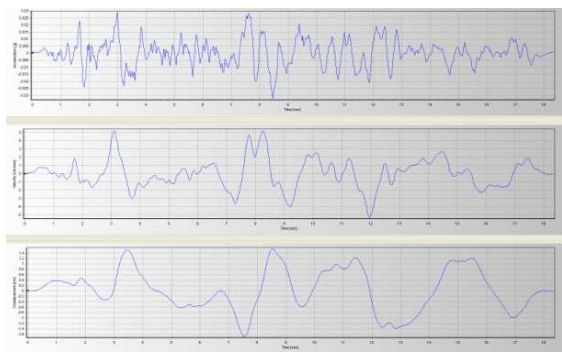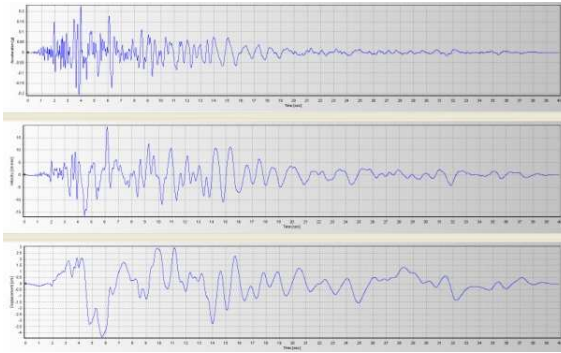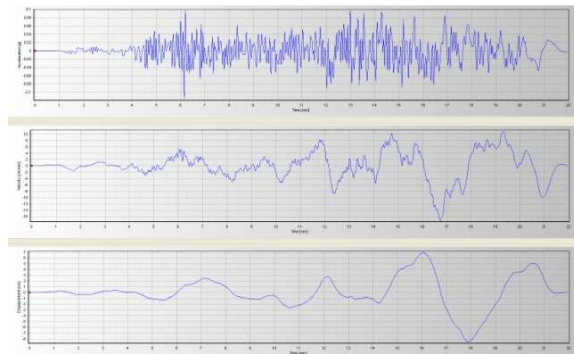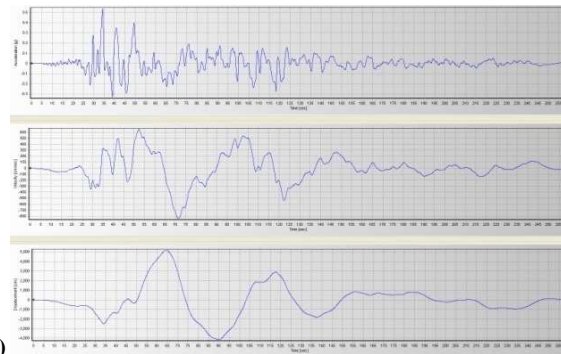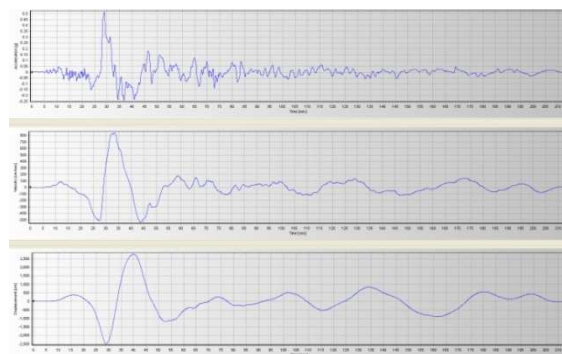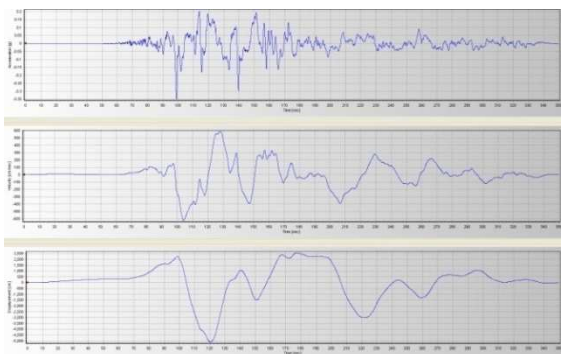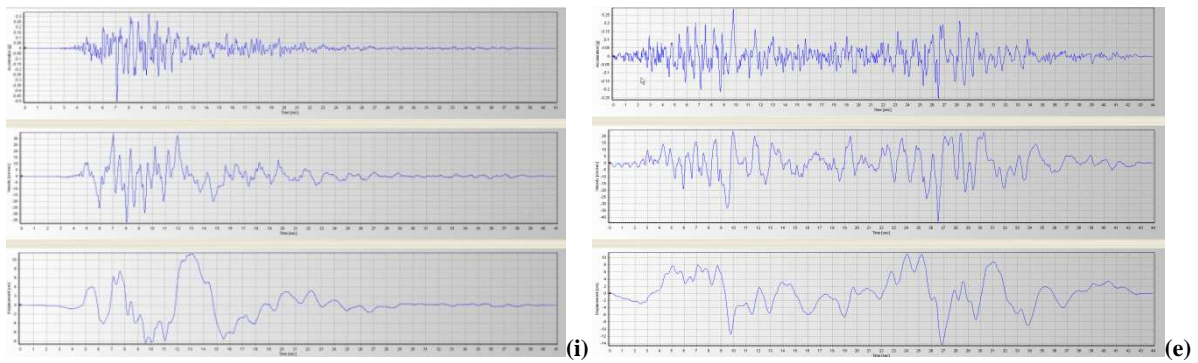
Figure 52 Groun Motion record : (a) Parkfield (b) El centro, (c) Victoria Mexico, (d) Morgan Hill, (e) Superstition hill, (f) Duzce Turkey, (g) Erzican Turkey, (h) Kocaeli Turkey, (i) Kobee Japan, (e) Landers

The results are shown below:

Figure 53 PSA House type one dir.x
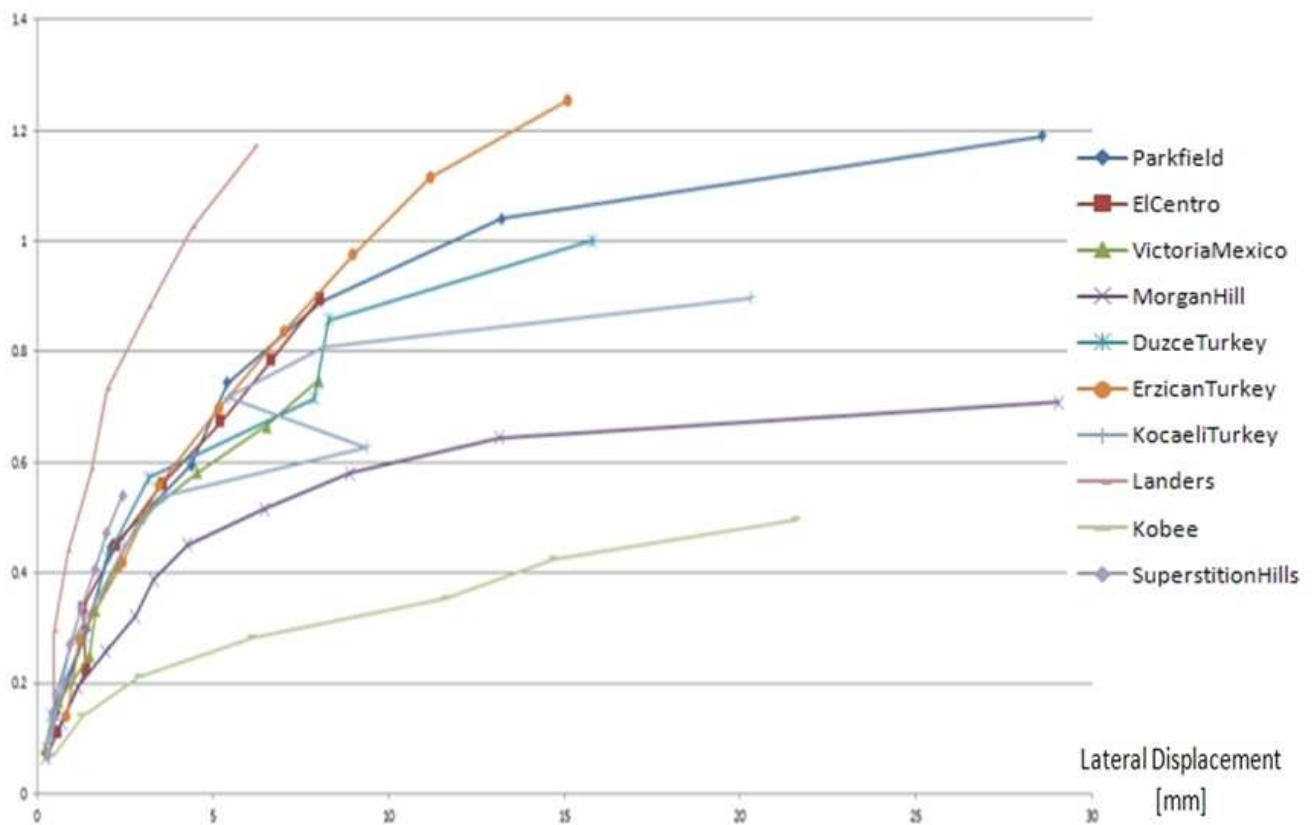
"In-Plane Cyclic Behavior of Substandard Confined Masonry: Full-Scale Experiments, Finite-Element Modeling and Incremental Dynamic Analysis"

Chapter 6

"First Mode" spectral acceleration PSA(T1,5%) [g]
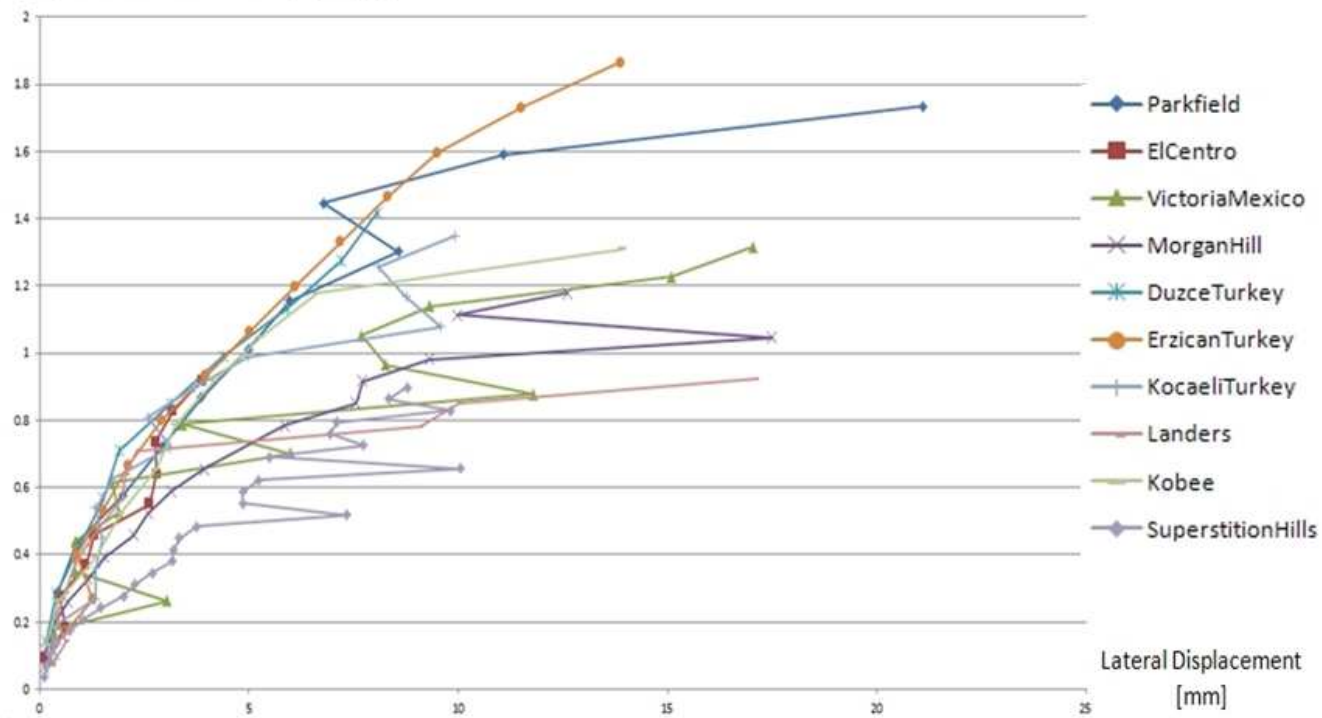
Figure 53 PSA House type one dir.y

"First Mode" spectral acceleration PSA(T1,5%) [g]
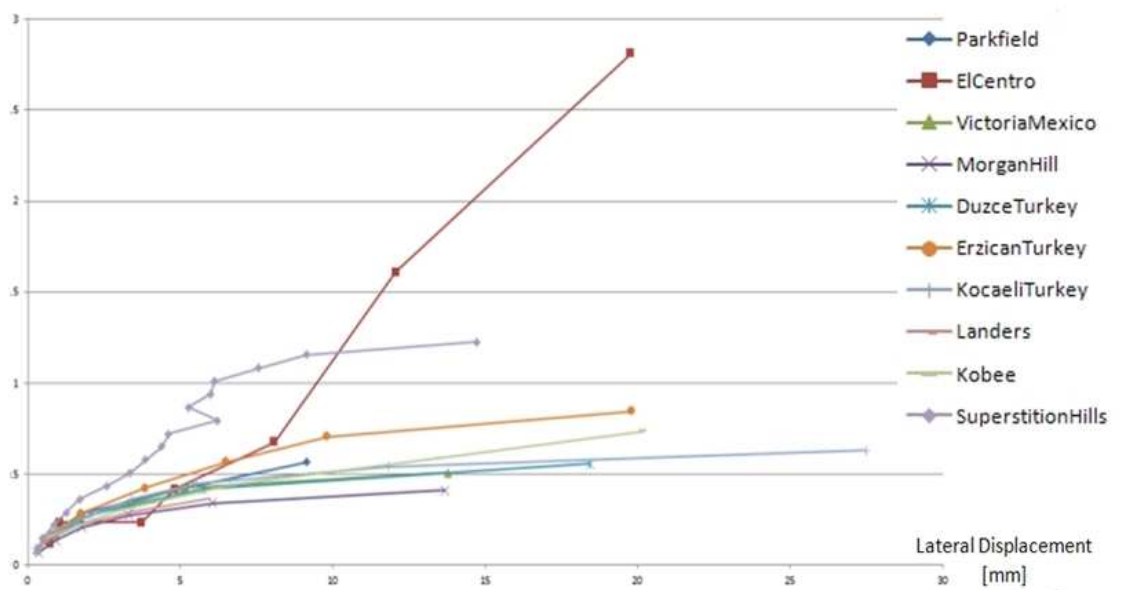
Figure 53 PSA House type two dir.x

"In-Plane Cyclic Behavior of Substandard Confined Masonry: Full-Scale Experiments, Finite-Element Modeling and Incremental Dynamic Analysis"

Chapter 6

"First Mode" spectral acceleration PSA(T1,5%) [g]
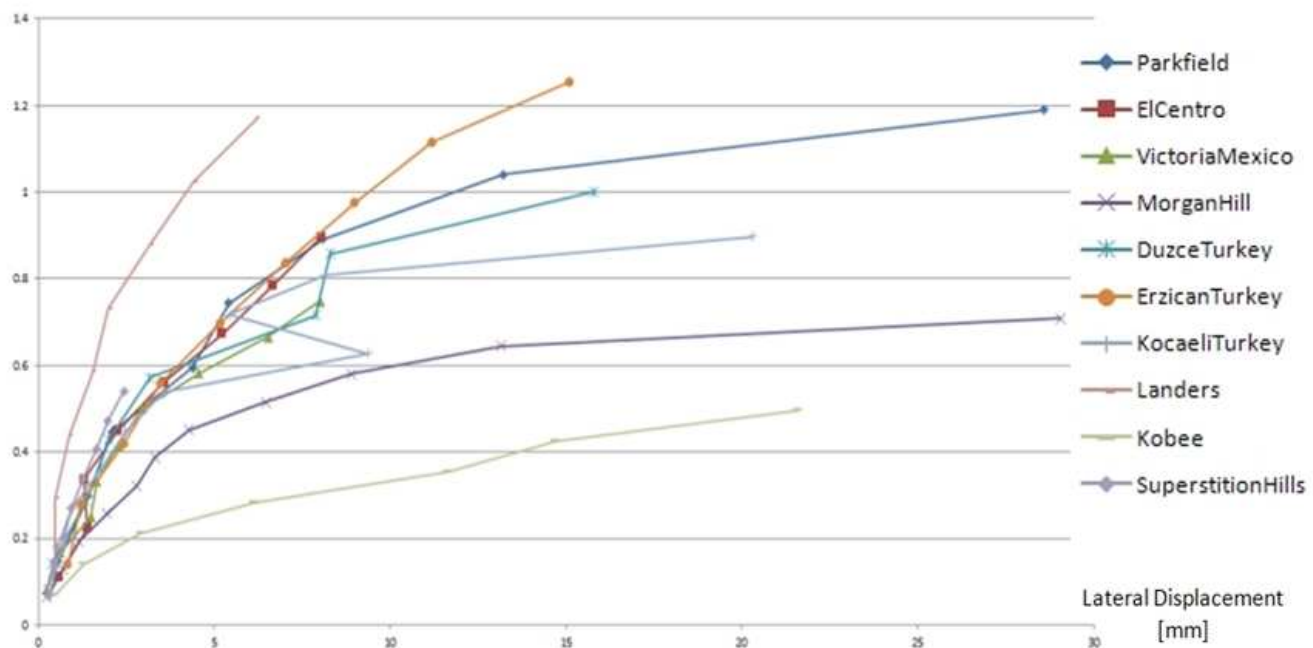
Figure 53 PSA House type two dir.y

"First Mode" spectral acceleration PSA(T1,5%) [g]
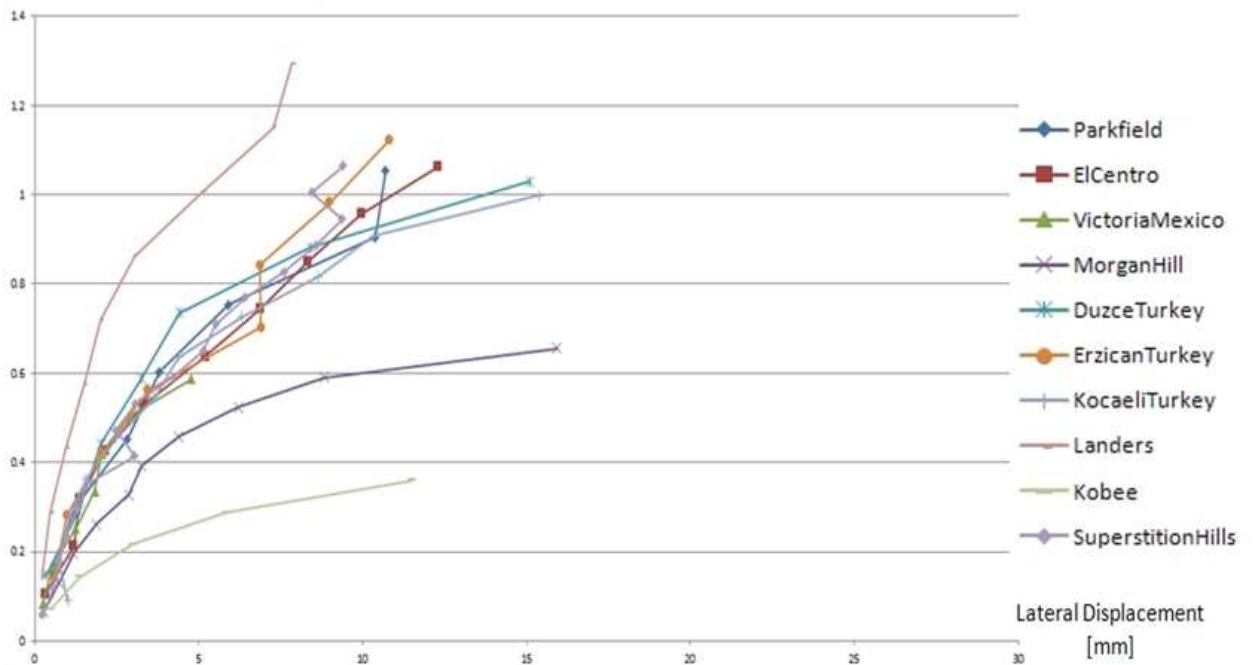


Figure 53 PSA House type three dir.x

"In-Plane Cyclic Behavior of Substandard Confined Masonry: Full-Scale Experiments, Finite-Element Modeling and Incremental Dynamic Analysis"

Chapter 6

"First Mode" spectral acceleration PSA(T1,5%) [g]
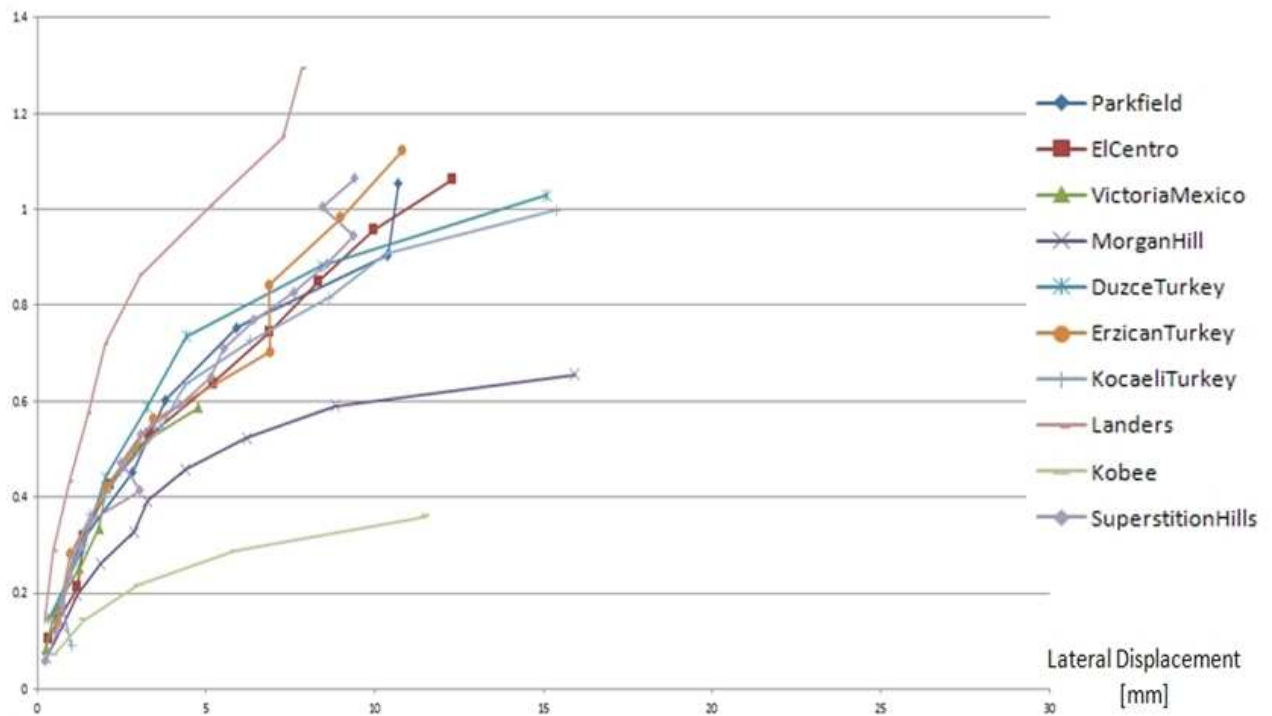
Figure 53 PSA House type three dir.y

6.4 Push Over Test

In order to quantify q factor, six push over tests in displacement control were done.

The following figures show the results.
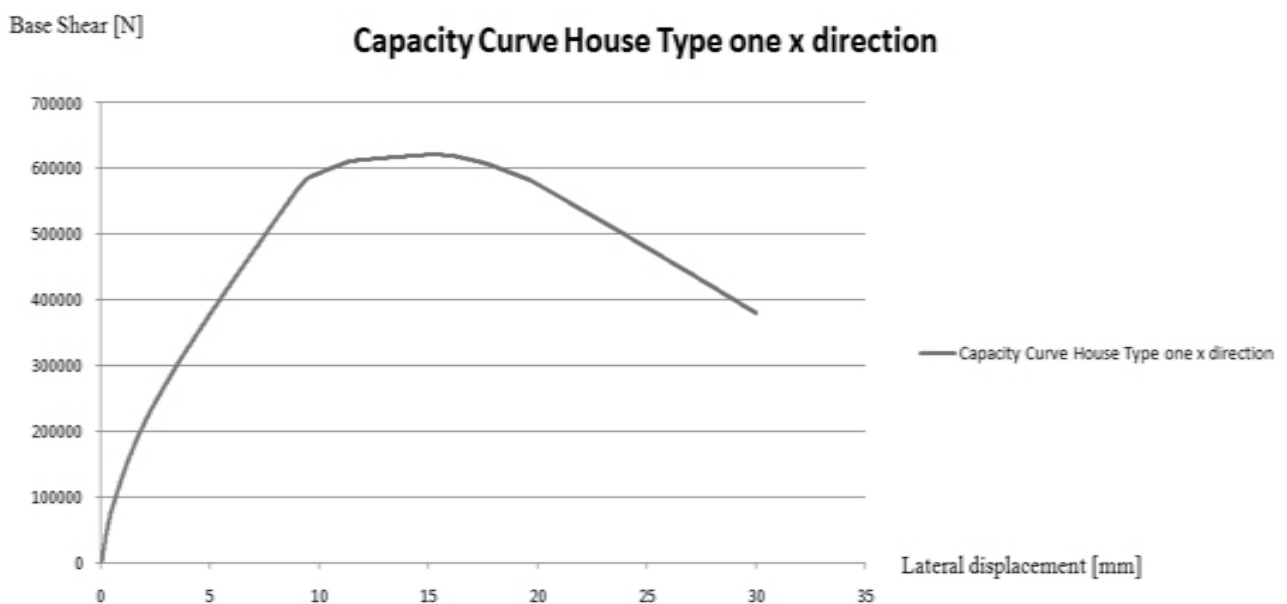

Figure 54 Capacity Curve

"In-Plane Cyclic Behavior of Substandard Confined Masonry: Full-Scale Experiments, Finite-Element Modeling and Incremental Dynamic Analysis"

Chapter 6
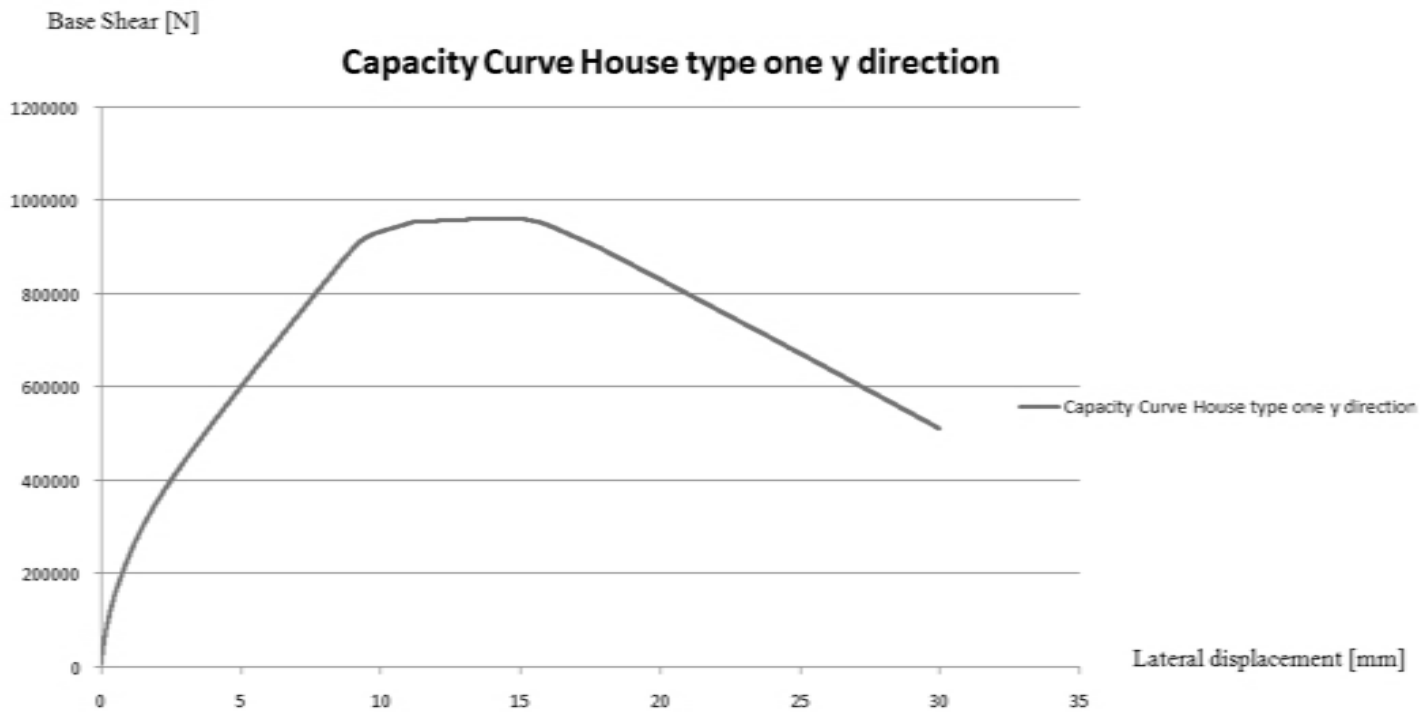
Figure 55 Capacity Curve
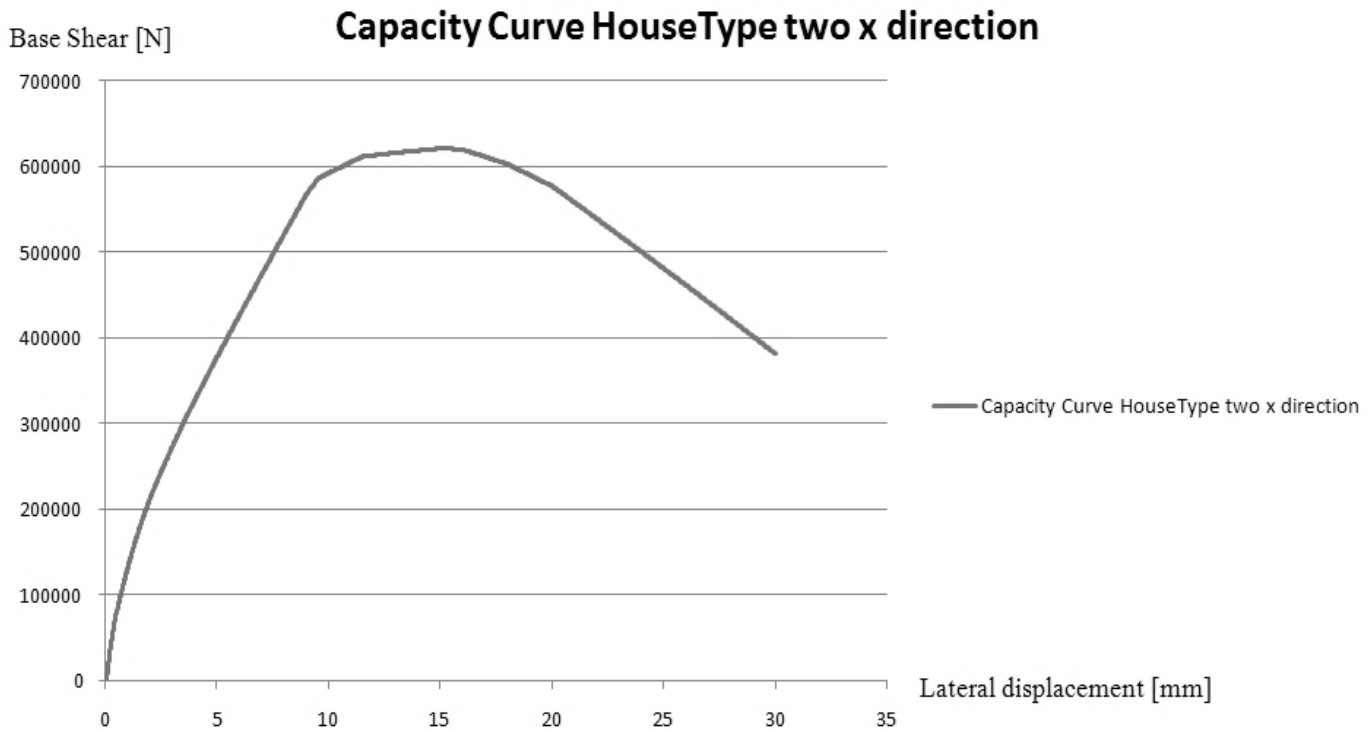
Figure 56 Capacity Curve

"In-Plane Cyclic Behavior of Substandard Confined Masonry: Full-Scale Experiments, Finite-Element Modeling and Incremental Dynamic Analysis"

Chapter 6
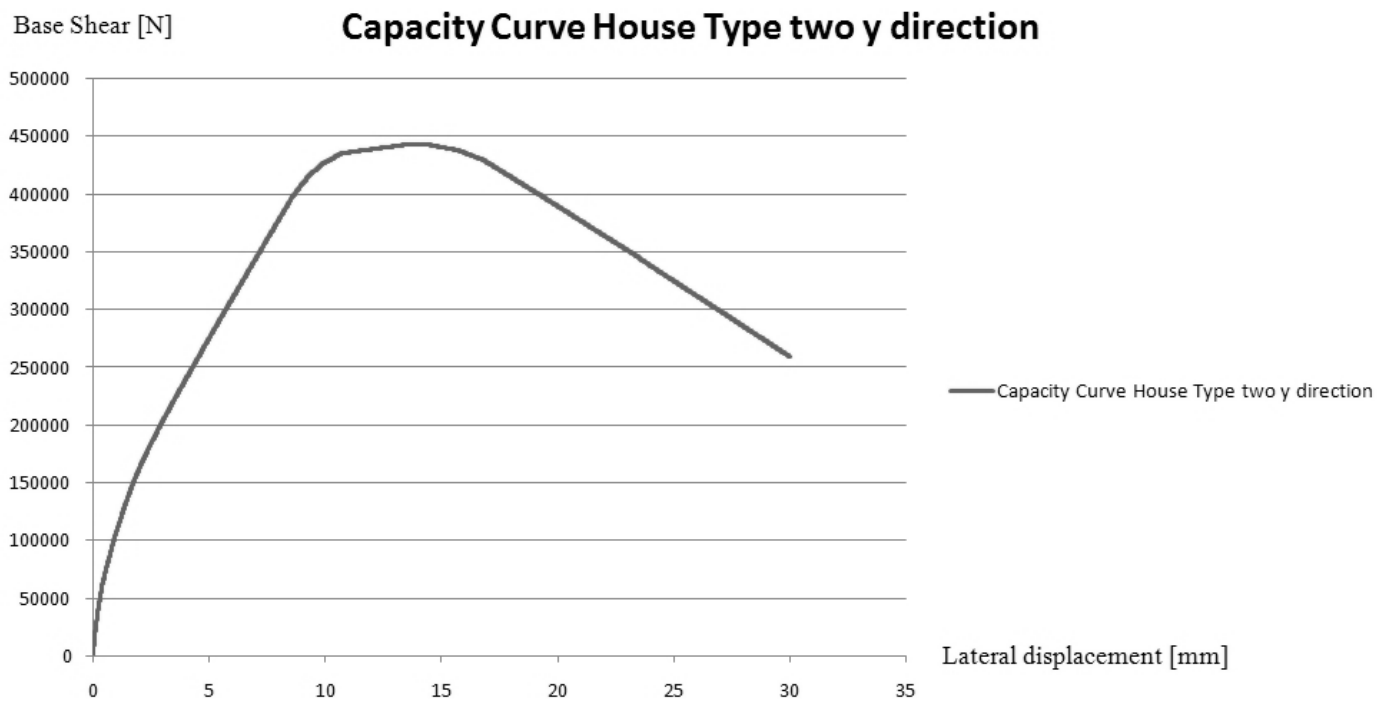
Figure 57 Capacity Curve
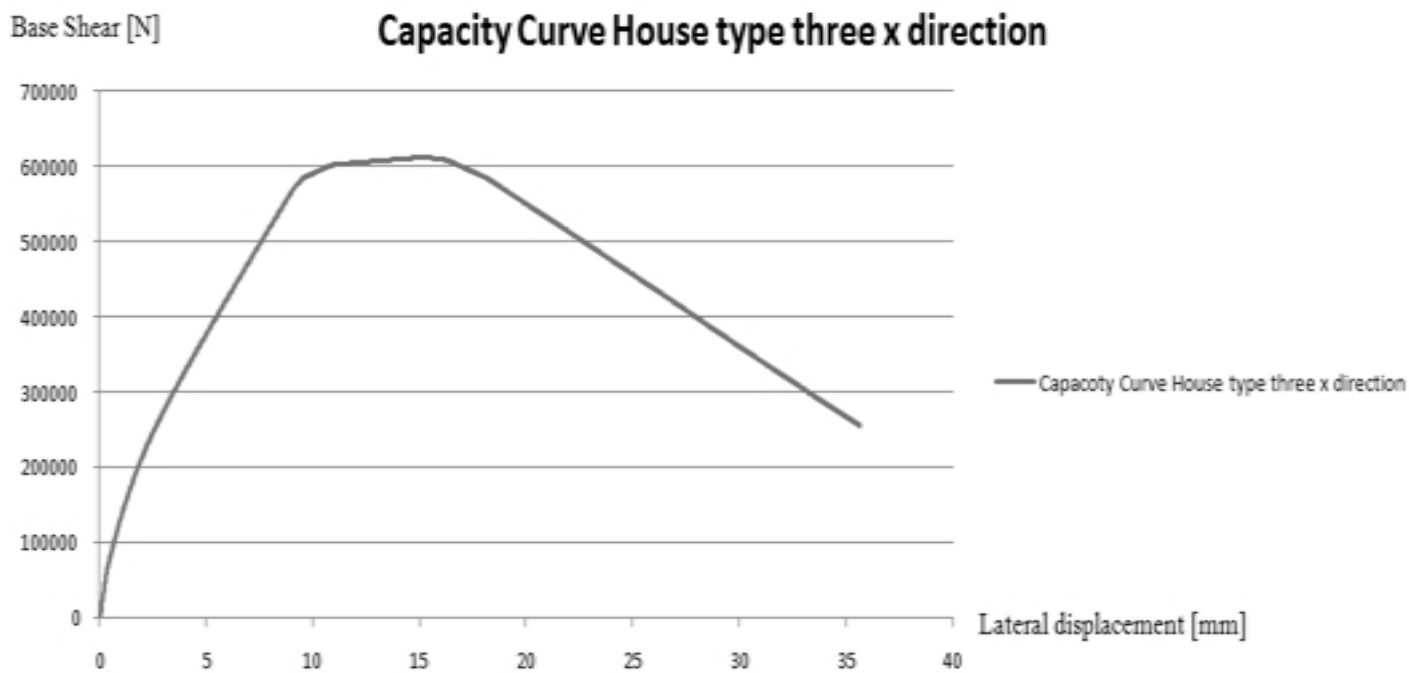
Figure 58 Capacity Curve

"In-Plane Cyclic Behavior of Substandard Confined Masonry: Full-Scale Experiments, Finite-Element Modeling and Incremental Dynamic Analysis"

Chapter 6
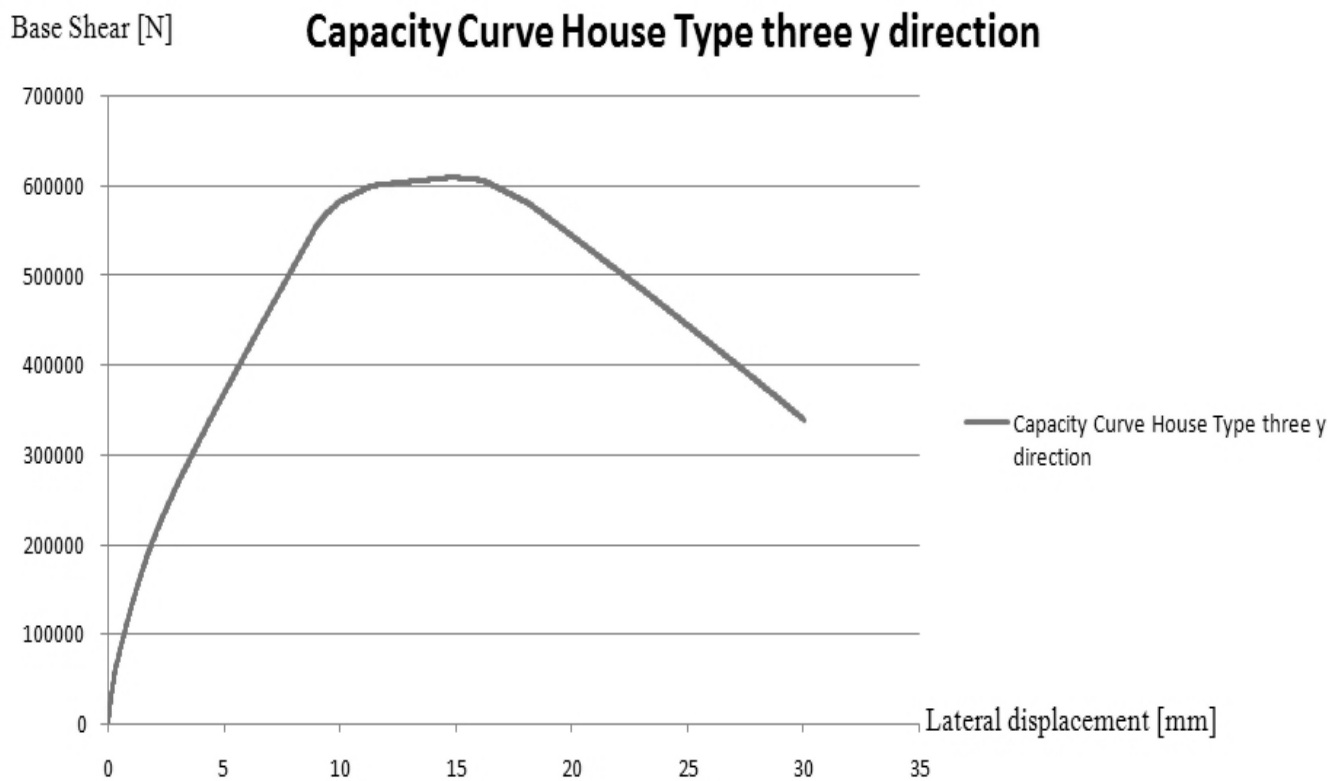
Figure 59 Capacity Curve

6.5 Results

Seismic force reduction factor q, have been evaluated by performing push over test and validating it with Incremental Dynamics Analysis. A bi-linear idealization was done for each push over test on three structures factors were defined for each main direction.

As it results from the below diagrams, IDA and push over test represent the same houses' behavior, and for this reason it was used the push over to quantify q.

"In-Plane Cyclic Behavior of Substandard Confined Masonry: Full-Scale Experiments, Finite-Element Modeling and Incremental Dynamic Analysis"

Chapter 6
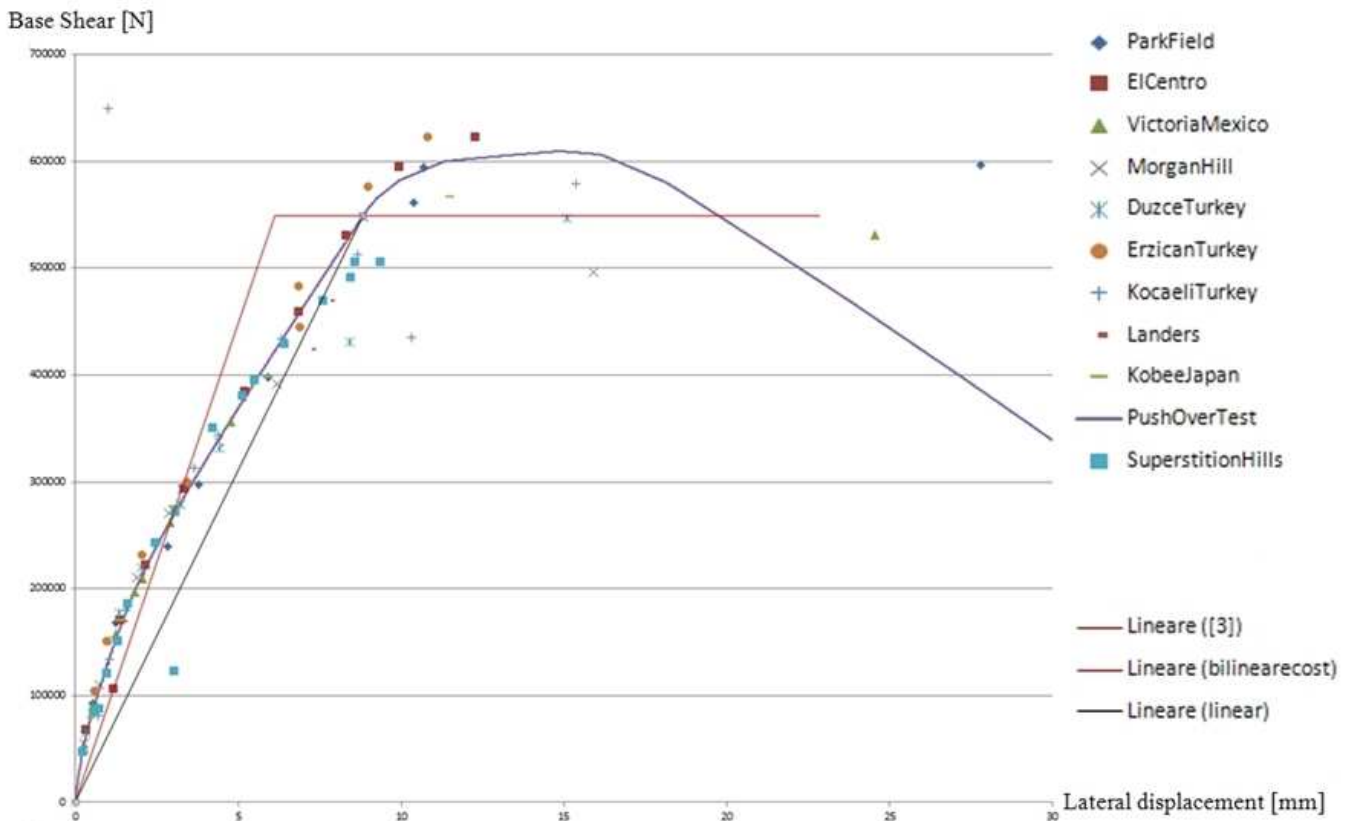
Figure 60 Validation and idealization of Type one house, x direction
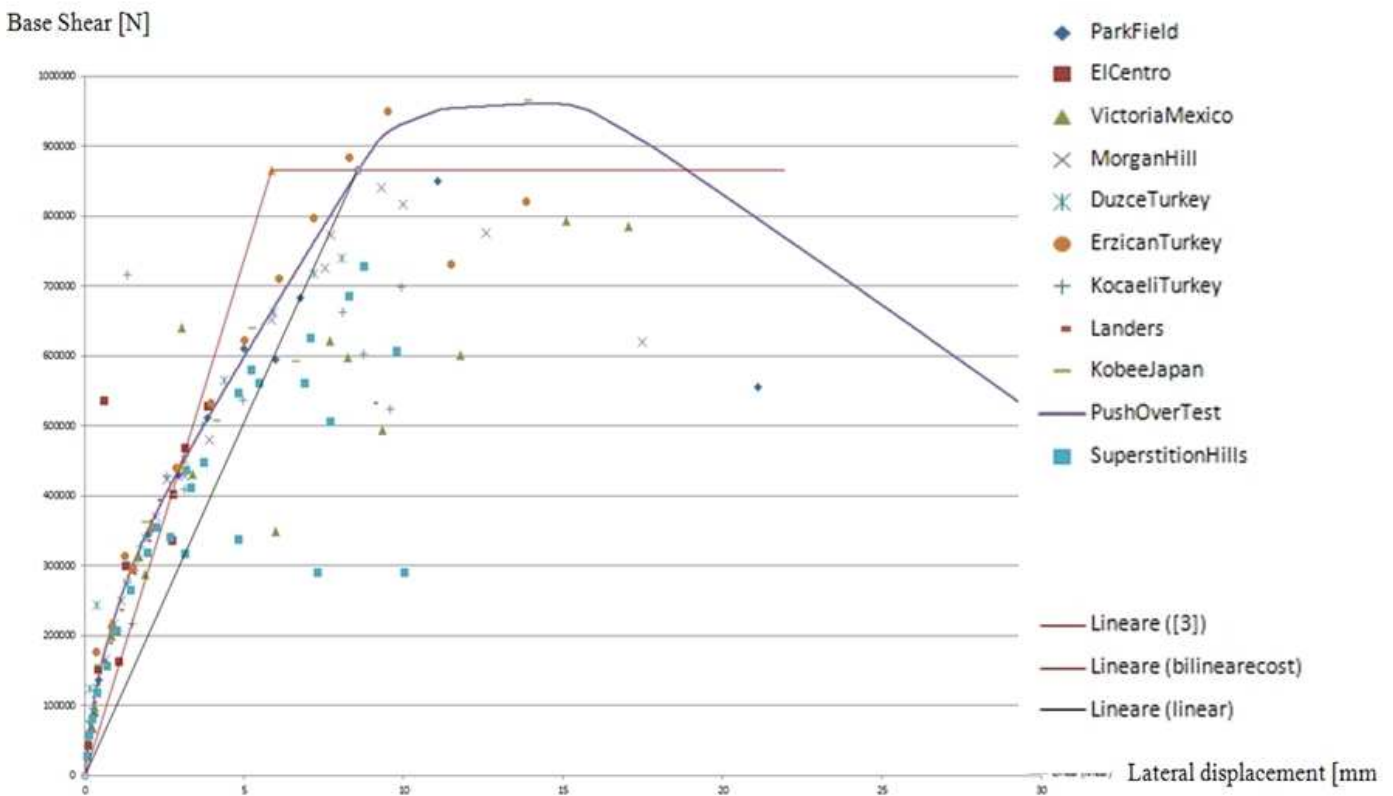
Figure 61 Validation and idealization of Type one house, y direction

"In-Plane Cyclic Behavior of Substandard Confined Masonry: Full-Scale Experiments, Finite-Element Modeling and Incremental Dynamic Analysis"

Chapter 6
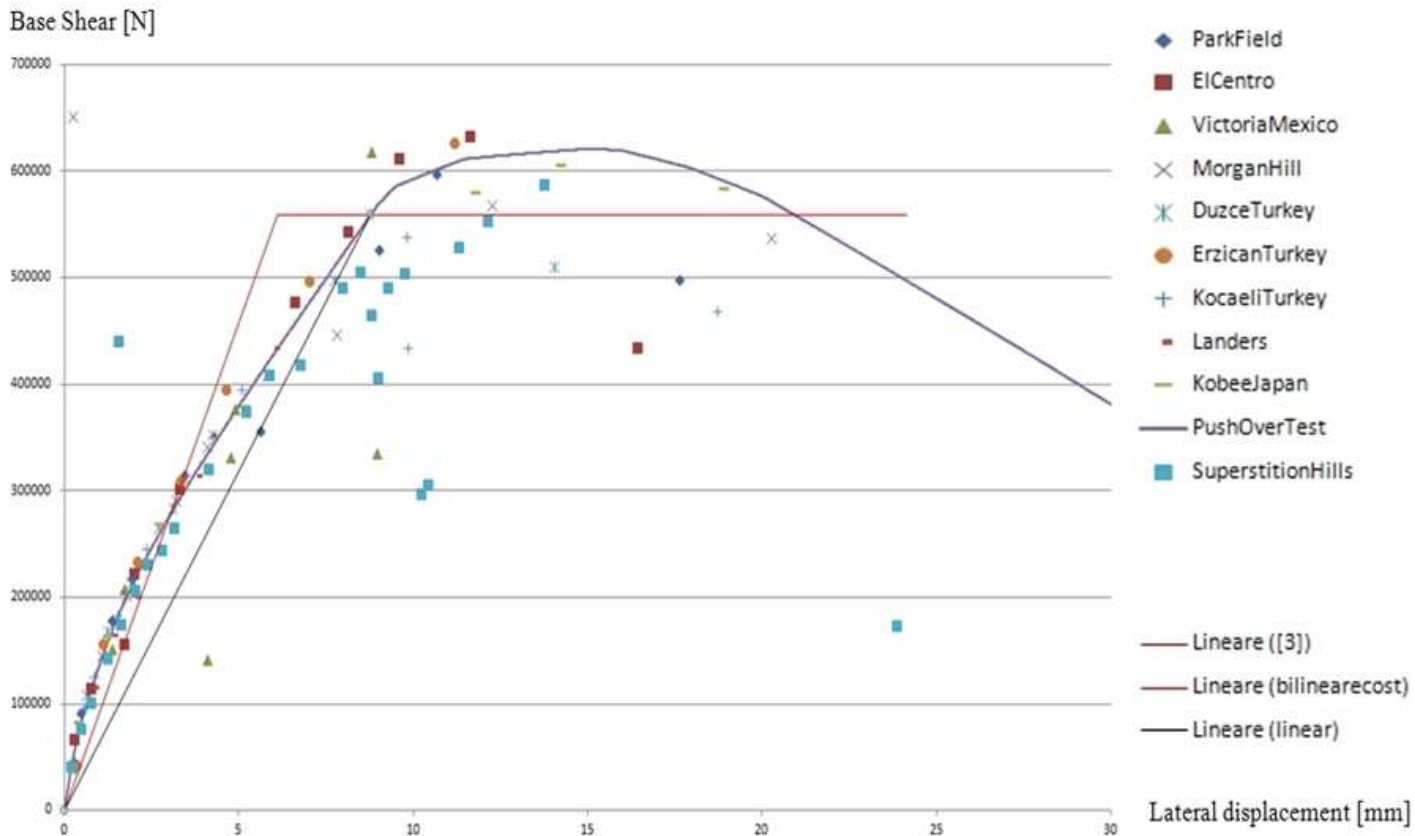
Figure 61 Validation and idealization of Type two house, x direction
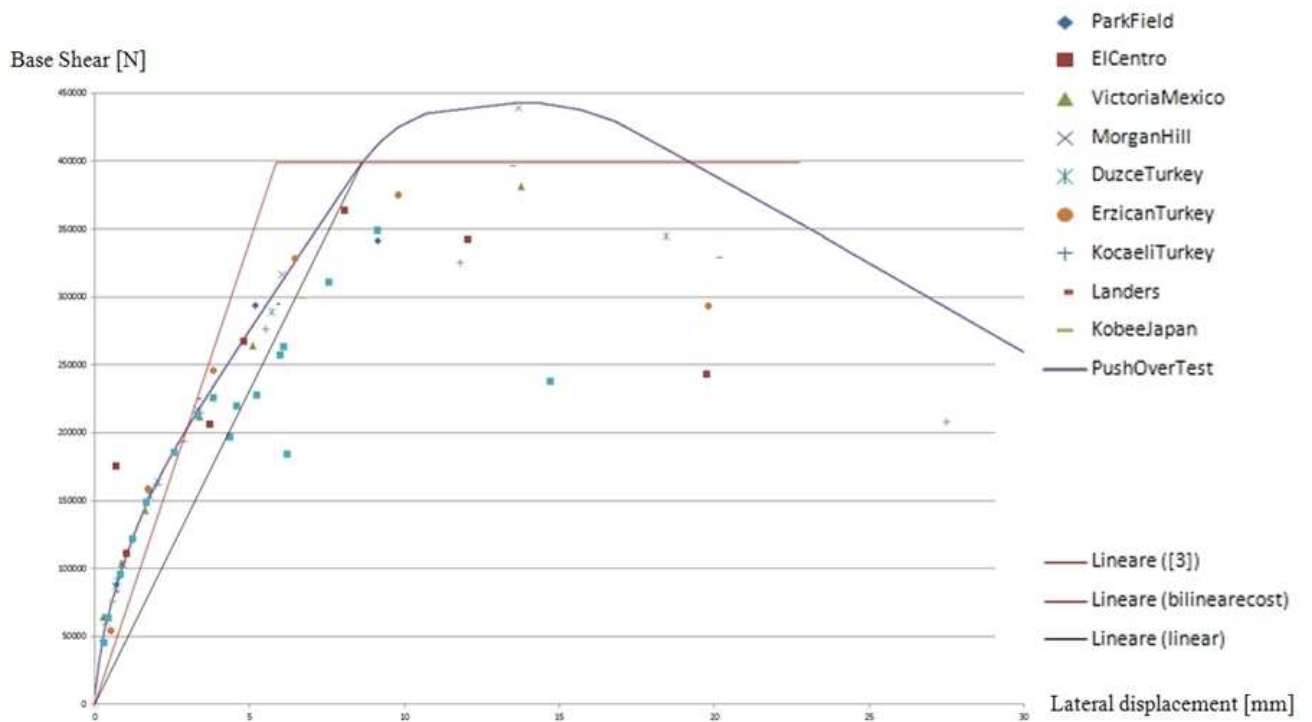
Figure 62 Validation and idealization of Type two house, y direction

"In-Plane Cyclic Behavior of Substandard Confined Masonry: Full-Scale Experiments, Finite-Element Modeling and Incremental Dynamic Analysis"

Chapter 6
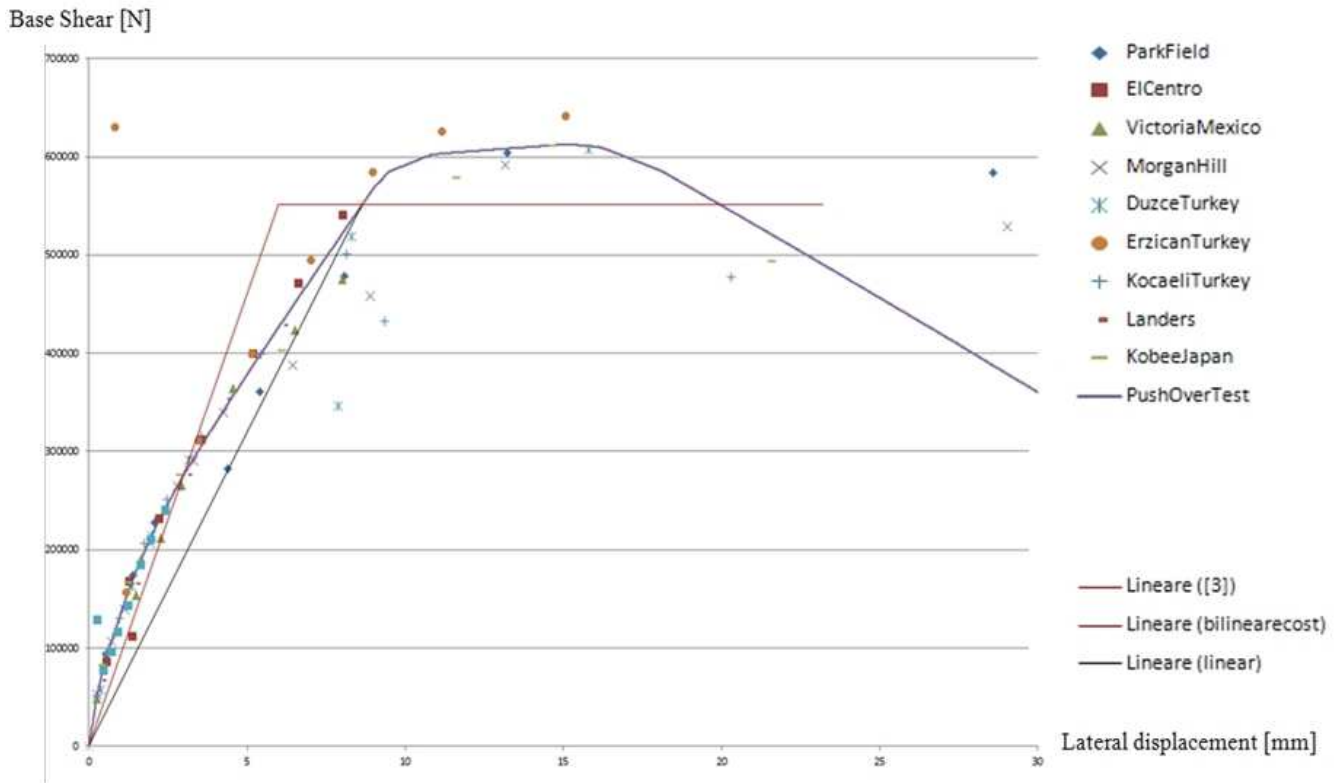
Figure 63 Validation and idealization of Type three house, x direction
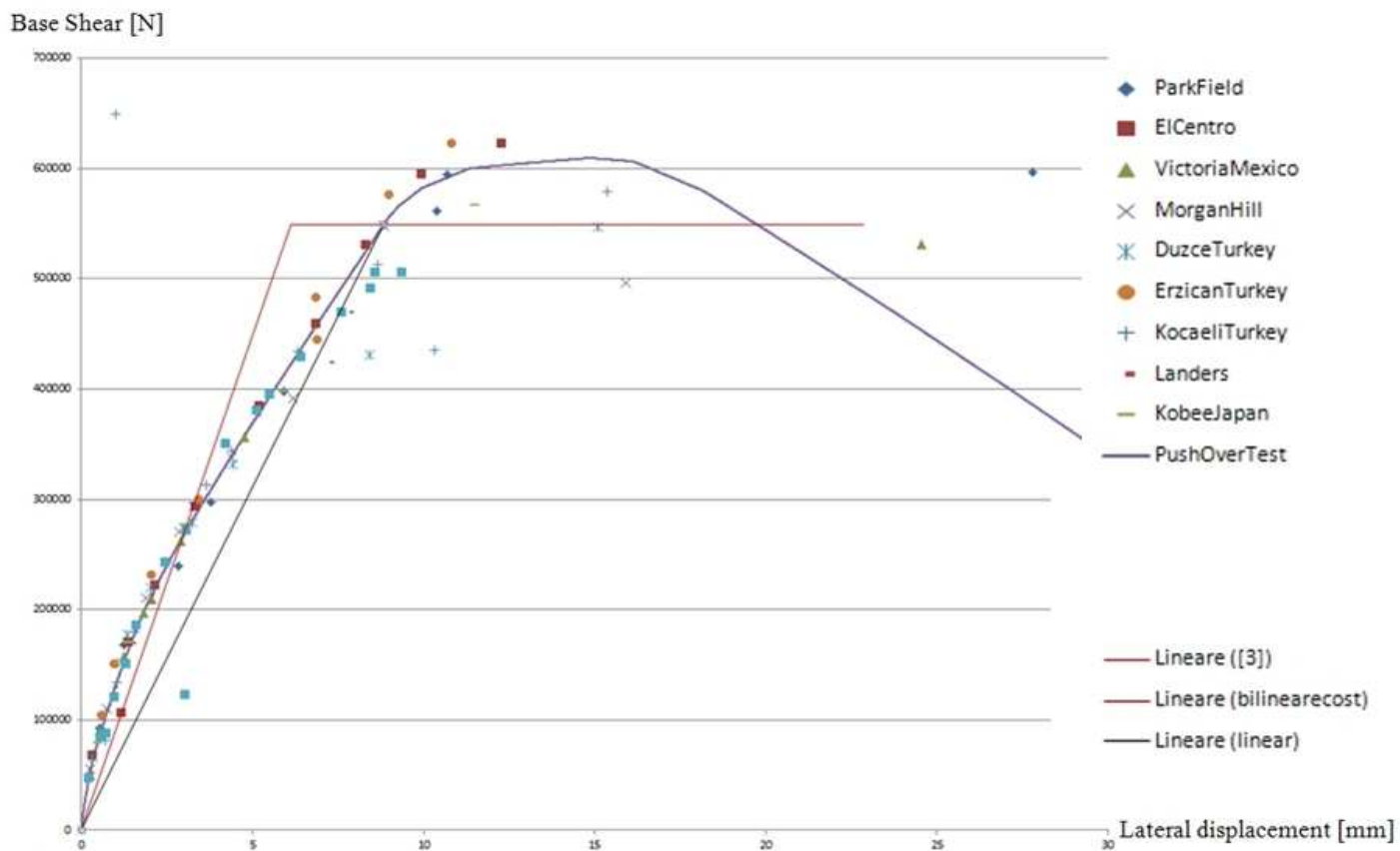
**Figure 64 Validation and idealization of Type three house, y direction**

"In-Plane Cyclic Behavior of Substandard Confined Masonry: Full-Scale Experiments, Finite-Element Modeling and Incremental Dynamic Analysis"

Chapter 6

As done for the elementary archetypes, also in this case the idealization was done using [3] theory (red line) and a more conservative approach (black line). Also the assumption of same displacement and same areas to quantify q was done. The results are illustrated in table 19.

Table 19 red value[3], black value conservative approach

	Type1 x	Type 1 y	Type 2 x	Type 2 y	Type 3 x	Type 3y
$q=\mu$	3.94	3.745	3.97	3.87	3.88	3.728
$q=\sqrt{2\mu-1}$	2.62	2.5475	2.63	2.6	2.6	2.54
$q=\mu$	2.73	2.56	2.75	2.636	2.694	2.592
$q=\sqrt{2\mu-1}$	2.11	2.032	2.12	2.06	2.09	2.045

"In-Plane Cyclic Behavior of Substandard Confined Masonry: Full-Scale Experiments, Finite-Element Modeling and Incremental Dynamic Analysis"

Chapter 7

7. Conclusions

- Through a complete literature review and a designed number of laboratory experiment it is possible to define clearly the mechanical behavior of CM walls under cyclic load;
- Following a global approach modeling, for CM elements, it is possible to define the elementary archetype behavior under seismic load;
- Once defined the elementary archetype, designed a structures typologies space, through Incremental Dynamic Analysis and Pushover analysis it is possible to define the Global ductility factor and the structure factor;
- Using the idealization technique [3] it is obtained a ductility factor in the range with the normal CM structures;
- Using a more conservative idealization technique it is possible to define a more plausible structure factor but the fundamental period it is not taken;
- From the results obtained, emerge that the global ductility factor is almost the same for all the structure so, it is possible to build structure whit less element with the almost same dissipate capacity.

Suggestions for a future research

- An energy dissipation analysis have to be done in order to define the maximum energy input;
- Using IDA results, it is possible to define the structure factor using this formulation:

$$q = \frac{PSA\,(T1,SF)m}{0.9Fmax}$$

with the following meaning:

q = structure factor;

PSA it is the pseudo-acceleration that corresponds to the fundamental period of the structures and the scaling factor value;

m = the mass of the system;

Fmax = maximum base shear defined by pushover test.

- Using the same modeling approach it is possible to model also the retrofitted wall.

"In-Plane Cyclic Behavior of Substandard Confined Masonry: Full-Scale Experiments, Finite-Element Modeling and Incremental Dynamic Analysis"

Contents

References

[1] FEMA P695/June 2009. "Quantification of building Seismic Performance Factors".

[2] Kuldeep S. Virdi Engineering Structures research centre, City University, London and Mr Ronson D.Rashkoff, www.staff.cityac.uk./earthquakes/Foreward.

[3] Miha Tomazevic. "Earthquake-Rsistent design of masonry buildings".

[4] Theodosios P.Tassios. "Meccanica della muratura".

[5] A. Giuffrè. "In-plane seismic behavior of historical masonry walls".

[6] G. Magenes and G.M. Calvi. "In-plane seismic responce of brick masonry walls"

[7] A. Penna, A. Galasco and S. Lagomarsino. "Analisi sismica non lineare a macroelementi di edifici in muratura".

[8] NTC 2008.

[9] ASCE 7.

[10] Evaluation of CM guidelines final draft

[11] F. Crisafulli. "Seismic behavior of reinforced concrete structures with masonry infills".

[12] Maria O. Moroni, Maximiliano Astroza, Juan Gomez, and Rafael Guzman. "Establishing R_w and C_d Factors for Confined Masonry Buildings".

[14] Inpres-Cirsoc 103. [1983] "Normas Argentinas para construciones sismoresistentes". Parte 3. Construciones de mamposteria.

[15] Gideon P.A.G. van Zijl. "Modeling Masonry Shear-Compression: Role of Dilatancy Highlighted".

[16] E. Smyro, C. Blandon, S. Antoniou, R. Pinho, F. Crisafulli. "Implementation and verification of a masonry panel model for nonlinear dynamic analysis of infilled RC frames".

[17] A. Anthoine. "Derivation of the in-plane elastic characteristic of masonry through homogenization theory".

[18] Chiara Calderini and Sergio Lagomarsino. "Continuum Model for In-Plane Anisotropic Inelastic Behavior of Masonry".

[19] Paulo B. Lourenco and Jan G. Rots. "Multisurface Interface Model for Analysis of Masonry Structures".

[20] Hamid R. Lotfi and P. Benson Shing. "Interface Model Applied to Fracture of Masonry Structures".

[21] B. Shieh-Beygi, S. Pietruszczak. "Numerical Analysis of structural masonry: mesoscale approach".

"In-Plane Cyclic Behavior of Substandard Confined Masonry: Full-Scale Experiments, Finite-Element Modeling and Incremental Dynamic Analysis"

Contents

[22] Armando Calabrese a , João Pacheco Almeida and Rui Pinho. "Numerical Issues in Distributed Inelasticity Modeling of RC Frame Elements for Seismic Analysis".

[23] Tim Gudmand-Høyer. "Yield line Theory for Concrete Slabs Subjected to Axial Force".

[24] Mohd. Zamin Jumaat and Bona Murty. "Yield load prediction of nailed timber joints using nail diameter and timber specific gravity".